

## MIT Open Access Articles

*Biological growth and synthetic fabrication  
of structurally colored materials*

The MIT Faculty has made this article openly available. **Please share**  
how this access benefits you. Your story matters.

**Citation:** McDougal, Anthony et al. "Biological growth and synthetic fabrication of structurally colored materials." Journal of Optics 21, 7 (June 2019): 073001 © 2019 IOP Publishing Ltd

**As Published:** <http://dx.doi.org/10.1088/2040-8986/aaff39>

**Publisher:** IOP Publishing

**Persistent URL:** <https://hdl.handle.net/1721.1/126616>

**Version:** Final published version: final published article, as it appeared in a journal, conference proceedings, or other formally published context

**Terms of use:** Creative Commons Attribution 3.0 unported license



TOPICAL REVIEW • OPEN ACCESS

## Biological growth and synthetic fabrication of structurally colored materials

To cite this article: Anthony McDougal *et al* 2019 *J. Opt.* **21** 073001

View the [article online](#) for updates and enhancements.

### Recent citations

- [Stability and Selective Vapor Sensing of Structurally Colored Lepidopteran Wings Under Humid Conditions](#)  
Gábor Piszter *et al*
- [Iridescence and thermal properties of \*Urosaurus ornatus\* lizard skin described by a model of coupled photonic structures](#)  
José G Murillo *et al*
- [Biological Material Interfaces as Inspiration for Mechanical and Optical Material Designs](#)  
Jing Ren *et al*



**IOP | ebooks™**

Bringing together innovative digital publishing with leading authors from the global scientific community.

Start exploring the collection—download the first chapter of every title for free.

## Topical Review

# Biological growth and synthetic fabrication of structurally colored materials

Anthony McDougal , Benjamin Miller, Meera Singh and Mathias Kolle 

Department of Mechanical Engineering, Massachusetts Institute of Technology, 77 Massachusetts Avenue, Cambridge, MA 02139, United States of America

E-mail: [mkolle@mit.edu](mailto:mkolle@mit.edu)

Received 9 January 2018, revised 29 May 2018

Accepted for publication 16 January 2019

Published 11 June 2019



### Abstract

Nature's light manipulation strategies—in particular those at the origin of bright iridescent colors—have fascinated humans for centuries. In recent decades, insights into the fundamental concepts and physics underlying biological light-matter interactions have enabled a cascade of attempts to copy nature's optical strategies in synthetic structurally colored materials. However, despite rapid advances in bioinspired materials that emulate and exceed nature's light manipulation abilities, we tend to create these materials via methods that have little in common with the processes used by biology. In this review, we compare the processes that enable the formation of biological photonic structures with the procedures employed by scientists and engineers to fabricate biologically inspired photonic materials. This comparison allows us to reflect upon the broader strategies employed in synthetic processes and to identify biological strategies which, if incorporated into the human palette of fabrication approaches, could significantly advance our abilities to control material structure in three dimensions across all relevant length scales.

**Keywords:** structural color, photonic materials, biological optics and bio-inspired photonics, structure formation processes, biological growth, nanofabrication and microfabrication, functional morphology

(Some figures may appear in colour only in the online journal)

## 1. Introduction

The control of material morphology and composition from the atomic to the macroscopic scale, with the aim of achieving specific material properties, is a key theme in biology and a major area of focus in science, engineering, and advanced technology development [1]. Biological and biologically inspired photonic materials—in particular when structural coloration is the desired core functionality—are great examples of the efforts of biological organisms and humans to

control material structure and composition across length scales [2–4]. In this review, we contrast nature's strategies for creating functional hierarchical structures with human approaches to do the same. Specifically, we focus on material morphologies that enable structural coloration. This permits us to assess the structural outcome simply by visual inspection, allowing us to draw conclusions about the potential of specific processes to ensure correct formation of color-inducing structures.

The science and engineering of structural color have historically intertwined biological phenomena with human-made devices. In *'Opticks: or, a treatise of the reflexions, refractions, inflexions and colors of light'*, published in 1704, Isaac Newton described how 'the finely color'd Feathers of some Birds ... appear of several Colors ... after the very same



Original content from this work may be used under the terms of the [Creative Commons Attribution 3.0 licence](https://creativecommons.org/licenses/by/3.0/). Any further distribution of this work must maintain attribution to the author(s) and the title of the work, journal citation and DOI.

manner that thin Plates were found to do ...' [5]. Since then, humans have aimed to understand, replicate, and expand upon a vast variety of biological optical structures [4, 6–14]. While in many instances human-made optical materials exceed natural materials with regards to application-specific performance characteristics—after all, humans did not need nature to build sophisticated lens systems, lasers, imaging devices, and much more—biological optical materials possess some significant advantages.

- (1) Their hierarchical nature, with structure control from atomic to macroscopic levels, enables beneficial synergies between quantum-optical, wave-optical, and ray-optical phenomena, yielding unique macro-scale optical characteristics.
- (2) This same hierarchical nature also confers the ability to integrate optical functions with other properties, such as tailored interfacial interactions, mechanical robustness, or thermo-regulation, to name just a few.
- (3) Biological optical systems often represent highly-evolved synergistic combinations of their intrinsic material properties and structure-imposed emergent behavior. They may therefore offer ideas for how to create a desired optical property in a synthetic system. Although major fundamental light manipulation concepts are well explored, the design of an optical material that satisfies a defined set of performance requirements under specific constraints in the most resource-efficient way is frequently a non-trivial task. Since resource-efficiency, robustness, and optimized performance is often crucial to any organisms' survival, the study of natural optical materials can help the optical designer in bounding challenging optimization scenarios by identifying promising starting points in large parameter spaces.
- (4) Natural optical materials provide insight into design principles that allow for the emergence of dynamic, adaptive, and reconfigurable optical performance.
- (5) Finally, biological optical systems are formed at or close to room temperature, and rely exclusively on biocompatible materials and sustainable chemical processes; these are factors of increasing importance in the context of energy-efficient, sustainable material design and resource management.

To date, much of the success in the field of biologically inspired optics comes from careful attention to the structures and material composition that enable nature's light manipulation concepts across the animal world, the plant kingdom, and other parts of the tree of life (figure 1) [15–25]. However, little progress has been made toward understanding how these structures form; instead, we still largely rely on conventional synthetic fabrication strategies to form bioinspired optical materials. Alternative processes that bear similarities with biological structure formation strategies are only slowly entering our manufacturing toolbox. This may be due to the lack of detailed knowledge about the processes that organisms harness to achieve the structural control required to form material morphologies that enable a specific optical effect. In this review we argue that bioinspired photonics research can contribute

significantly to optical technology advancements, provided we develop a robust understanding of the biological processes that enable structure formation and adopt relevant principles in human fabrication strategies. An in-depth understanding of the differences between human approaches and natural processes in the generation of structurally colored materials could help to pinpoint strategies for overcoming current limitations in our ability to design and manufacture materials with true control over the material structure in all three dimensions, across all relevant length scales. Just as the emulation of natural material morphologies and microstructures have enabled novel optical materials, a stronger focus on understanding and harnessing the processes underlying structure formation will lead to new insights and strategies for the design and fabrication of novel functional materials.

The next section of this review begins with a few brief comments on the physics of structural color and then continues with a discussion of select examples of biological structural color with a focus on structural diversity, dynamics, and material constituents. Subsequently, we will briefly review an exemplary selection of synthetic structurally colored materials. The third section then forms the review's core. After providing a brief categorization of structure formation processes, we assess what is known about the processes involved in the formation of biological optical materials and then discuss synthetic structure formation strategies. In the final section, we compare and contrast biological and human structure formation concepts, and synthesize a few recommendations for opportunities to advance human manufacturing strategies for advanced optical materials.

## 2. Biological and synthetic structurally colored materials

### 2.1. Physics of structural color

Light manipulation is vital for many biological organisms and also critical in a diverse range of human application scenarios including vision and image capture systems, optical detectors, energy conversion, information processing, and communication. The underlying physics is discussed throughout the literature on biological and bioinspired photonic materials, and considered with particular attention to structural colors in [36–38]. In essence, adequate manipulation of light-matter interactions can only be achieved by employing materials that feature the right structural design to exploit a set of specific effects from a wide range of optical phenomena (figure 2).

Absorption and luminescence (inherently quantum-mechanical effects) necessitate control of structure and composition on the atomic scale, which is far below the characteristic wavelength of visible radiation. Photonic structures on the scale of a few hundred nanometers to several micrometers can exploit diffraction and interference phenomena in the visible optical spectrum and also greatly assist in tailoring absorption and emission originating from light-matter interactions on much smaller scales. Finally, three-dimensional patterns on the scale of tens of micrometers to several



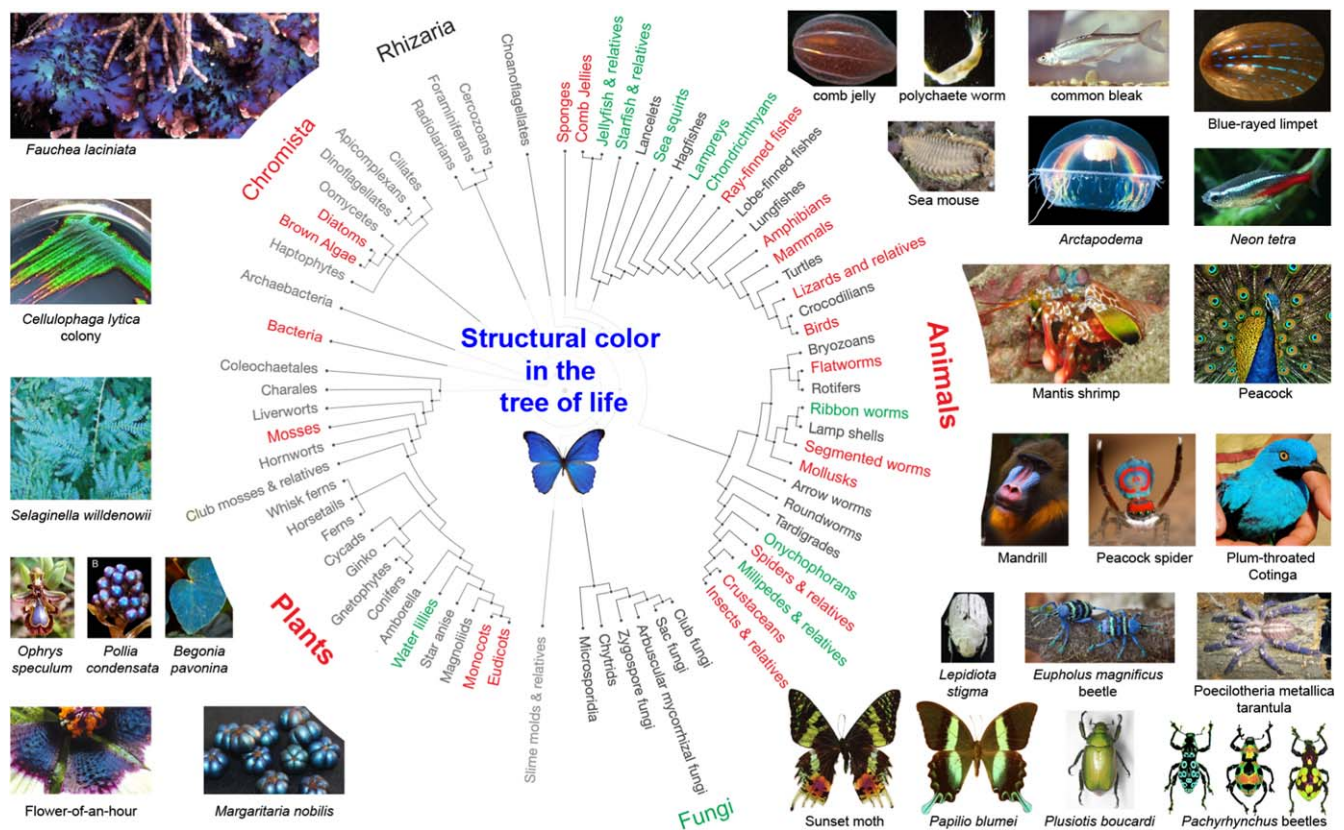


**Figure 1.** Structural color in the biological world. Structural color has evolved convergently in most major biological groups and is particularly abundant among animals and plants. Terrestrial species, such as birds, insects and fruits, have been studied intensely for several decades; over the last few years, research has increasingly focused on the light manipulation strategies of marine organisms. Groups and clades that contain species which employ structurally colored materials and have been the subject of scientific research efforts and publications are marked in red. Groups that also likely employ structural color are shown in green, although to our knowledge no scientific study has focused on them in this regard. Image credits: *Faucheia laciniata*—Reproduced with permission from Lovell and Libby Langstroth © California Academy of Sciences. *Cellulophaga lytica* reproduced from [26]. CC BY 4.0. *Selaginella willdenowii* republished with permission of The Royal Society, from [22]; permission conveyed through Copyright Clearance Center, Inc. *Ophrys speculum*—this ‘Ophrys speculum subsp. Speculum’ image has been obtained by the author(s) from the Wikimedia website where it was made available under a CC BY-SA 2.5 licence. It is included within this article on that basis. It is attributed to Esculapio. *Pollia condensata* reproduced with permission from [28]. *Begonia pavonina* reprinted by permission from Springer Nature: Nature, Nature Plants, [29], 2016. *Hibiscus trionum* [30] John Wiley & Sons. © 2014 The Authors. New Phytologist © 2014 New Phytologist Trust *Margaritaria nobilis* reproduced from [31]. CC BY 4.0. Comb jelly—reproduced with permission from Kevin Raskoff. Polychaete worm—reproduced with permission from Andrew Parker. Common bleak—this ‘Alburnus alburnus photographed in Tiszafüred, river Tisza, Hungary’ image has been obtained by the author(s) from the Wikimedia website where it was made available by Etrusko25 under a CC BY 3.0 licence. It is included within this article on that basis. It is attributed to Arkos Harka. Limpet Reproduced from [32]. CC BY 4.0. Sea mouse—reproduced with permission from Dave Harasti. *Arctapodema*—reproduced with permission from Lawrence P. Madin. *Neon tetra*—this ‘Neon Tetra, Paracheirodon innesi, Family: Characidae’ image has been obtained by the author(s) from the Wikimedia website where it was made available under a CC BY 3.0 licence. It is included within this article on that basis. It is attributed to Holger Krisp. Mantis shrimp—this ‘A colourful stomatopod, the peacock mantis shrimp (Odontodactylus scyllarus), seen in the Andaman Sea off Thailand’ image has been obtained by the author(s) from the Wikimedia website where it was made available by Zaneselvans under a CC BY 2.0 licence. It is included within this article on that basis. It is attributed to Silke Baron. Peacock—this ‘A peacock showing off its colours, Sultanpur National Park’ image has been obtained by the author(s) from the Wikimedia website where it was made available under a CC BY-SA 4.0 licence. It is included within this article on that basis. It is attributed to Jatin Sindhu. Mandrill—this ‘Mandrillus sphinx.’ image has been obtained by the author(s) from the Wikimedia website where it was made available under a CC BY 2.0 licence. It is included within this article on that basis. It is attributed to Matt Sabbath. Peacock spider republished with permission of The Royal Society, republished with permission of The Royal Society, from [33]; permission conveyed through Copyright Clearance Center, Inc. Plum-throated cotinga—reproduced with permission from Thomas Valqui. *Lepidopta stigma* reprinted by permission from Springer Nature: Nature, Scientific Reports, [34], 2014. *Eupholus magnificus*—this ‘Français: Boîte pédagogique sur les insectes de l’indomalais insulaire. Eupholus magnificus.’ image has been obtained by the author(s) from the Wikimedia website where it was made available under a CC BY-SA 4.0 licence. It is included within this article on that basis. It is attributed to Édouard Hue. *Poecilotheria metallica* tarantula—reproduced from [https://commons.wikimedia.org/wiki/File:Poecilotheria\\_metallica.JPG#/media/File:Poecilotheria\\_metallica.JPG](https://commons.wikimedia.org/wiki/File:Poecilotheria_metallica.JPG#/media/File:Poecilotheria_metallica.JPG). Image stated to be in the public domain. Sunset moth and *Papilio blumei* reprinted by permission from Springer Nature: Springer Netherlands, Encyclopedia of Nanotechnology, [35], 2012. *Plusiotis boucardi*—reproduced with permission from Brett Ratcliffe. *Pachyrhynchus* beetles—Reproduced with permission from Estan Cabigas.

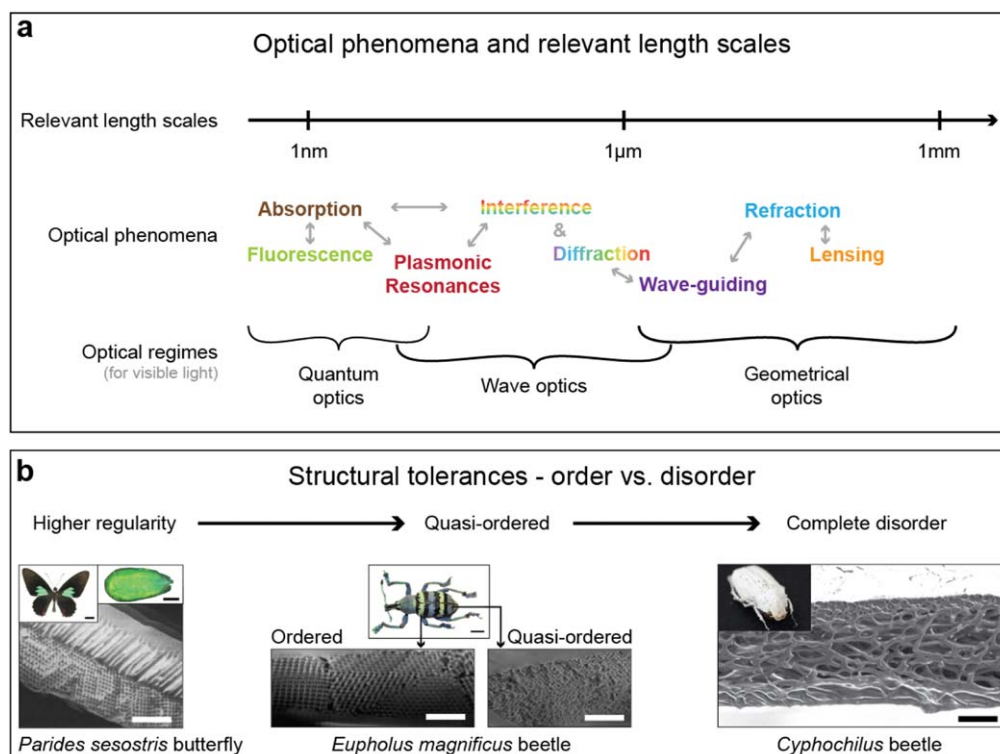


**Figure 2.** Optical phenomena, relevant length scales, and the role of order in photonic materials. (a) A large diversity of phenomena are involved in the interaction of matter with light on different length scales. Many of these phenomena are exploited in biological photonic materials and certainly also play a role in synthetic optical systems. (b) The brightness and hue of a structural color material depends on a variety of parameters and their variations. One of them is the degree of order. Regular ordered architectures usually provide bright coloration and frequently show some iridescence; the example shown here is the gyroid structure found in the butterfly *Parides sesostris*. The weevil *Eupholus magnificus* has differently colored regions on its elytra. The brighter green stripes result from a highly-ordered 3D photonic crystal, while the blue stripes originate from a quasi-ordered 3D photonic structure. Such quasi-ordered structures usually show less angle-dependent color variation. *Cyphochilus* beetles have a completely disordered fibrillar architecture in their scales, which causes their bright white reflections. ((B) right) Reproduced from <https://www.cam.ac.uk/research/news/the-beetles-white-album> by Lorenzo Cortese and Silvia Vignolini. CC BY 3.0.

centimeters are required to exploit lensing and focusing effects, refraction, and wave-guiding.

The degree of regularity in the color-generating structure has a direct impact on the resulting coloration [42]. The brightest, most iridescent colors usually result from structures with tight geometric tolerances and a high degree of order [28, 43, 44]. Angle-independent hues arise through coherent scattering from quasi-ordered material structures [41, 45, 46]. The most brilliant whites are caused by incoherent scattering of light from completely disordered nano- and microstructures [34, 47–51].

In short, the most stunning visual displays in nature usually rely on sophisticated hierarchical material structures that synergistically exploit several different physical phenomena to create unique coloration effects.

## 2.2. Biological structural color—structural diversity, dynamics, and materials

In our discussion of select structural color examples in biology, we focus on three specific attributes that we consider as primarily important in the context of this review.

- (1) Structural diversity, signifying the interplay of several different processes and control mechanisms involved in structure formation,

- (2) Color dynamics, enabled by the organism's ability to stimulate controlled structural variations *in situ*, and
- (3) Material constituents that provide intrinsic optical and mechanical attributes, which are modified by imposing structure and are crucial for dynamic, reversible structure variation.

**2.2.1. Structural diversity.** The stunning diversity of hierarchical photonic architectures in butterfly scales exemplifies the ability of biological systems to evolve and reliably produce structural elements with fine-tuned optical functionality (figure 3). A generic morphology of ridges, cross-ribs, and lamellae forms the basic blueprint for scales across lepidopteran species [52]. However, a rich variety of modifications to this generic building plan results in a range of strategies to display colors of tailored intensity and spectral composition, satisfying the organisms' requirements for conspecific and cross-species communication, camouflage, thermal management, air flow modification, or wetting control [53–59].

Butterflies of the *Morpho* family utilize specialized ridge designs [43, 61, 65, 66]; the sunset moth *Chrysiridia rhipheus* relies on perforated lamellae located in the scales between the ridges [67, 68]; *Papilio palinurus*, *Papilio ulysses* and others,



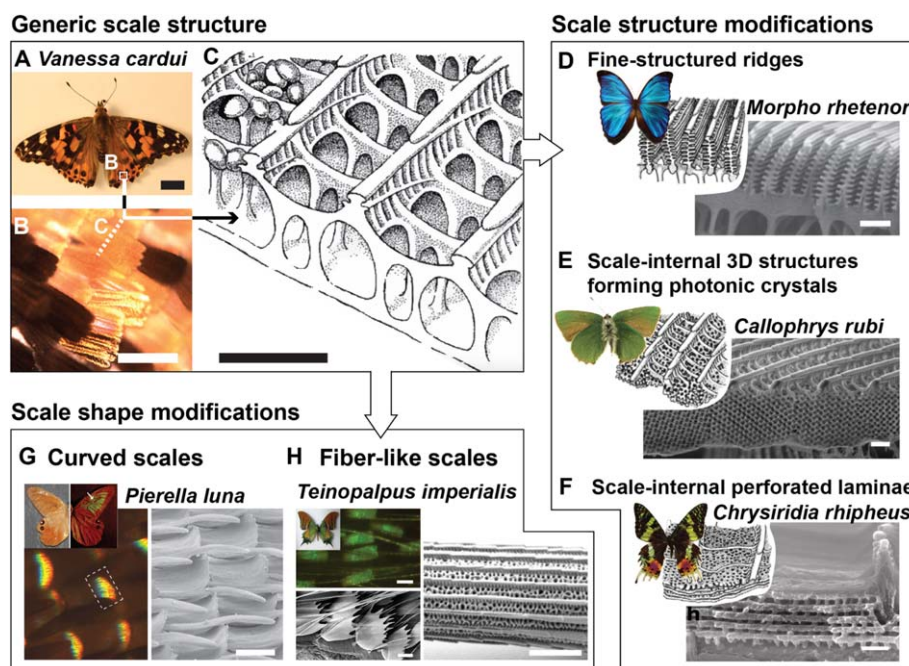


**Figure 3.** Structural diversity in butterfly wing scales. (A) The ‘Painted Lady’ butterfly *Vanessa cardui* (scale bar 1 mm) and (B) its orange and black wing scales (scale bar 100  $\mu\text{m}$ ), which (C) display a generic scale architecture (scale bar  $\sim 1 \mu\text{m}$ ). (D)–(F) This generic design is modified by many butterfly species to enable unique color displays. (D) Fine-structured ridges on the wing scales of many *Morpho* species (scale bar 1  $\mu\text{m}$ ). (E) Three-dimensional photonic crystal structures in the wing scales of the ‘Green Hairstreak’ butterfly *Callophrys rubi* (scale bar 1  $\mu\text{m}$ ). (F) Perforated lamella forming a Bragg reflector in the scales of the sunset moth *Chrysiridia rhipheus* (scale bar 500 nm). (G) and (H) Other butterfly species harness changes in the overall scale shape to produce structural colors. (G) The ‘Moon Satyr’ *Pierella luna* produces varying coloration effects by curving its scales to orient the fine-scale cross-rib architecture such that it forms a vertical diffraction grating (scale bar 50  $\mu\text{m}$ ). (H) The ‘Kaiser-i-Hind’ butterfly *Teinopalpus imperialis* displays scales and long fibers with very similar micro- and nanoscale architecture on its wings (scale bar 2  $\mu\text{m}$ ). (C) Republished with permission of The Royal Society, from [52]; permission conveyed through Copyright Clearance Center, Inc. (D) This ‘blue morpho butterfly’ image has been obtained by the author(s) from the Wikimedia website where it was made available by Lycaon under a CC BY-SA 3.0 licence. It is included within this article on that basis. It is attributed to Gregory Phillips. (D), (E) and (F) [60] John Wiley & Sons. © 1998 Wiley-Liss. (D) SEM) Republished with permission of The Royal Society, from [61]; permission conveyed through Copyright Clearance Center, Inc. (E) This ‘*Callophrys rubi* insect collections SLU, Uppsala’ image has been obtained by the author(s) from the Wikimedia website where it was made available under a CC BY-SA 3.0 licence. It is included within this article on that basis. It is attributed to Vítězslav Maňák. (E) SEM) Republished with permission of The Royal Society of Chemistry, from [62]; permission conveyed through Copyright Clearance Center, Inc. (F) Reprinted by permission from Springer Nature: Springer Netherlands, Encyclopedia of Nanotechnology, [23], 2012. (F) SEM) Reprinted by permission from Springer Nature: Springer Netherlands, Encyclopedia of Nanotechnology, [24], 2012. (G) Reproduced with permission from [64]. (H) This ‘*Teinopalpus imperialis* (male) verso’ image has been obtained by the author(s) from the Wikimedia website where it was made available under a CC BY-SA 3.0 licence. It is included within this article on that basis. It is attributed to Anaxibia.

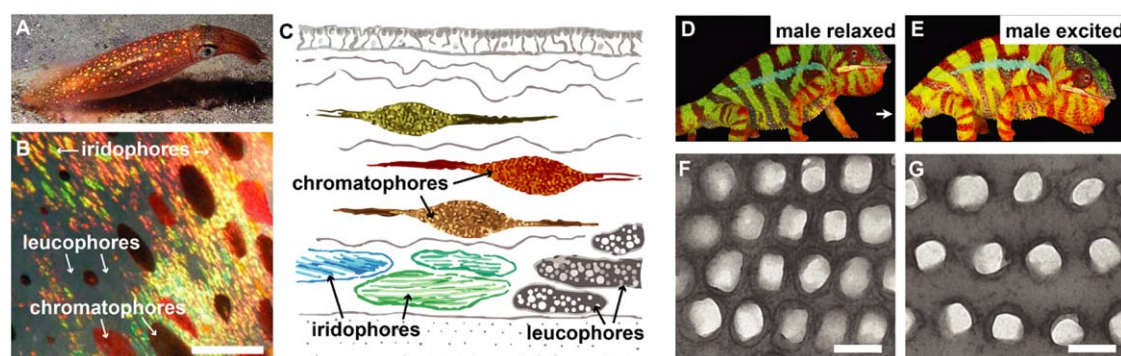


**Figure 4.** Dynamic coloration. (A) The squid *Loligo pealeii* is capable of changing its coloration using three different types of optical elements within its skin. Reproduced with permission from Laptew Productions. (B) and (C) Chromatophores are cells filled with brown, red, and yellow pigments that can expand and contract to cover more or less skin area. Iridophores contain regular layered protein structures that reflect blue, green, yellow, and red colors. Leucophores are cells that are filled with randomly arranged, poly-disperse, highly scattering spheres. They provide a white canvas for the colors of iridophores and chromatophores (scale  $\sim 1 \text{ mm}$ ). (D) and (E) The panther chameleon (*Furcifer pardalis*) native to Madagascar is capable of dynamically changing color to facilitate courtship and male rivalry. (F) and (G) The color change is enabled by controlling the lattice period of a regular arrangement of guanine crystals within the chameleon’s skin tissue (scale 200 nm). (A) Reproduced with permission from Mike Laptew. (B) and (C) Adapted with permission of The Royal Society, from [82]; permission conveyed through Copyright Clearance Center, Inc. (D), (E), (F) and (G) Reprinted by permission from Springer Nature: Nature, Nature Communications, [86], 2015.

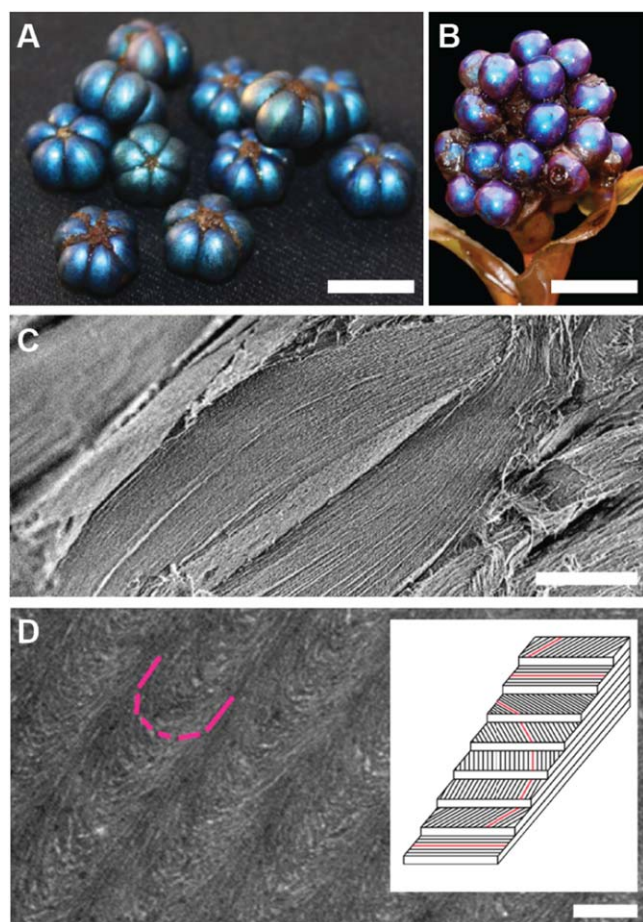


**Figure 5.** Cellulose photonics. (A) Fruits of the plant *Margaritaria nobilis* native to tropical Central and South America (scale  $\sim 1$  cm). (B) Fruits of the plant *Pollia condensata* an African forest species (scale  $\sim 1$  cm). (C) Scanning electron micrograph of a section through a single pericarp cell of *M. nobilis* showing a multilayered architecture (scale  $10\ \mu\text{m}$ ). (D) A transmission electron micrograph of a section of this multilayer architecture reveals the Bouligand arch pattern, which is a clear signature of a helicoidal cell-wall architecture (scale  $250\ \text{nm}$ ). This micrograph was taken from *P. condensata*, which like *M. nobilis* creates color with a regular helicoidal arrangement of cellulose microfibrils in its cells. The inset shows a schematic of the arrangement of the cellulose microfibrils to form a chiral structure with a well-defined pitch. (A) and (C) Reproduced from [31]. CC BY 4.0. (B) and (D) Reproduced with permission from [28].

impose microscopic curvature on such multilayers to create specific optical effects [69, 70]; and *Parides sesostris*, *Callophrys rubi*, and *Teinopalpus imperialis* form continuous three-dimensional periodic networks that act as photonic crystals [71–74]. While the optical working principles of such structures are well characterized and some research has been devoted to the processes underlying their formation [72, 75], a clear understanding of the formation mechanisms remains elusive.

Birds appear to have perfected the art of forming quasi-ordered, and amorphous photonic materials with a short-range periodicity but no long-range order [46, 76–79], an approach to create non-iridescent structural color. Quasi-order has also been found to be employed in some scarab beetles [41].

**2.2.2. Dynamic coloration.** Even more intriguing examples of the ingenuity of biological organisms in harnessing micro- and nanoscale structures for light manipulation can be found in the dynamic coloration of cephalopods and chameleons. Exploiting intracellular pigmentation- and structural coloration-based architectures, cephalopods are capable of changing their skin coloration using a sophisticated combination of chromatophores, iridophores, and leucophores [80–82] (figures 4(A)–(C)). One exciting aspect that we are slowly beginning to understand is the neural control of this dynamic coloration [83]. In contrast to cephalopods, which employ proteins to form their dynamic iridophores [84, 85], chameleons embed regularly organized guanine crystals in expandable skin structures, allowing the animal to vary the resulting structural color by expanding or contracting the tissue [86] (figures 4(D)–(G)).

**2.2.3. Material constituents for biological structural color systems.** The photonic architectures found in tropical fruits, such as *Pollia condensata* and *Margaritaria nobilis* [28, 31], represent inspiring examples of the use of cellulose (figure 5), earth's most abundant biopolymer [87]. These structures intrigue by their nano-scale arrangement of cellulose nano-crystals in a regular helicoidal chiral architecture, which strongly reflects circularly polarized light of the same handedness as the cellulose structure.

In insects, functional biophotonic architectures are mainly composed of chitin, guanine, pterins and melanins [77, 88]. Fish and copepods use regular guanine arrangements [89–91]. Birds have evolved strategies to pattern keratins, melanins, and carotenoids in their feathers [77, 92] and in addition use collagen structures in their skin [45], similar to some of the color-generating structures in mammals [93]. Mollusks have found ways to extracellularly structure calcium carbonate, and intracellular proteins, such as reflectin [32, 85, 94]. Finally, plants and insects apply a variety of waxes (in addition to the cellulose and chitin discussed above) to create photonic architectures [27, 95].

### 2.3. Synthetic structural color—exemplary man-made materials and devices

In this section, we complement the previous discussion of representative examples of biological structural color with a perspective on exemplary man-made materials and devices that involve structural color. As in the previous section, we emphasize the color-generating structures, dynamics, and material constituents.

**2.3.1. Silk inverse opals—modulation of photonic lattices with water and light.** Opals and inverse opals consist of close-packed, nano-scale, high refractive index colloids within a low-index matrix, or low refractive index pores within a high-index matrix, respectively. Opal- and inverse opal-like photonic architectures can be found in nature [21, 96–98], and have also been synthetically fabricated using a wide



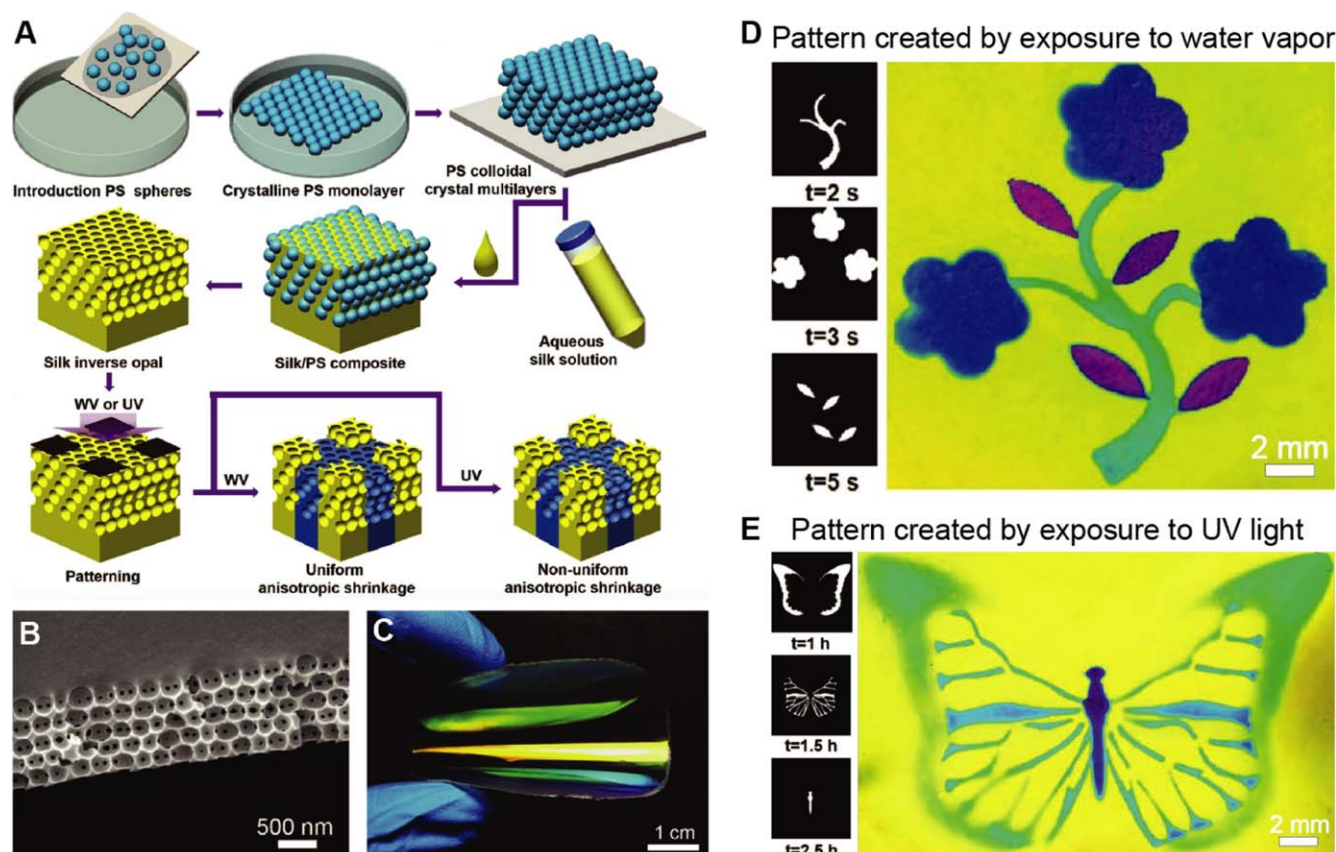


**Figure 6.** Painting patterns in silk inverse opals. (A) The fabrication process consists of the deposition of a direct opal by repeatedly scooping up polystyrene colloid monolayers from an air-water interface (top row), before infiltrating the opal with aqueous silk solution, followed by drying and removal of the of the colloids with solvent to obtain the inverse opal (middle row). The inverse opal is then patterned by local exposure to water vapor or ultraviolet light. (B) Scanning electron micrograph of a silk inverse opal. (C) Photograph of film as it is bent, showing its excellent flexibility. (D) Exposure of a silk inverse opal to water vapor through different porous stencil masks is used to enable a multicolor pattern. (E) Similar effects can be achieved by exposing the silk to UV light through patterned photomasks. [109] John Wiley & Sons. © 2017 WILEY-VCH Verlag GmbH & Co. KGaA, Weinheim.

variety of strategies [98–107]. One common strategy for fabricating inverse opals is to create a colloidal crystal of polymer spheres, casting a matrix material onto the crystal, and subsequently removing the spheres [108].

This method has recently been applied to creating large-area, highly ordered silk inverse opals [109] (figure 6). Silk, a biopolymer sourced in industrial quantities from domesticated silkworms, is an excellent optical material due to its transparency, low surface roughness, nanoscale processability, and mechanical durability [110, 111]. It has been used to form many useful optical components, including photonic crystals, microlens arrays, color-tunable diffraction gratings, and even random lasers [112–114]. Silk is usually processed in aqueous solutions. Control over the solution chemistry and water evaporation kinetics allows for tuning the material's nanoscale morphology to tailor its macro-scale properties. The silk inverse opals are iridescent and highly flexible. After formation of the inverse opal, the structural properties of the silk can be modified through exposure to water vapor or ultraviolet light [115, 116]. This allows for controlled modulation of the photonic crystal's lattice parameters to inscribe structural color variations and patterns into the

inverse opal films. This represents a promising new strategy for facile creation of stimuli-responsive photonic materials with tunable structural color, which could be beneficial in biosensors, including direct antigen-detection in colorimetric immunosensors [117].

**2.3.2. Full-color reflective MEMS displays.** Microelectro-mechanical systems (MEMS) are microscale devices that contain both electrical and mechanical functionality. Advanced MEMS micromachining approaches have unique advantages for the creation of miniaturized optical devices (called micro-opto-electro-mechanical systems, short optical MEMS or MOEMS). The precision mechanics of MEMS combined with industrial surface micromachining processes that are compatible with optically relevant materials have enabled a diverse range of rapidly reconfigurable, tunable, micro-optical elements, including lenses, mirrors, and filters. These components have made significant impact in a wide variety of commercial applications [118–120]. Digital micro-mirror devices—invented at Texas Instruments over 35 years ago—are an example of MEMS based optical systems [121], which

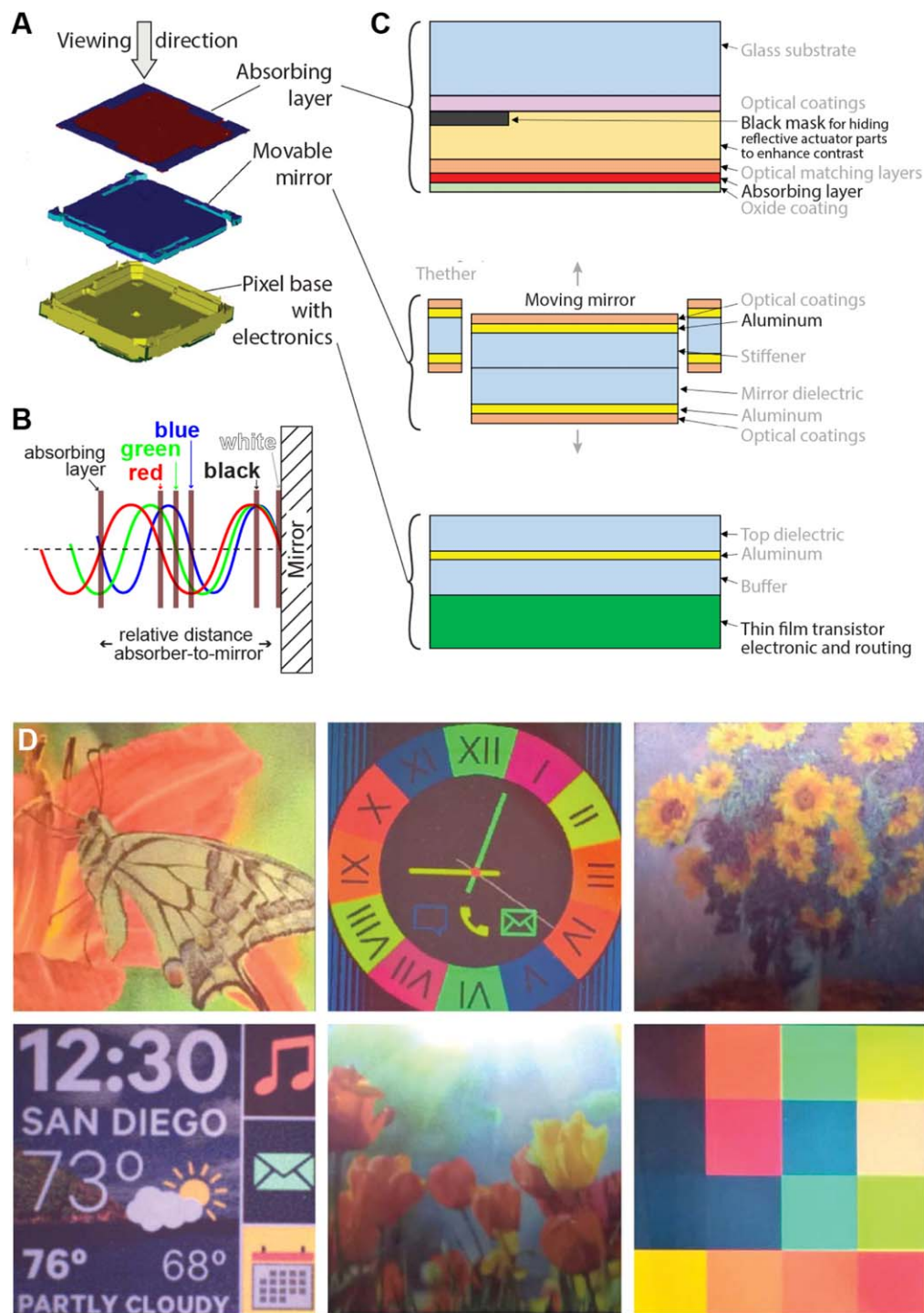


**Figure 7.** A reflective MEMS-based single mirror interferometric display. (A) Overview of the device layout showing the fixed absorbing layer, the moving mirror, and the pixel base. (B) Schematic depicting the display's working principle. Precise positioning of the absorber in the standing wave field enables controlled spectrally-selective absorption. (C) Detailed schematic of the pixel architecture, fabricated in an elaborate surface micromachining process. (D) Full color images displayed by a  $483 \times 483$  pixel array. (A), (C) and (D) © [2017] IEEE. Reprinted, with permission, from [124]. (B) Reprinted with permission from ref [123], OSA.

have tremendous technological and commercial value in digital projection displays and other applications [122].

Newer MEMS display technologies specifically make use of structural color to enable energy-efficient, large-area reflective displays that eliminate the need for device-internal light sources, thereby drastically reducing energy demand. One of the more

recent examples of this type of technology is the single mirror interferometric display by Qualcomm [123, 124]. Each of the display's pixels consists of a thin layer of a light-absorbing molybdenum chromium alloy suspended over an aluminum mirror (figure 7(A)). In this geometry, incident light interferes with light that reflects off the mirror, which results in standing

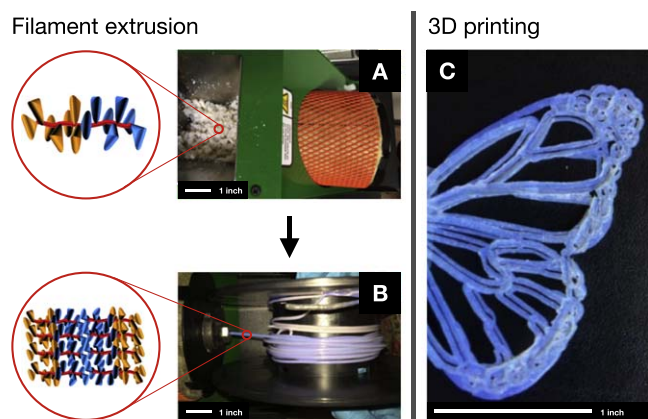


**Figure 8.** 3D-printing with structural color. (A) Colorless block copolymer granules are loaded in the filament extruder. (B) Emergence of structural color during filament extrusion, caused by molecular-scale self-assembly of the polymer (inset diagrams suggest molecular structure). (C) The same filament 3D printed via fused deposition modeling in the shape of a butterfly wing. Reprinted with permission from [125]. Copyright (2017) American Chemical Society.

wave patterns. The position of extrema and zeros in the light field varies with the light wavelength, which can be exploited to induce spectrally selective absorption via controlled positioning of the absorbing layer (figure 7(B)). If the absorber is placed at a location of maximally varying amplitude in a specific wavelength's standing wave pattern, light of that particular wavelength is absorbed, while light in different spectral ranges can pass. In the actual device, positioning of the absorbing layer within the standing wave field is achieved through moving the pixel's mirror using the integrated high-precision MEMS actuator infrastructure that is controlled by a thin-film transistor circuit within each pixel. The elaborate pixel infrastructure, shown schematically in more detail in figure 7(C), is produced in a series of surface micromachining steps. Prototype devices can switch their pixels at 120 frames per second, display 16 primary color states, and have a display density of 346 points per inch (figure 7(D)). Since these devices do not require internal illumination, they only consume energy to switch and hold the displayed information, promising significantly higher energy efficiency than current displays. In principle, the fabrication process is amenable to flexible substrates, which in the future could provide avenues for flexible reflective display designs that could be used in optically adaptive, color- and information-changing wearables.

**2.3.3. 3D-printing with block copolymer-based structurally colored filaments.** 3D printing, in particular fused deposition modeling, has significantly gained in popularity in recent years, both in a professional manufacturing context and as a hobbyist tool. Commonly, colored parts are created by mixing a pigment dispersed within the polymer of interest. More recently, that coloration has instead been achieved by making use of structural color [125]. As shown in figure 8, the polymer of interest is a block copolymer, which self-assembles during the filament heating and extrusion process to create an ordered nanostructure that exhibits structural color. This filament can then be used for 3D printing. Adjusting the molecular weight of the BCP alters

the dimensions of the nanostructure, which in turn alters the wavelength of reflected light.

### 3. Processes that drive the formation of structurally colored materials

#### 3.1. Processes—preliminary comments

In the preceding sections, a few representative examples for biological photonic systems and man-made materials that rely on structural color were chosen to emphasize three important process attributes that are the focus of this review.

- (1) Control over the material structure to allow for a wide variety of architectures,
- (2) Control over the local material composition, and
- (3) Control over the materials' dynamic properties.

These examples show that biological and synthetic processes have unique characteristics that determine 'what goes where' during the structure formation. In this review, we chose to specifically focus on processes that create materials with structural color for several reasons.

- (1) The structural outcome is immediately apparent.
- (2) The structures at the origin of structural color have a varying but controlled degree of order on distinct length scales.
- (3) The underlying formation processes must be robust, as can be seen in the impressive degree of reliability with which biological microstructures are realized.
- (4) Many of the prominent biological structurally colored materials are based on easily handled, abundant biomaterials, including cellulose, chitin, and calcium carbonate, which readily lend themselves to the full spectrum of materials analysis techniques.
- (5) Hierarchical designs are prevalent, and often each component of the hierarchy adds to the material's functionality.
- (6) The perceived color is a proxy for the structures' optical qualities; visual / spectral assessment of their optical characteristics on the macro- and microscale provides a convenient pathway to assessing changes that might be imparted by modifying the formation processes.
- (7) Understanding processes that lead to the formation of structurally colored materials could help to identify avenues for realizing synthetic analogs for a wide range of optical applications.

#### 3.2. Process classification

The controlled formation of morphologies that induce structural color in biological and in synthetic material systems usually depends on the interplay of several processes. In this review, we broadly classify structure formation processes into the following categories (figure 9).

- *Additive processes:* material is added sequentially to an existing structure. In biology, this includes the secretion of chitin in insect cuticles and the deposition of calcium





Figure 9. Process categories.

carbonate in mollusk shells. Examples of synthetic additive processes are the formation of thin metal oxide layers on an optical filter by atomic layer deposition or chemical vapor deposition, as well as the 3D-printing of complex micromorphologies.

- *Subtractive processes*: an initial material volume is modified by spatially selective removal of material. In biology, this includes the degradation of insect cuticles (for instance occurring during ecdysis, or the digestion of actin scaffolding structures during the formation of butterfly wing scales). A plethora of subtractive processes are used in synthetic manufacturing, ranging from metal machining on larger scales to a variety of micromachining approaches that employ physical and chemical etching procedures for structure formation on smaller length scales.
- *Continuous processes*: material with the desired shape and structure is continuously extruded or drawn. We consider the biological growth of hairs, bristles, and scales broadly as such a continuous process. A synthetic analog might be found in the extrusion of layered polymer architectures with controlled internal morphology or the drawing of photonic crystal fibers.
- *Net-shape processes*: an initial mass of material is deformed until it gains the final desired shape, without a significant change in the material's initial mass. A biological example for such processes are anisotropic cell deformations occurring in flower petal formation. Molding of nano-scale surface structures by nano-imprinting, or casting and curing onto a template, are examples of shaping processes in synthetic manufacture.
- *Assembly processes*: building blocks with desired base characteristics are assembled into complex functional material architectures. If this happens autonomously, just driven by the interactions of the unit elements and their surrounding medium, the process is termed 'self-assembly'. The formation of regular three-dimensional photonic structures in butterfly and beetle scales is likely driven in part by self-assembly. Synthetic opaline and inverse opal photonic crystals are usually formed through self-assembly.

We note that it is not necessarily easy or straightforward to fit natural processes into these specific categories. This is primarily due to the fact that in nature many of these processes occur in parallel and are difficult to separate neatly, while in synthetic manufacture processes occur primarily in sequence. Additionally, the classification of a process depends on where the system boundaries are defined; when

viewed in different contexts, a single physical phenomena may be best described by different categories. However, the classification that we employ here provides benefits for the comparison between biological and synthetic structure formation processes and enables us to propose potential strategies for advancing human manufacturing concepts by gaining inspiration from biological processes.

### 3.3. Biological processes

In broad terms, processes that enable the formation of biological structures have one of three purposes.

- They contribute to the generation of constituent materials;
- They are involved in organizing these materials into structures;
- They facilitate clean-up and/or continuous maintenance of the final structure to ensure persistent functionality.

These processes may occur sequentially, but often they are integrated with some degree of overlap.

The generation of material constituents is prescribed by the organism's genetic code: information encoded in DNA is transcribed into RNA, which then is translated into a protein by assembling amino acids at a ribosome [126–128]. The protein must then move via some method of cellular transport to a new location inside or outside the cell [129–131]. At its new location, the protein may interact with other molecules in its environment, pulling, pushing, and bending the aggregate structure into shape [132]. However, non-protein materials (carbohydrates, lipids, minerals, purines, and pterins) are not produced directly via gene expression [128]. Instead, these materials are gathered, modified, and assembled by a collection of enzymes. Since enzymes are proteins, the organism's genes still control this palette of constituent materials, albeit more indirectly. In some cases, the material is produced at the site of its final destination [133, 134]; otherwise, it is transported to that destination, where it integrates with the aggregate structure [132]. Thus a unique aspect of biological growth as a fabrication process for micro- and nanostructured materials is that, in general, the structure-forming cell synthesizes the materials and shapes the forming structures all within itself or in a region closely surrounding the cell.

Processes contributing to biological structure formation can be broadly classified within the categories outlined in section 3.2. Because cells typically produce their own raw material needed for structure formation, all biological processes have at least some stages that can be described as 'additive': on-site synthesis, secretion, and various methods

of intracellular transport are all indicative of additive processes. Reciprocally, subtractive processes are rarer in biological structure formation; when they do occur, their main function tends to be removal of a mold that has supported structure formation. Subtraction of temporary material is generally achieved by degradation, such as enzymatic digestion [135–137]. In various cases, materials can be formed in a continuous fashion, by linearly propagating a given shape: examples are lipid extrusion through a pore or linear growth of cytoskeletal elements; examples of larger macro-structures are bristles and feathers [138–143]. We also find that an abundance of processes in nature shape a given net volume of material using other elements, such as membranes or biological scaffolds, as a template or mold [144]. Lastly, a wide variety of intermolecular forces contribute to the assembly of various materials.

While we generally know how to identify the material constituents and structural components that impart function, we know little about how these materials are formed by living organisms. Control and regulation of multiple processes across various length scales are required to form the material morphologies that enable specific structural color effects. Structure formation has to be controlled from the nano- to the macro-scale to enable the harnessing of different light–matter interaction principles, such as absorption and fluorescence (quantum-optical regime), diffraction and interference (wave-optical regime), and refraction or lensing (ray-optical regime); yet, our understanding of biological structure control and regulation is still in its infancy. In fact, many of the biological structure formation processes that we discuss below are, at best, incompletely understood.

In the following section, we describe the phenomena that have been observed during the formation of structurally colored materials in different organisms. In addition—where possible—we outline hypotheses that have been formulated regarding the underlying physical phenomena. We hope to capture the ‘status quo’ of the current scientific understanding of the formation of material structures used in nature to manipulate light, and specifically focus on structures in butterfly wing scales, cephalopod iridophores, bird feathers, and flower petal surfaces as representative examples.

**3.3.1. Diversity of processes. Example, scale formation in lepidopterans:** the formation of scales on the wings of Lepidoptera (butterflies and moths) is a complex process that has interested scientists for well over a century [145, 146]. Although the wing scales of butterflies and moths develop during metamorphosis, the tissue for the wing already starts forming as an ‘imaginal disc’ in the larval stages [147, 148]. As the larva initiates pupation, the disc initiates a dramatic pace of growth. The wing tissue begins to grow and thicken, after which differentiated scale precursor cells become readily identifiable by their larger size (figure 10(A)).

A number of historical and recent seminal studies have provided phenomenological insights into scale formation once the final stage of morphogenesis—the pupation—has started [15, 40, 148, 150–154]. This provides the basis for identifying the scale components relevant to structure formation and for forming hypotheses about their interactions and the mechanisms

leading to the formation of the final chitin-based scale architectures. Based on these studies, we know that each scale is formed by a single scale cell that extrudes a scale protrusion, which is seated in a socket formed by an adjacent socket cell. Furthermore, we can establish the following (rough) timeline for scale development. In this phenomenological overview of scale formation, we state the developmental stages in percentages relative to the overall pupation duration; this duration changes from species to species and depends significantly on exterior conditions such as temperature [155].

At around 15% of pupal development, the epithelial cells have aligned on the wing membrane. Socket and scale cells have formed from a common mother cell (figure 10(B)). At this point the scale cell begins to build a protrusion that is to become the scale (figure 10(C)). The membrane of the scale cell is extended by actin filaments, pushing through the middle of the toroid-shaped socket cell in the fashion of a continuous process. As the scale cell reaches about a third of its final length at around 25% of pupal development, the actin filaments begin to assemble in regularly spaced bundles running the length of the scale; these bundles are essential in the following ‘netshape’ stages of molding the membrane [148]. The scale protrusion is still circular (figure 10(D)). At around 30% of pupal development, regular F-actin filament structures are apparent in the scale protrusion, which is in the process of flattening (figure 10(E)). Soon after, stationary undulations appear across the top surface of the scale, lining up with the actin bundles (figure 10(F)). Although the actin has been demonstrated to be crucial to the formation of the membrane mold [148], the precise physical phenomena behind the actin-membrane interactions are unknown. While buckling phenomena have been hypothesized to be responsible for the formation of undulations on the scale cell surface [15], the mode and control of this buckling have not been elucidated.

With the mold in place, the cuticle (chitin fibrils in a matrix of supporting proteins) begins to appear to form a single-cell exoskeleton (figure 10(G)). The polymerization of chitin is enabled by an enzyme, chitin synthase, which is reported to operate at the apices of a membrane [156–158]; which, in the case of the wing scales, are located along the tops of the ridges. The cuticle is thus secreted in an additive fashion; in addition to the molded configuration, the surface takes different morphologies, likely due to internal forces within the cuticle aggregate [15, 159], which may be thought of as self-assembly. During the production of chitin, the membrane template does not remain fixed, but rather retracts from its original position. The chitin is then sclerotized and the cuticle is hardened. At around 60% of pupal development, the scale ridges show pronounced features and the cell cytoplasm appears to retract and degrade (a subtractive process) (figure 10(H)). At this point, substantial amounts of chitin have been secreted at the apices of pleats in the top surface of the scale cell membrane (figure 10(I)). It is likely that the membrane and cell cytoplasm retraction contribute to the final shaping of the end product: a non-living scale.

This growth of butterfly scales exemplifies how the cell’s plasma membrane can function as a template mold, while the internal actin skeleton in turn appears to structure this mold;

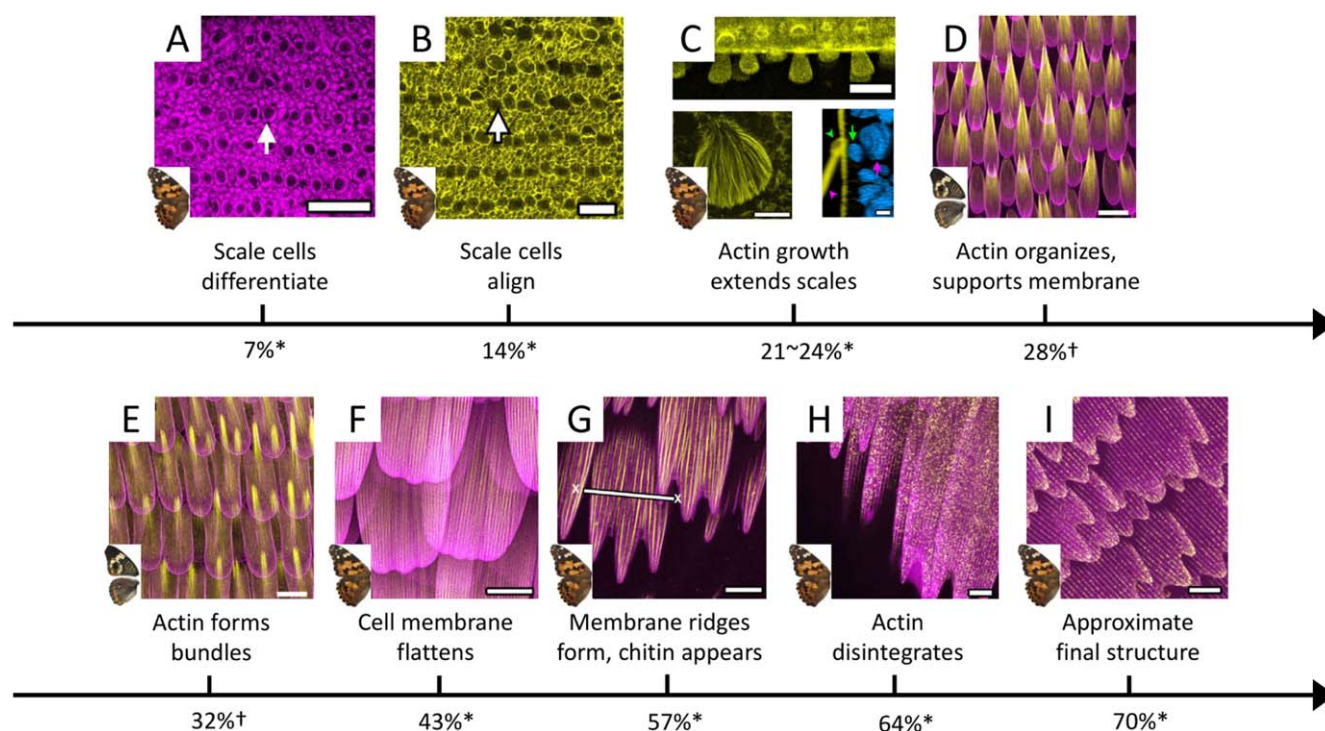


**Figure 10.** Timeline of scale structure formation in two butterfly species. Percent duration of pupation in *Vanessa cardui* denoted by \*; *Junonia coenia* denoted by †. Magenta shows plasma membrane, and yellow shows actin. (A) After the caterpillar pupates, specific cells on the wing tissue differentiate into scale precursor cells (large cells as denoted by arrow) (scale 30  $\mu\text{m}$ ). (B) The precursor cells align in distinct rows that lead to the tissue-wide organization of the wing scales (scale 30  $\mu\text{m}$ ). (C) *Top*, Scale cells begin to grow actin and extend away from the wing surface (scale 15  $\mu\text{m}$ ); *bottom left*, close up of actin growth (scale 5  $\mu\text{m}$ ); *bottom right*, cross section of yellow scale cell actin and blue scale cell nucleus (pink arrows), as well as the supporting socket cell structures (green arrows) (scale 5  $\mu\text{m}$ ). (D) As the scale cell is extended, actin begins to take on a more regular order, and supports the growing membrane (scale 15  $\mu\text{m}$ ). (E) Actin bundles further organize into regularly spaced bundles (which will later support membrane undulations) (scale 15  $\mu\text{m}$ ). (F) The cell membrane flattens and maintains the actin in their bundles (scale 15  $\mu\text{m}$ ). (G) The cell membrane then begins to 'wrinkle' in a controlled fashion consistent with the actin bundles; around the same time, chitin secretion accelerates (scale 15  $\mu\text{m}$ ). (H) Chitin expression continues; the actin disintegrates (scale 15  $\mu\text{m}$ ). (I) Toward the last third of the pupa stage, the scale cell begins to appear in its final structure; the cuticle hardens, pigment appears, and the cell dies leaving behind the cuticular scale (scale 15  $\mu\text{m}$ ). (Fluorescence) Reprinted from [148], with permission from Elsevier. (Wings) Reproduced with permission from [149].

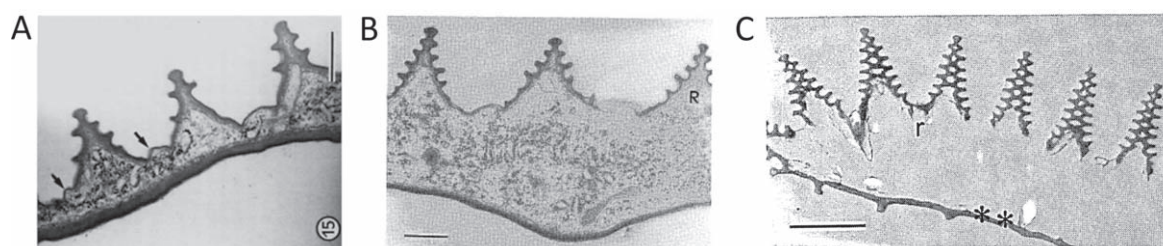


**Figure 11.** Cross sections of scales of *Colias eurytheme* at different stages of development. (A) Developing scale of *C. eurytheme* with ridges clearly defined, with cuticle being expressed at the lower lamina and the ridges, but not at the windows (arrows) (scale 0.5  $\mu\text{m}$ ). (B) Developing scale of *C. eurytheme* with multiple lamellae developing on the ridge cuticle (scale 0.5  $\mu\text{m}$ ). (C) Mature scale cell of *C. eurytheme*, with lower lamina (\*\*), ridges, and multiple lamellae formed on the ridges (scale 1  $\mu\text{m}$ ). (A) [40] John Wiley & Sons. © 1994 Wiley-Liss, Inc. (B) and (C) Reprinted with permission from ref [15], OSA.

yet it also illustrates how the other modes of production such as the secretion of chitin (additive processing), and the retraction of the cell cytoplasm and membrane (subtractive processing) are utilized in biological structure formation.

As the result of this complex structure formation process, all scales have an undulating upper surface of ridges connected by cross-ribs (figure 11); these cover a lower lamina, with intermittent trabeculae connecting the upper and

lower portions. Lepidopterans follow this basic blueprint but variations on this theme reveal a wide range of geometries that achieve structural color (figure 3). For instance, a variety of butterflies and moths forms regular perforated laminae in the scale interior, which act as multilayer reflectors. Layered photonic architectures are prevalent in nature and besides their just mentioned presence in the scales of many lepidopteran species, are found in the cuticles of beetles and



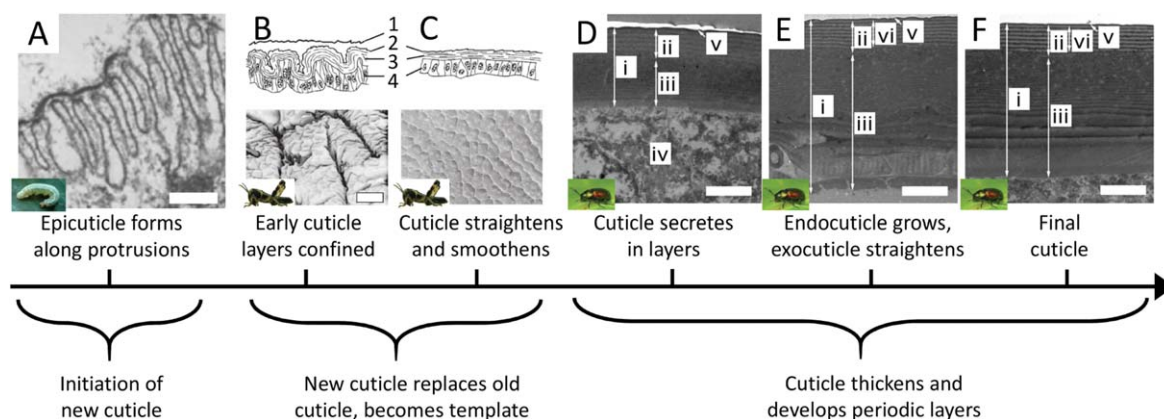


**Figure 12.** Secretion of cuticle multilayer. Although the research on cuticle growth is spread among various arthropods and life cycle stages, we can gather an overall sense of cuticle formation. (A) To begin growing a new cuticle, microvilli of epidermal cells secrete the outermost epicuticle (scale  $0.5\ \mu\text{m}$ ). (B) The young, unhardened cuticle grows to a surface area larger than the older cuticle, causing many folds to develop (shown here in larval *Schistocerca gregaria*); (1) old molting cuticle, (2) epicuticle, (3) procuticle, (4) epidermis (scale  $3\ \mu\text{m}$ ). (C) After molting, the new cuticle is allowed to straighten and smooth as it takes the place of the older cuticle, becoming in effect a template for future layers (*S. gregaria*). (D) As the procuticle (exocuticle and endocuticle) begin to grow, cyclic growth patterns result in alternating bands of distinct chitin arrangements (shown here in imago of *Gastrophysa viridula* after ecdysis; (i) dorsal elytral cuticle; (ii) exocuticle; (iii) endocuticle; (iv) hemolymph space under the cuticle; (v) epicuticle; (vi) reference length (scale  $1\ \mu\text{m}$ ). (E) With time, the cuticle grows, and the layers may undergo slight changes in uniformity and electron density (*G. viridula*) (scale  $1\ \mu\text{m}$ ). (F) The fully developed cuticle of *G. viridula* (scale  $1\ \mu\text{m}$ ). (A) Reprinted from [161], Copyright (1979), with permission from Elsevier. ((A) inset) Reproduced with permission from [68]. ©2000 University of Florida IFAS. (B) and (C) Reproduced with permission from [162], Cambridge University Press. ((B) and (C) insets) Reprinted by permission from Springer Nature: Springer, Applied Entomology and Zoology, [169], 2008. ((D) to (F)) Reprinted by permission from Springer Nature: Nature, Scientific Reports, [160], 2017. ((D) to (F) insets) Adapted with permission of The Royal Society, from [170]; permission conveyed through Copyright Clearance Center, Inc.

spiders, the scales of fish, the skin of cephalopods and the waxes of plants [20, 35].

**Multilayer secretion:** in general, layered biological morphologies that cause structural coloration appear to conform to a support structure, which operates as a template or a mold to help define the final material conformation. This approach commonly occurs in carbohydrate structures (such as chitin and cellulose) which tend to be secreted along a surface that defines its shape. Although the information available on cuticle formation is spread over diverse organisms, we can build an approximate, representative framework of the processes involved [160–166]. For instance, the leaf beetle *Gastrophysa viridula* secretes a chitin surface like its fellow arthropods, the butterflies; unlike them however, it forms the cuticle above tissue rather than on individual cells, and yet it also deposits in layers, each surface supporting the last [160] (figure 12). Cellulose too is secreted, forming the iridescent, pixelated reflectors found on the fruits of *Pollia condensata* and *Margaritaria nobilis* [28, 31]; in these plants the deposited cellulose nanocrystals form helicoidal structures, which give the material its unique abilities to strongly reflect circularly polarized light. This secretion likely involves additional physical processes that result in regular chirality. Curiously, similar physics might be at play in the formation processes of the helical circularly-polarized light reflecting cuticle nanoarchitectures found in some beetles, which have been compared to cholesteric liquid crystal structures [95, 167].

Minerals, which are often deposited alongside with organic materials [171, 172], can also be formed into a layered photonic structure as found in the case of blue-rayed limpets [32]. In general, mollusk shells are formed by

calcification underneath the periostracum, a thin elastic membrane at the growth edge that is secreted by the mantle and links it to the forming shell. The stiffness differences between the calcified material and the mantle can lead to various shell configurations [173, 174], but the impact on the microstructure is still not well understood.

Other layered photonic structures, notably iridophores, are made by filling a mold rather than coating a template-like surface. In cephalopods, the protein reflectin fills a multilamellar membrane (discussed further below). Guanine crystal structures are likewise formed by filling intracellular membranes, in some cases with further support from fibrous structures [89, 175]. Two recent studies on copepods and scallop eyes have demonstrated that these small marine organisms can generate either highly regular hexagonal or square crystal elements that are then assembled into more complex architectures in their soft tissues to create specific optical effects [91, 176]. The extremely regular shape and size of guanine crystals are a clear sign of the exquisite control that the two organisms can exert on the underlying formation processes.

**Mechanical stress deformation:** mechanical stresses can modify the morphologies of secreted flat layers, leading to microscale undulations and patterns that cause light diffraction thereby producing color. In many situations, these mechanical stresses occur in response to material growth, in turn affecting the growing structures. In some butterfly species, pronounced chitin structures develop on the ridges, such as the Christmas tree-like cross-sectional pattern in *Morpho* species. Ghiradella proposed that lamellae formation in butterfly scales occurs by buckling [15]. The notion of buckling poses an interesting question for mechanical stresses

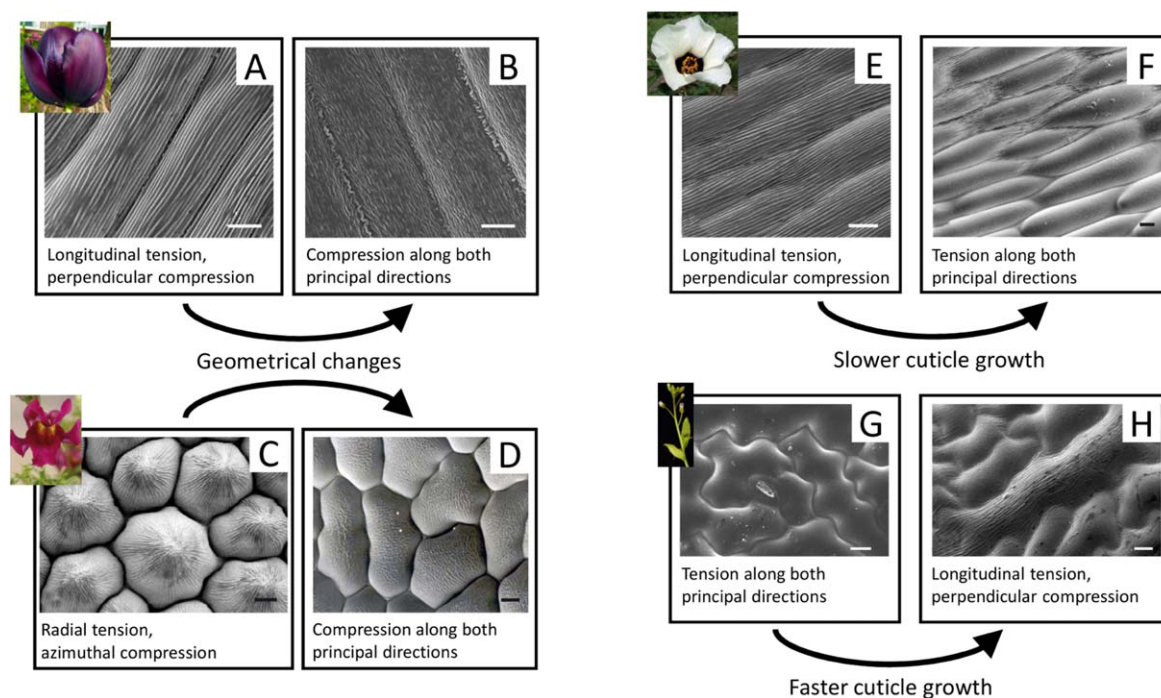


**Figure 13.** Proposed models of cuticle pattern formation in petals and leaves. *Geometrical changes can regulate ridge morphology*: (A) in the ‘Queen of the Night’ tulip, parallel ridges are consistent with wrinkles that form under longitudinal tension and compression in the perpendicular direction. (B) In the non-iridescent petals of the tulip, minimal geometrical changes are capable of changing the stress conditions causing disorder in ridge orientation. (C) Similarly, the radial ridges in the snapdragon (*Antirrhinum majus*) are consistent with radial tension and azimuthal compression. (D) Mutations that lower the cone protrusion of these cells decrease the radial tension and introduce disorder in ridge material. *Cuticle growth rates affect ridge formation*: (E) in the dark iridescent center of *Hibiscus trionum*, parallel ridges also form due to the particular anisotropic conditions. (F) In the transition to non-iridescent white, the cellular cuticles are smooth, consistent with models that demonstrate slower cuticle growth, despite similar geometries. (G) The opposite is proposed to occur in the leaves of *Arabidopsis thaliana*, whose wild type is smooth. (H) When the organism is modified to increase cuticle growth, ridges appear. (Scale for all, 10  $\mu\text{m}$ .) Adapted with permission of The Royal Society, from [182]; permission conveyed through Copyright Clearance Center, Inc.

in biological materials, because of the various approaches taken to understand buckling [177]. Some of these different frameworks include: quantifying residual stresses due to the growth of a material [178], prestrain of a substrate layer that supports a thinner layer [179, 180], and comparisons between stretching energies and substrate stiffness [181].

On the macroscale, mollusk shell growth provides an interesting case study for how stresses between soft mantle tissue and hard secreted shell determine the forming shell morphology. The mollusk’s growing mantle, which deposits new shell at the growth edge, is constrained in its expansion by the already deposited shell. This leads to characteristic mantle deformations, the shape of which is then ‘frozen’ into the forming shell morphology as the mantle secretes the shell mineral [173, 174]. However, it is not yet known exactly if and how mechanical stresses and strains occurring between soft secreting cells and tissues and the harder secreted materials manifest themselves at the micro- and nanometer scale of the lamellar morphologies in structurally colored mollusks and other animals.

Recent models suggest that striated flower petal architectures, which are implicated in structural color generation, may result from mechanical deformation phenomena during petal development (figure 13). The petal’s growth and associated mechanical boundary conditions have been characterized according to cuticle growth rate and developing principal

stretches along two axes [182]. Various combinations can lead to tension in both directions (promoting smooth cells), compression in both directions (promoting disordered wrinkles), or compression in one direction and tension in another (promoting organized wrinkles). By regulating the initial geometry of the cell and the ensuing cuticle growth rate, flower petals may produce ridge patterns that cause diffraction as the origin of their structural coloration [183, 184].

Mechanical stresses and buckling thus may be instrumental in creating some of the morphologies found in structurally colored materials. However, to our knowledge, the role of mechanical stresses have not yet been verified *in situ* during the actual development of any structurally colored biological material. Nevertheless, careful assessment of material morphology and boundary conditions during the formation of specific photonic structures (such as striations on flowers), combined with mechanical modeling, could provide deeper insights into the role of mechanical effects during their growth.

*Variety in two-dimensional structures*: in order to achieve material structures with two-dimensional periodicity, nature draws from a wide variety of processes (figure 14). Regularly packed collagen fibers in the coloration structures of various birds and mammals are hypothesized to form by self-assembly, which in the case of collagen is driven by inter-fiber physics [45, 93, 185–187] (figures 14(A)–(C)). Other biological 2D periodic material structures are highly

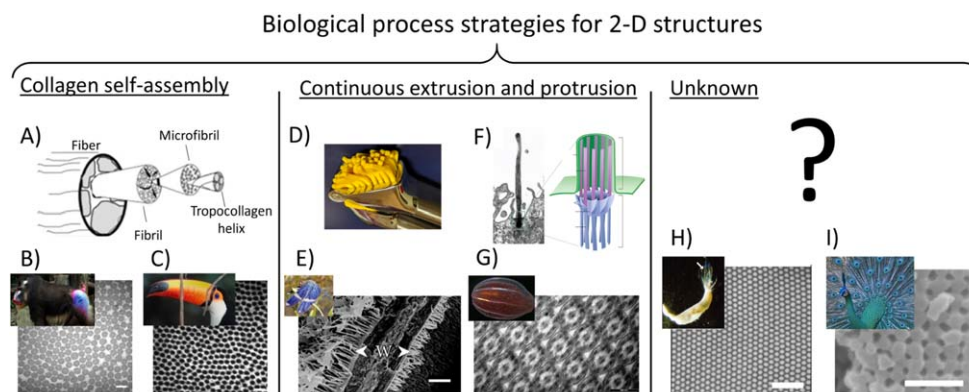


**Figure 14.** Biological process strategies for 2D structures. (A) Collagen fiber assembly begins with the self-assembly of the tropocollagen helix that is organized into microfibrils and fibrils, which then form a fiber. The direction, size, and spacing of these fibers are critical to the structural coloration. Collagen fibers yield 2D quasi-order in (B) the blue skin of *Mandrillus sphinx* (scale 250 nm) and (C) the blue skin around the eye of *Ramphastos toco* (scale 200 nm). (D) In extrusion, material is forced through a specified shape (as when clay is forced through a press). (E) Wax pillar forests extrude through pores in the cuticle of the dragonfly *Zenithoptera lanei* (scale 2  $\mu$ m). (F) Cilia grow from cells due to the growth of nine microtubules protruding from the cell surface (cilia exist in a wide variety of cells; shown here is a cilia in the canary brain together with a microtubule schematic) (scale 1  $\mu$ m). (G) In the comb-jellyfish *B. cucumis*, cilia are grown immediately next to one another, resulting in bright rainbow colors as they beat (scale 200 nm). (H) The mechanism driving the 2D order of the cylindrical voids in the chitinous setae of *Pherusa* is unknown (scale 2  $\mu$ m). (I) Likewise, we do not yet know the physics that regulates melanin granule size and organization in avian feathers, such as those on *Pavo muticus* (scale 500 nm). (A) Reprinted from [192], Copyright (2003), with permission from Elsevier. (B) This ‘Mandrill at Singapore Zoo’ image has been obtained by the author(s) from the Wikimedia website where it was made available by Avala under a CC BY 2.0 licence. It is included within this article on that basis. It is attributed to Robert Young. ((B) SEM) Reproduced with permission from [93], The Journal of Experimental Biology. (C) This ‘Toco toucan (*Ramphastos toco*) adult’ image has been obtained by the author(s) from the Wikimedia website where it was made available by Charlesjsharp under a CC BY 4.0 licence. It is included within this article on that basis. It is attributed to Charles J Sharp. ((C) SEM) Reproduced with permission from [45], The Journal of Experimental Biology. (E) Reprinted from [189], Copyright (2015), with permission from Elsevier. ((F) Singla) From [193]. Reprinted with permission from AAAS. ((F) Alvarez-Buylla) Republished with permission of Society for Neuroscience, from [Primary Neural Precursors and Intermittent Nuclear Migration in the Ventricular Zone of Adult Canaries, Arturo Alvarez-Buylla, 18, 3, 1998]; permission conveyed through Copyright Clearance Center, Inc. ((F) Anderson) Republished with permission of Rockefeller University Press, from [The three-dimensional structure of the basal body from the Rhesus monkey oviduct, Richard G. W. Anderson, 54, 2, 1969]; permission conveyed through Copyright Clearance Center, Inc. ((F) Preble) Republished with permission of Genetics Society of America, from [Extragenic Bypass Suppressors of Mutations in the Essential Gene BLD2 Promote Assembly of Basal Bodies With Abnormal Microtubules in *Chlamydomonas reinhardtii*], Andrea M. Preble, 157, 1, 2001]; permission conveyed through Copyright Clearance Center, Inc. (G) Reproduced with permission from Kevin Raskoff. ((G) TEM) Reprinted figure with permission from [188], Copyright (2007) by the American Physical Society. (H) Reproduced with permission from Andrew Parker. ((H) SEM) Reprinted figure with permission from [139], Copyright (2009) by the American Physical Society. (I) This ‘*Pavo muticus* - Hai Hong Karni’ image has been obtained by the author(s) from the Wikimedia website where it was made available by JJ Harrison under aCC BY-SA 3.0 licence. It is included within this article on that basis. It is attributed to JJ Harrison. ((I) SEM) Reproduced with permission from [191]. Copyright (2003) National Academy of Sciences, U.S.A.

suggestive of continuous processes. For example, the repeated axial symmetry in the cilia of the comb-jellyfish are composed of a central axoneme surrounded by microtubules, which are frequently involved in cilia structures and other cell protrusions [188] (figures 14(F), (G)). Other examples of continuous processes are found among members of the Odonata, who produce a wax pillar forest (with a low degree of order, yet two dimensional) via continuous extrusion through cuticle pores [138, 189, 190] (figures 14(D), (E)).

Melanin structures in some avian feathers result in two-dimensional structurally colored morphologies (figure 14(I)). During their formation, regular melanin granule structures must be generated and assembled in an orderly fashion [191, 197]. Although some older studies provide hints about the internal timeline of granule location [198], the underlying processes and related physics are generally unknown.

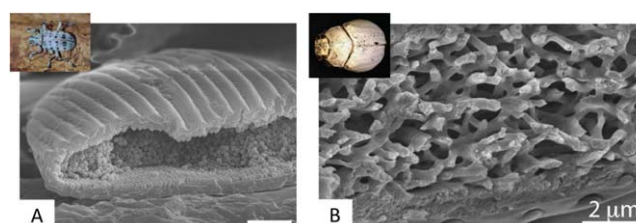


**Figure 15.** 3D photonic structures in beetles. (A) Although the actual processes leading to quasi-ordered 3D organization as found in the longhorn beetle *P. waterhousei* are unknown, both phase separation and colloidal packing can lead to similar configurations. (B) Unknown processes enable disorder of thinner structures among larger voids to achieve highly scattering white in *Cyphochilus* beetles. (Scale for both: 2  $\mu$ m.) (A) Reprinted figure with permission from [201], Copyright (2001) by the American Physical Society. (B) Reprinted by permission from Springer Nature: Nature, Scientific Reports, [34], 2014.



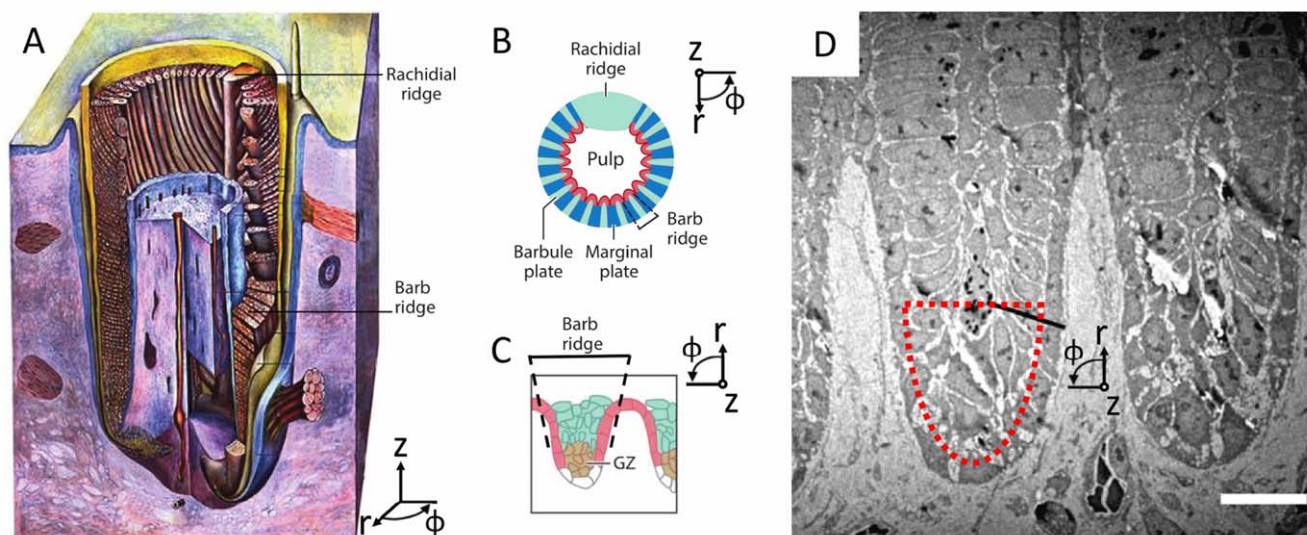


**Figure 16.** The growing feather. (A) Feather growing from feather follicle in the dermis (purple): the epidermis (blue cross section and yellow-blue surface) invaginates the dermis (purple), leaving a central core, the dermal pulp (also purple); the rachis, barbs, and barbules grow in the cavity. (B) A representative cross-sectional schematic of the growing feather; the barb ridges wrap around the pulp, meeting at the rachis. The feather grows out and away from the surface out of the follicle collar; unlike typical plant growth, where tips grow at the leading edge, the feather first grows the distal tips and then proceeds to grow the proximal regions of the feather. (C) A close-up cross-sectional schematic of the developing barb ridge, showing the region that will form the marginal plate (red) and the growth zone (GZ, brown); the pulp is toward the bottom of the image. (D) Along a cross-section of the growing feather, multiple barb ridges are shown, with the center of the follicle toward the bottom of the image; outlined in red is the general region shown in figure 17 (scale  $10\ \mu\text{m}$ ). (A) Reproduced from [223]. (B) Reprinted from [224], Copyright (2007), with permission from Elsevier. (C) Republished with permission of Annual Reviews, from [220]; permission conveyed through Copyright Clearance Center, Inc. (D) Republished with permission of The Royal Society, from [222]; permission conveyed through Copyright Clearance Center, Inc.

Polychaete worms offer another puzzle related to the formation of 2D periodic structures (figure 14(H)): the setae of the genera *Aphrodita* and *Pherusa* have well-ordered cylindrical voids in a chitin matrix [139, 199]. The authors of one study propose that chitin fibril defects may force the regular positioning of the chitin structure [139], but we do not know the time line nor the physics of the development of this structure.

**Three-dimensional structures and self-assembly:** three-dimensional photonic structures appear to rely heavily on self-assembly processes [144, 200]. In some butterflies, gyroid structures—regular three-dimensional continuous network architectures—are found between the upper and lower surfaces of the scale. Gyroid morphologies are believed to be formed with the assistance of internal membranes (just as we saw in the case of multilayer formation) [71, 72, 75, 144]. Three-dimensional photonic structures observed in bird feathers offer strong indications for phase separation to be involved in the structure formation process (discussed in further detail below). Beetles also exhibit a variety of three-dimensional geometries, the formation of which is not fully understood (figure 15). Various beetles, including *Pachyrhynchus argus* and *Pseudomyagrus waterhousei*, use chitin to create 3D morphologies of ordered or quasi-ordered spheres [19, 201], which could be reminiscent of either phase separation or colloidal packing. The *Cyphochilus* beetle produces a different 3D geometry, employing bulk disorder to achieve brilliant white; this geometry is particularly intriguing since this particle size and distribution have not been manufacturable [202]. Disordered colloidal morphologies

also form the basis for the whites produced by leucophores in cephalopod skin, although disordered multilayers have also been found to be the source of bright whites in squids [203, 204]. Little to nothing is known about the formation of these leucophore structures.

**Hierarchical elements:** the various features of the butterfly scale also typify the hierarchical nature of biological materials. Biological shapes are frequently appreciated for being hierarchical [205–207]. One useful definition for hierarchy is pattern or order at various length scales [107]. Hierarchical design of material structures might be essential to ensure a particular function, as well as enabling multifunctional behavior [42, 208].

For example, the hierarchical silica frustules of diatoms are of interest not only for their optical behavior [209–211], but also for a wide range of applications, from drug delivery to fluid filtering [212]. In diatoms, organization of actin and microtubules appear to be closely related to their silica structure patterns [213], perhaps hinting at a templating-like process similar to those in butterfly scales. Yet a broad range of components seem to impact the structures at various orders of magnitude, from silica deposition to the overall valve structure [214–216]. However, the physical processes driven by these components and, moreover, their combined effects is still an open question.

Although biology is particularly adept at integrating diverse structural motifs across many length scales, little is known about the biological processes that define and control hierarchy throughout the  $100\ \text{nm}$ – $10\ \mu\text{m}$  range.

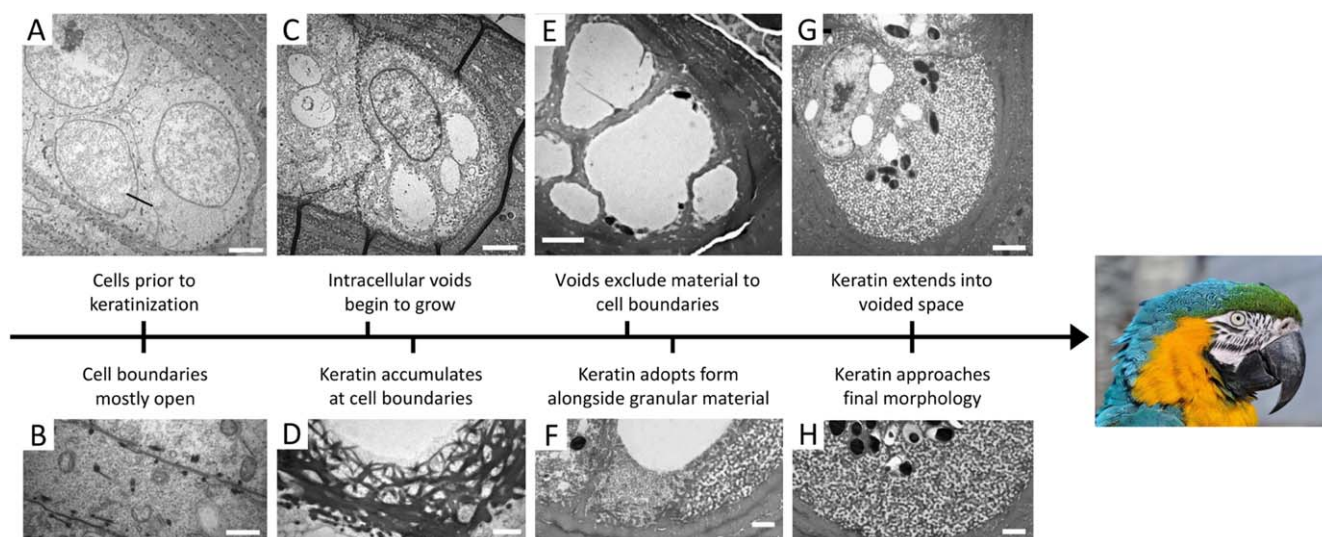


**Figure 17.** Development of keratin structures in feathers of the macaw *Ara ararauna*. (A) Prior to keratinization, medullary cells have enlarged nuclei (scale  $2\ \mu\text{m}$ ). (B) Unknown structures are found along cell boundaries, which are otherwise mostly free (scale  $1\ \mu\text{m}$ ). (C) The cells then develop voids in the cytoplasm (scale  $2\ \mu\text{m}$ ). (D) At the same time, keratin begins to accumulate at cell boundaries (scale  $1\ \mu\text{m}$ ). (E) Later in development, the cytoplasmic voids have filled almost the entire cell (scale  $3\ \mu\text{m}$ ). (F) Keratin begins to develop its tortuous channel, spinodal form alongside other 'granular' material (scale  $1\ \mu\text{m}$ ). (G) The keratin structures spread and the voids shrink (scale  $2\ \mu\text{m}$ ). (H) The keratin network is nearly fully developed (scale  $1\ \mu\text{m}$ ). Republished with permission of The Royal Society, from [222]; permission conveyed through Copyright Clearance Center, Inc. (Parrot) This 'Portrait of a Blue-and-yellow Macaw (*Ara ararauna*) in the Vogelburg (bird park) Hochtaunus, Weilrod, Germany' image has been obtained by the author(s) from the Wikimedia website where it was made available under a CC BY-SA 3.0 licence. It is included within this article on that basis. It is attributed to Quartl.

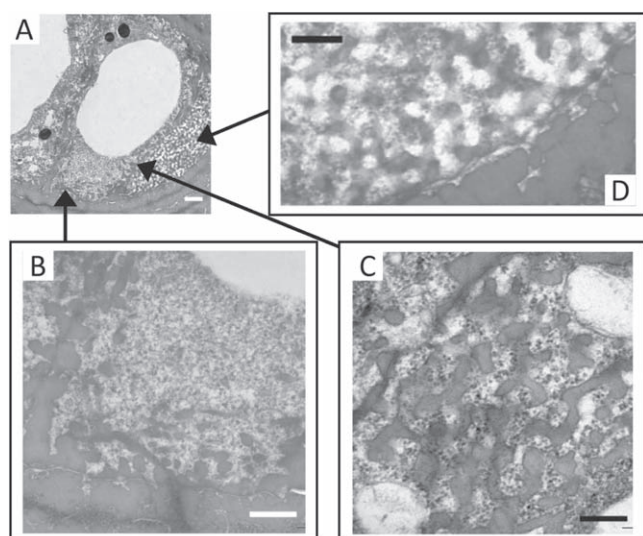


**Figure 18.** Various stages of keratin structure formation. (A) Various stages of structure development are present in medullary cells (scale  $1\ \mu\text{m}$ ). (B) Granular material interspersed with 'unformed' keratin (scale  $600\ \text{nm}$ ). (C) Keratin structure undergoing formation (scale  $300\ \text{nm}$ ). (D) Keratin begins to take final form (scale  $300\ \text{nm}$ ). Republished with permission of The Royal Society, from [222]; permission conveyed through Copyright Clearance Center, Inc.

**3.3.2. Self-assembly.** Example, *keratin self-assembly in avian feathers*: self-assembly processes appear to occur in the formation of biological photonic materials and they carry significant potential for technical understanding and synthetic material design. Keratin development in bird feathers offers an exemplary case study of the self-assembly of three-dimensional

structurally colored biological materials. In addition to the nanostructuring that imparts coloration, the development of feathers is of interest for their varied hierarchical morphologies, which has implications for the function of feathers [140, 197, 217–221]. A bird's feather grows from a follicle on the birds' skin (figure 16). The follicle begins as a proliferation of epidermal cells, which form into a budding papilla, dipping below the surface of the epidermis to form the cavity and rising to form the initial protrusion. Inside the bulk of the papilla is the dermal pulp, which is surrounded by exterior cells called the collar. The cells in the collar then differentiate and begin to form into barbs (some of which merge into the main vain, the rachis); later cells further differentiate into barbules. As the papilla grows upward, the barbs marvelously grow 'backward,' their tips extending back to eventually merge with the rachis. During this progression in cellular arrangement, keratin is produced via normal protein production within the cells [133] (figure 17). The keratin aggregates, with keratin fibrils elongating as the feather grows. Later, the cells dehydrate, altering the relative composition and arrangement of the cell, before finally leaving behind the keratinous structure of the feather [133, 222].

The resulting microstructure of the feather is remarkably similar to the structures that self-assemble during polymer phase separation [46, 79, 222] (figure 18). The study of polymer blend systems has shown that phase separation can proceed in two different ways: spinodal decomposition (which leads to winding or tortuous channels), or nucleation and growth (which leads to spherical or inverse sphere structures) [225, 226]. Transmission electron microscopy studies of feathers from various species illustrate that the spatial distribution of keratin closely matches the structures



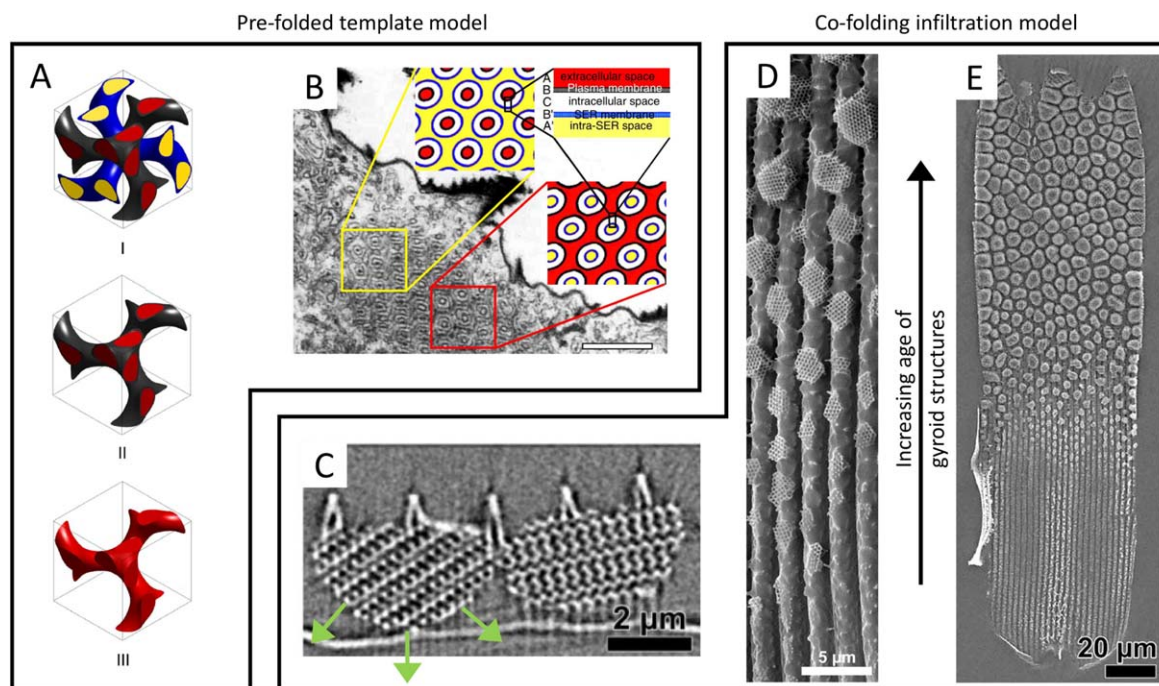


**Figure 19.** Proposed models of gyroid formation in butterflies. (A), The prefolded template model suggests that a double gyroid is formed within the intracellular space, with one gyroid system composed of the smooth endoplasmic reticulum (SER) membrane (blue) surrounding the intra-SER space (yellow), and the other gyroid composed of the plasma membrane (black) surrounding the extracellular space (red). Chitin grows and fills the extracellular space. The SER system and the plasma membrane templates die away, leaving the single gyroid of chitin. (B) The prefolded template model illustrated on one of H. Ghiradella's classic transmission electron micrographs (scale 1  $\mu\text{m}$ ). (C) The co-folding infiltration model proposes that chitin and membrane cooperate to fold into the cell. (D) The size of gyroid crystal grains are found to vary gradually in the scales of butterflies such as *Thecla opisena*. (E) The co-folding model suggests that the gyroids fold into the cell, beginning first at the tip of the scale and progressing back toward the socket. (A) and (B) Reproduced with permission from [72]. (C) to (E) Reprinted/adapted from [75]. © The Authors, some rights reserved; exclusive licensee American Association for the Advancement of Science. Distributed under a Creative Commons Attribution NonCommercial License 4.0 (CC BY-NC) <http://creativecommons.org/licenses/by-nc/4.0/>. (Inset) [154] John Wiley & Sons. © 1989 Wiley-Liss, Inc.

from one of either of these two phase-separation processes [79]. Additionally, another study of feathers at mid-development reveals no sign of template or mold features like those observed in the butterfly, but rather show a progression of aggregation and voids in the cellular space [222]. However, the authors of that study point out that the structural growth is not identical to 'simple' phase separation, but rather is likely modified by spatially varying composition changes within the cell. Moreover, some targeting must be involved in the initial keratin production, since keratin growth begins at the periphery of the cell [133, 222]. Thus, when considering self-assembly in biology we must be careful to account for other guiding processes that contribute to structure formation.

**Tolerance control:** tolerances in the formation of particular features are worth considering when studying biological growth of structurally colored materials, since the materials' interaction with light is closely determined by optical path lengths and structural order. For feathers, timing is key to halt spinodal decomposition, when the channels are the exact right size [222]. Many feathers demonstrate short-range order but less long-range order [79]; additionally, feathers can achieve a smooth color gradient by having cells create one of only two structural colors [222]. In beetles of the genus *Eupholus*, different degrees of long-range order in three-dimensional photonic structures leads to differences of

brightness and color in the beetle's scales, resulting in a characteristic stripe pattern [41].

**Gyroids, a debate in self-assembly:** self-assembly is also believed to drive the structural formation of gyroid morphologies in butterfly wings. Lipid membranes have a variety of stunning phases that are compatible as scaffolds for chitin growth [144]; in the butterfly scales, the plasma membrane and the smooth endoplasmic reticulum membrane are thought to define a double-gyroid phase, allowing chitin to fill the space excluded by the plasma membrane [72] (figures 19(A), (B)). Yet, an alternative model recently proposed that, instead of any phase separation process, the chitin and the plasma membrane co-fold [75] (figures 19(C)–(E)). Under this model, the chitin and plasma membrane gradually self-assemble a gyroid and grow into the cell interior; this process initiates at different sites: it appears to be first occurring at the scale tip and progressing backwards from there.

The differences between these models of butterfly gyroid formation, as well as the unknown aspects of keratin structure development, highlight important questions regarding growth and self-assembly processes. For one, there is a tension between approaches that consider self-assembly primarily as interactions among individual molecules (or unit elements) and descriptions that emphasize energy minimization across the entire system. In either case, however, we still lack



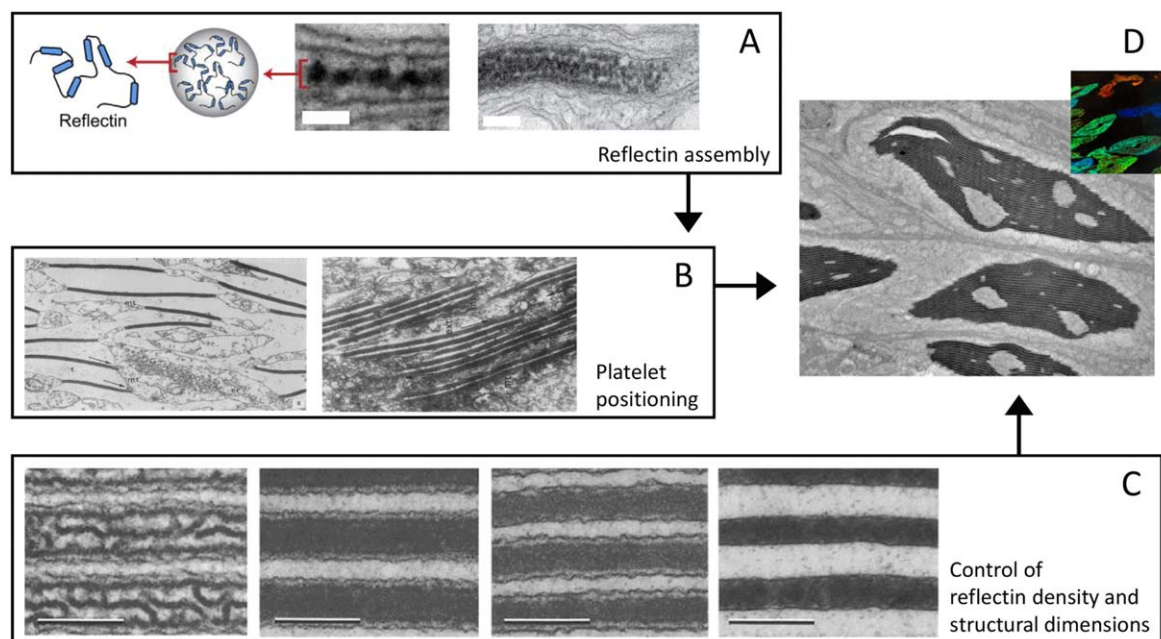


**Figure 20.** Iridophore creation in cephalopods. (A) Reflectin aggregates into ‘beads’ and forms ‘beads-on-a-string’, which fill the platelet space (scales: middle, 100 nm; right, 200 nm). (B) Platelets are transported (possibly by microtubules) to the edges of the cell. (C) Acetylcholine adjusts the water concentration in iridophores, which changes the reflectin density and the structural dimensions (scale 250 nm). (D) Full iridophores in tissue, which are further manipulated by the organism. (A) Reprinted from [231], Copyright (2010), with permission from Elsevier. (B) Reprinted from [229], Copyright (1967), with permission from Elsevier. (C) Reprinted by permission from Springer Nature: Springer-Verlag, Cell and Tissue Research, [80], 1990. (D) Reproduced with permission from [94].

knowledge on the conditions, phenomena, and components that are necessary for self-assembly. Many questions remain: During molecular interactions, what controls consistency across the entire structure? During system-wide changes, how does growth and expansion of the structure impact the conditions for self-assembly? What conditions allow for self-assembly? What components are needed in self-assembly-based structure formation? These questions and many others must still be answered in order to understand the physical principles and specific contexts of self-assembly in developing organisms.

**3.3.3. Process requirements for dynamic coloration. Example, iridophore formation in cephalopods:** cephalopods are widely celebrated for their tunable coloration [81, 82]. While other creatures also exhibit the ability to change their color [86, 227, 228], the cephalopods exhibit superb control of ‘what goes where’ over various length and time scales. Although cephalopods can actively change their chromatophores and iridophores, here, we will focus primarily on iridophore development (figure 20). Similar to lepidopteran scales, the iridophore formation process appears to begin with a basic template, which is filled in by the proteinaceous material that provides the optical functionality. In addition, iridophores are ‘wired up’ to a neural control network that allows the organism to tune the color. Iridophore development is heavily dependent on two distinct components: lamellar, membrane-bound regions and protein-based platelets filling this region.

Fifty years ago, Arnold suggested that microtubules participated in the transport of vesicles away from the Golgi

apparatus toward the periphery of the cell (figure 20(B)), where they aggregated to form ‘interconnecting spaces’; meanwhile, platelets—now known to be the protein reflectin—were observed to appear at the surfaces of these spaces [229]. However, very little is understood about the mechanisms that control the spatial location of these platelets within cells and of the cells within tissues [231], as most idiocyte development studies have focused on the reflectin rather than the formation of the lamellar region. As the reflectin collects in the lamellar regions created by folds of the cell membrane, it self-assembles into spheroids with roughly 15 nm radii. These spheroids further organize themselves as ‘beads-on-a-string’, fill the lamellar space, and form the platelet [230] (figure 20(A)). Such hierarchical self-assembly may be important to the ability of the protein to condense during active iridophore color tuning [85, 94, 232] (figure 20(C)). This condensation phenomenon is a local structural change that happens upon phosphorylation of reflectin, which is triggered by the neurotransmitter acetylcholine. For the cephalopod to achieve useful color, it must control changes at the protein length-scale consistently across the length scale of the cell, and further integrate cellular control across the entire tissue [233].

The dynamic behavior of materials with tunable color can potentially give us valuable insight about their development. Dynamic variations of structural color can be achieved through changes of the material’s geometrical structure, molecular composition, and placement relative to other system components (figure 21). However, the tuning of the material’s optical characteristics imposes new

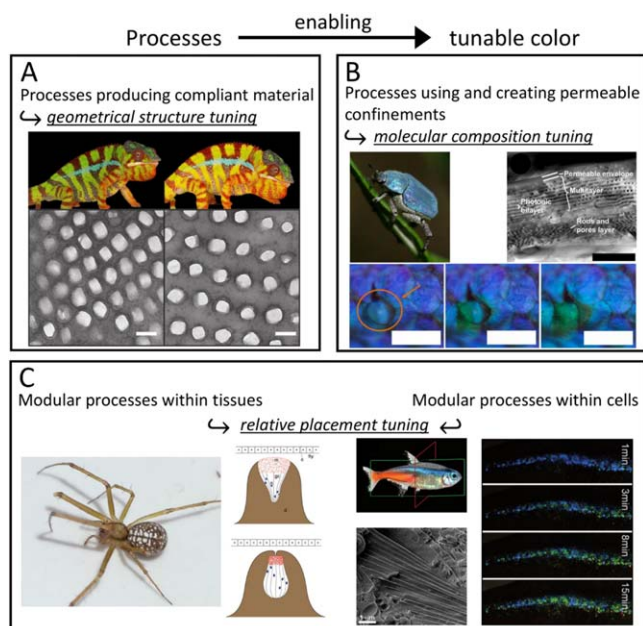


**Figure 21.** Process requirements for producing tunable structurally colored materials. (A) Processes that produce compliant material is necessary for geometrical structure tuning, as we see in the panther chameleon *Furcifer pardalis* (scale 200 nm). (B) Processes that create permeable, yet confined, spaces enable color tuning by altering molecular composition of the structure in beetles such as the *Hoplia coerulea* and other (scale: top right 2  $\mu\text{m}$ ; bottom row 100  $\mu\text{m}$ ). (C) Modular processes within tissues (suggested to occur in the *Floronia bucculenta* spider) and modular processes within cells (for example, the neon tetra fish *Paracheirodon innesi*) are important for control of the positioning of structurally colored materials (scale for SEM image 1  $\mu\text{m}$ ). (A) Reprinted by permission from Springer Nature: Nature, Nature Communications, [86], 2015. (B) Reprinted by permission from Springer Nature: Nature, Scientific Reports, [236], 2016. ((C) left) This 'Floronia bucculenta, female. Location: The Netherlands - Huijbergen - Staartsche Duinen west' image has been obtained by the author(s) from the Wikimedia website where it was made available by name of uploader Lymantria under a CC BY-SA 3.0 licence. It is included within this article on that basis. It is attributed to Frank van de Putte. ((C) middle left) Reprinted by permission from Springer Nature: Springer-Verlag Berlin Heidelberg, Spider Ecophysiology, [237], 2013. ((C) right) [227] John Wiley & Sons. © 2015 WILEY-VCH Verlag GmbH & Co. KGaA, Weinheim.

requirements on the processes at the origin of its formation; the processes that impart the material's molecular composition, structural geometry, and relative placement must now be compatible with its required dynamic and reversible optical behavior. Furthermore, processes related to the formation of additional components, such as dedicated chromatophore muscles [234] and the neural network in cephalopod skin [235], which effectuate and control the color tuning, require integration with the processes that form the optical structures. Just as the development of structural color in animals is not fully understood, many aspects of the development of the infrastructures that enables dynamic structural coloration remain a mystery. However, we can attempt to use the behavior of the tunable material after its formation to infer some of the requirements on the processes that produce it.

*Processes enabling geometrical changes:* in materials where the dynamic color relies on changes in geometry, the organism requires developmental processes that can produce sufficiently compliant materials to accommodate this change (figure 21(A)). In the cephalopod, the condensation of reflectin expels water from the interior of the lamellae, reducing the interior volume and changing the periodic thickness of the multilayer [80, 94, 229, 230]. The structural attributes of the protein and the plasma membrane together allow for this effect. Consequently, processes that tend to produce very stiff materials, including deposition processes such as mineralization in mollusks or secretion of cuticle in arthropods, are generally less compatible with this mechanism of color tuning. Conversely, proteins and materials that allow a high degree of water content may be more amenable to reversible dimensional changes. However, structurally colored materials must have at least two optically distinct materials or material phases. If one phase is deformable and can support a second, stiffer phase, color changes can still be produced by geometrical changes. In such cases, various processes must cooperate to produce each phase. For example, the panther chameleon *Furcifer pardalis* forms a periodic arrangement of guanine nanocrystals within an upper skin layer, which exhibits a color change when stretched [86]. This requires integration of guanine crystal formation and production of the pliable dermis, in addition to other processes that place the crystals. In both the chameleon and the cephalopod, the modular nature of the individual iridophore and of the guanine crystals enables some degree of separation of these processes. Thus, when tunable color is driven by dimensional or periodicity changes, the tunable structure requires processes that can produce at least one flexible material phase; if more phases are utilized, then additional processes are needed to produce, place, and orchestrate the combined execution of these processes.

*Processes enabling material changes:* when color dynamics are driven by changes in material composition or by replacing one material with another, we find that the composition change is generally occurring within a confining structure; additionally, the material exchange must be regulated in some way (figure 21(B)). For example, during the reflectin condensation in the cephalopod iridophore, water is removed, which alters the effective refractive index of the protein. During this activity, the lamellae serve to maintain the structure's geometry and define a boundary for the various materials involved (reflectin, acetylcholine, water) [94]. Thus, in addition to accumulating and organizing reflectin, developmental processes must simultaneously form and incorporate the bounding lamellae structure. This hints at the need for additional processes to produce supporting structures with reliable geometry that can accommodate the material exchange necessary for optical tuning. Modular compartmentalization of the cell into confined volumes appears to prove beneficial for these processes: the membrane offers a point of aggregation for reflectin, while establishing the confining structure for water exchange. Various beetles employ a variation on this principle [241]. For example, in the beetle *Hoplia coerulea*, water displaces the air within the cuticle. While the cuticle admits

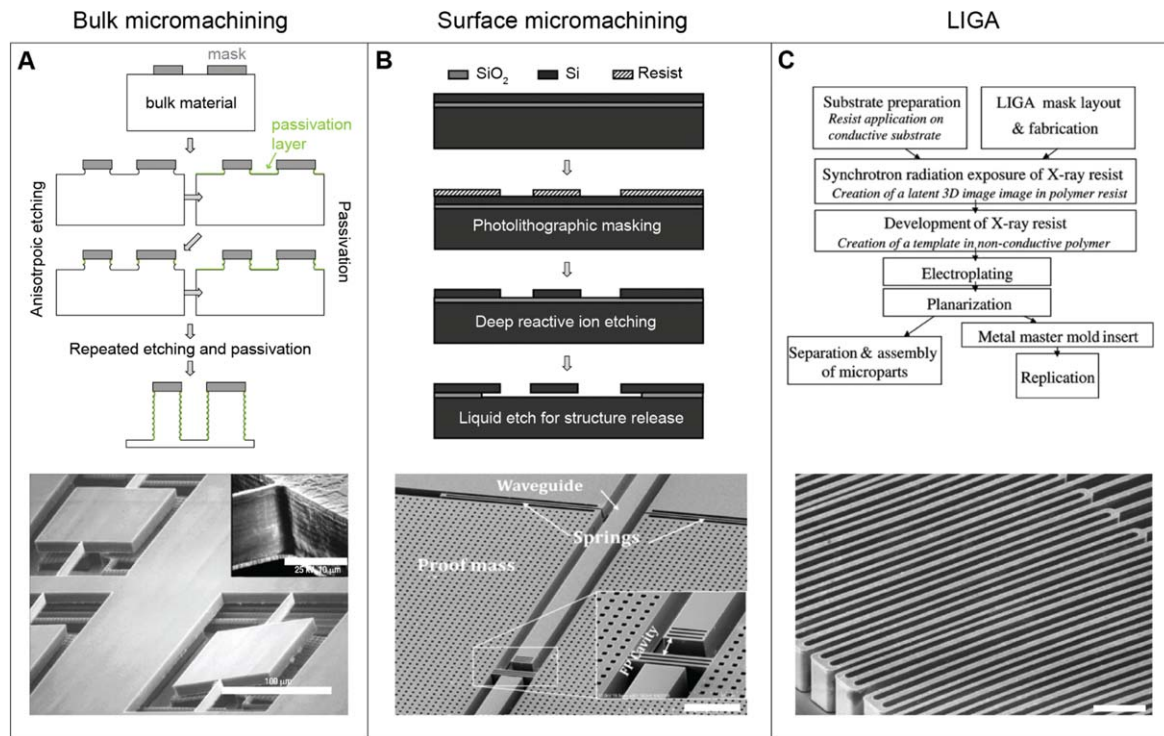


**Figure 22.** Common microfabrication approaches: Bulk micromachining, surface micromachining, and LIGA. The top sketches depict the processes schematically. Scanning electron micrographs at the bottom show examples of optical structures formed with these processes: (A) a bulk micromachined mirror array formed in titanium (scale 100  $\mu\text{m}$ , inset 10  $\mu\text{m}$ ). (B) A surface micromachined Fabry-Pérot-based accelerometer (scale 100  $\mu\text{m}$ ). (C) Spring flexures holding a high aspect ratio optical grating fabricated with LIGA (scale 50  $\mu\text{m}$ ). (A) Reprinted by permission from Springer Nature: Nature, Nature Communications [238], 2004. (B) & [2012] IEEE. Reprinted, with permission, from [239]. (C) Reproduced with permission from [240].

water, it is impermeable to ethanol [236]. This selective behavior is suggested to occur due to the cuticle's porous structure and the presence of salts distributed within the cuticle. The optical tunability of beetle cuticle depends on development processes that allow for suitable modification of the cuticle: firstly, to enable porosity that permits access to confined spaces within the cuticle, and secondly, to introduce salt additives as necessary. Therefore, tunability that is achieved through changes in molecular composition requires specialized processes that create structures where selective material exchange can controllably take place.

*Processes enabling reconfiguration of the photonic material's location:* tunable optical behavior that is driven by dynamic variations in relative placement of the optical structure's individual components (cells, tissue sections, intracellular elements, and so forth) depends on these components to be modular and/or to some degree independent (figure 21(C)). In the cephalopod, as well as some fish [242, 243] and lizards [244], the configuration of a chromatophore relative to an iridophore blocks or alters the structural color behavior of the iridophore. In the cephalopod, this is achieved by the unique developmental regimens of two separate layers: one with muscle-controlled chromatophores and another with acetylcholine-controlled iridophores [81]. We can infer, therefore, that these two systems have some separation during development and also unique processes that lead to their production. Cellular modularity allows for processes that lead to different structural outcomes within

microscale proximity. In cephalopods, this process strategy allows interference, scattering, and absorption phenomena in the interplay of chromatophores, iridophores, and leucophores. Sometimes, a material's functional components are developed in even closer proximity: in the *Floronia bucculenta* spider, a guanocyte layer is grown immediately under a layer of muscle; yet, the developmental processes for guanocytes and myocytes are clearly separate. Thus higher, tissue-level regulation coordinates their respective placement during development.

In other cases, organisms achieve color changes by repositioning scatterers and pigmented components within single cells, with the material's functional components developed within intracellular proximity: for example, the iridophores of the neon tetra fish *Paracheirodon innesi* develop a guanine multilayer within the cell [227]. The fish can rotate the angle of this intra-cellular multilayer to achieve a color change. This suggests that the structure, the actuator of the multilayer, and some part of the system controlling the actuator must all be developed intracellularly. Another example includes the grasshopper *Kosciuscola tristis* which produces pigmented and scattering elements dispersed within epidermal cells [241]. These cells alter the distribution of the scattering and pigmented elements to achieve a pronounced color change. In these cases, the modular *dynamics* at the cellular level is indicative of modular *processes* at the cellular level during development.



*Considerations for controlling color changes:* the discussion of processes that produce dynamic biological materials would be incomplete without some mention of the development of the infrastructure that controls the dynamic behavior. Since passive tunable systems (like the porous, water-permeable cuticle of *Hoplea coerulea*) are tightly integrated with the structurally colored material, the development of the associated regulation mechanisms likely occur simultaneously with the production of the structurally colored material. However, neural control in cephalopod skin requires integration of the nervous system, the dynamic optical elements, and any intermediating component (such as muscles) at some point during development. As previously indicated, there is evidence that neural control of structural color can develop as a somewhat independent ‘module’: in the cephalopod, for example, iridophores are controlled via a neural circuit that is separate from the circuit that controls chromatophores [235]. For either network however, the organism’s development must lead the neural connection to interface with the material. Interestingly, reflectin has been shown to be a highly favorable medium for human neural stem cell/progenitor growth, causing the authors of one study to wonder if reflectin itself helps establish neuron-iridophore contact [245]; however, currently there is no scientific evidence if and how reflectin impacts cephalopod neuron development. Much more work is needed in this realm to understand these types of questions at the intriguing junction between developmental biology, materials science, and neuroscience.

Cellular methods of control are perhaps understood even less and provide an alternative twist on the development of control. In examples such as the neon tetra and the grasshopper *K. tristis*, it is not entirely clear whether variations in the cell, the tissue, or the nervous system are triggering the coloration change. Yet, it is interesting to note that these color changes are not rapid (15 min in the neon tetra and 30 min in the grasshopper), which causes us to speculate whether the systems that actuate the intracellular reconfiguration (e.g. microtubule networks [241]) are produced on demand by the cell. If so, the organism is less encumbered by the production of actuation mechanisms during development, but perhaps at the cost of slower dynamics. Overall, dynamic control of structural color, as well as the development and fabrication of dynamic systems, is ripe for further research.

### 3.4. Synthetic structure formation processes

Over the last century, a wide range of synthetic processes have been conceived to realize devices whose functions rely on increasingly precise control of material morphology and composition at ever smaller length scales [246]. The advances in structure formation processes seen at the end of the last century came as a response to the high demand for smaller and more capable integrated circuits, and the need for sophisticated micro-electro-mechanical systems (MEMS) technology [247, 248]. This development has been fueled further by the rise of personal electronic devices that harbor more sophisticated communication, computation, imaging,

and sensing technology in very compact packages. In parallel, progress in microfluidic systems for biomedical applications has driven a larger demand for structure control across all length scales in a broader selection of materials, including soft solids and fluids [249, 250]. Microfluidic technology penetrates a wide range of application fields from lab-on-chip technology for drug discovery and medical diagnosis, to fluidic optical devices [251, 252]. Finally, the recent scientific, industrial, and public interest in additive manufacture has opened up opportunities for changing established paradigms in manufacturing [253]. In the following, we will provide a selective overview of representative synthetic manufacturing approaches, which are of relevance in the context of realizing advanced optical materials with structural color.

#### 3.4.1. Conventional micro- and nanofabrication techniques.

Although the processes used in semiconductor manufacturing and MEMS technology were initially not readily applicable to soft materials processing, they have evolved greatly to include a large variety of materials and are worth considering here [254]. Semiconductor processing approaches are among the most advanced capabilities of humankind for patterning materials at small scales. Beyond standard semiconductor and MEMS fabrication, these processes are currently applied to realize a wide variety of devices, such as optical MEMS, lab-on-a-chip systems, micro total analysis systems ( $\mu$ TAS), solar cells, and flat-panel displays. These newer technologies benefit specifically from translating microfabrication techniques into the domain of polymer processing [255]. Micro- and nanofabrication techniques, which are also used to realize the MEMS displays discussed in section 2.3.2, can therefore serve as a case study for the wide variety of mature human manufacturing processes used to create micro- to nanoscale systems. Different criteria can be used to classify standard microfabrication approaches. In the context of this review, we will distinguish between bulk micromachining [256], which relies on spatially controlled removal of material from a substrate (subtractive processes), surface micromachining [257, 258], which involves the sequential deposition and patterning of desired materials (additive and subtractive processes), and molding [259], where materials are cast into shape (net-shape processes) (figure 22).

Bulk and surface micromachining strongly rely on lithography processes, which enable the transfer of two-dimensional patterns onto the processed substrate (often a silicon or glass wafer). Photolithography, where spatially heterogeneous light distributions are used to transfer a pattern onto a photo-curable polymer, is most widely applied in industrial and academic microfabrication for the formation of planar micro- and nanoscale patterns.

Etching, a crucial component of bulk micromachining and surface micromachining, allows for selective material removal in desired locations. Spatial selectivity can be achieved through photolithographic deposition of protective masks. Furthermore, the resulting structure is strongly dependent on the specific etchant chemistry and its interaction

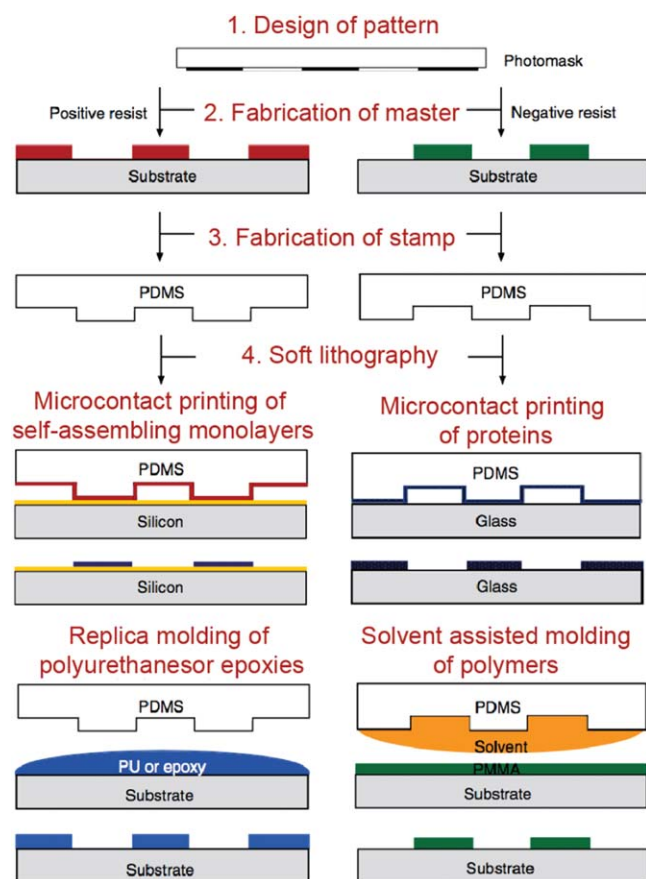


**Figure 23.** Soft lithography. Schematic illustrations of the four key steps involved in soft lithography and of a selection of major soft lithographic patterning approaches. Reprinted by permission from Springer Nature: Nature, Nature Communications [264], 2010.

with the materials. Careful etch process design allows for the creation of deep channels with vertical sidewalls in regions not covered by the protective mask, or alternatively can be used to create pronounced under-cuts. There are two common types of etching, wet and dry. Wet etching involves immersion of the substrate in a liquid etchant. Here, the etching dynamics between substrate and etchant (such as anisotropic etch rates) along different substrate crystallographic orientations define the resulting structure. Dry etching involves the use of reactive, activated gases. Gas activation can be achieved through heat or plasma, and directional delivery of the gas can allow for highly directional etching.

The complementary process to pattern creation via etching is the spatially selective deposition of material in thin films in areas that are not covered by the photoresist mask, a key concept in surface micromachining. There are a variety of techniques to deposit materials onto patterned or non-patterned substrates, such as sputtering, chemical vapor deposition, atomic layer deposition, layer-by-layer deposition, molecular beam epitaxy, and polymer film deposition via spin coating, to name just a few. The specific choice of deposition technique is strongly dependent on the required precursors, the intended characteristics of the deposited material, its

desired thickness and thickness variation, the substrate, and the photoresist pattern.

Finally, the process of micromolding has found applications in microscale device design and MEMS technology since the early 80s. In particular, a process called LIGA (Lithographie, Galvanoformung, Abformung) is used to produce metal- or polymer-based MEMS devices with a high aspect ratio [259]. For LIGA a mold is first etched into a photolithographically patterned photoresist and then back-filled by electroplating metals or conductive polymers, before finally removing the photoresist template.

More detailed discussion of the micro- and nanofabrication processes that were only briefly described in the preceding paragraphs, as well as many other techniques not mentioned here, can be found in dedicated textbooks [260, 261].

**3.4.2. Soft lithography and transfer printing.** In recent decades, scientists and companies have increasingly focused on different strategies for adapting classical semiconductor microfabrication approaches to patterning soft materials [262].

Soft lithography, a technique conceived in the early 90s [263], employs soft stamps that are formed by casting and curing an elastomer (such as polydimethylsiloxane) onto patterned surfaces that were etched in silicon or formed in photoresist. This cast can then be used as a stamp or mold, greatly expanding the set of materials that can be used for pattern creation [264] (figure 23). Taking this concept even further, transfer printing employs elastomer stamps to manipulate a variety of ‘inks’ at the nanoscale [265], as shown in figure 24. These robust, low-cost, large-scale adaptable patterning techniques have greatly increased our ability to impose structure on biocompatible, soft materials in non-planar geometries at length-scales ranging from  $\lesssim 50$  nm to several 100s of micrometers. This enables advanced device design in biotechnology, medical diagnostics, lab-on-chip systems, and plastic electronics [266].

Methods for structure formation that rely on semiconductor microfabrication, soft lithography, or transfer printing are among the most essential process strategies that humans have refined for industrially viable high-end manufacturing and low-cost pattern creation on the nano- and microscale. We have become extremely good at the generation of patterns on planar surfaces using sequential processes. This allows us to manufacture a wide variety of two-dimensional structures easily with a resolution down to a few nanometers. By systematic combination of these sequential processing strategies, even structures with complexity in three dimensions can be built in a sequential layer-by-layer fashion, including the complex architectures of current state-of-the-art microprocessors, dynamic MEMS devices, or even faithful replicas of butterfly wing structures [267] (figure 25). However, there are also profound limitations associated with these approaches related to their sequential nature and the trade-offs that have to be made between resolution, structural sophistication, large area processing at high throughput, and

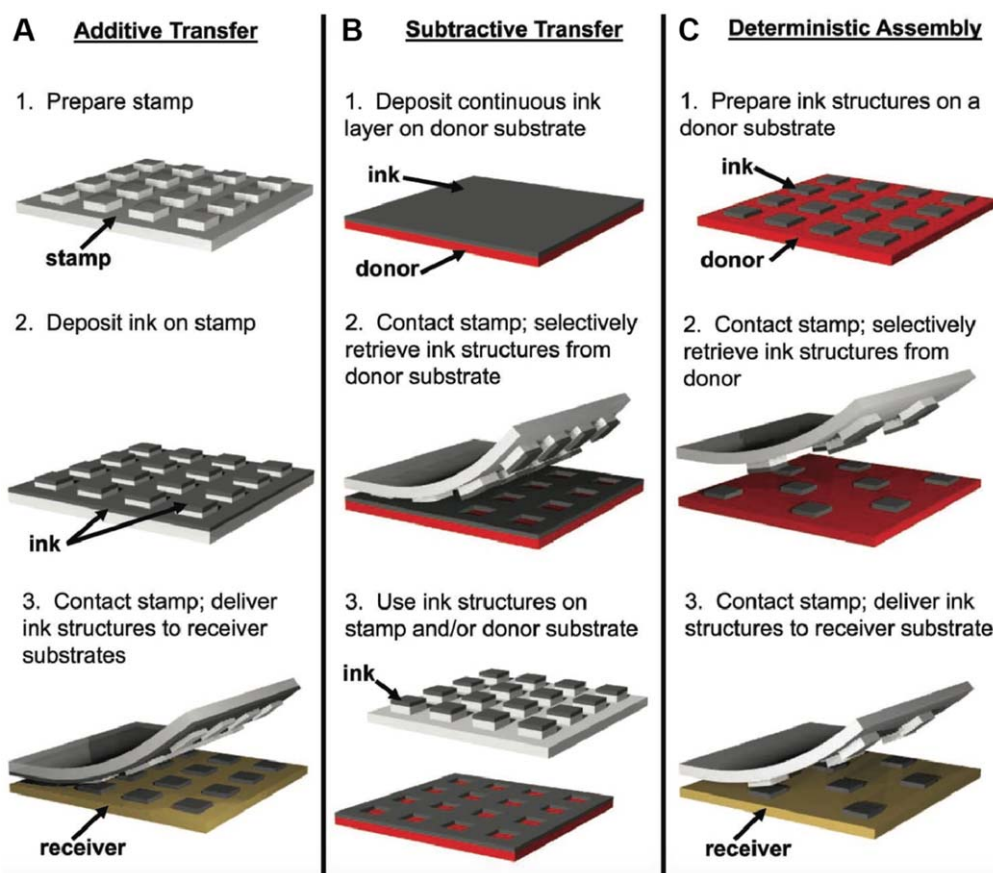


**Figure 24.** Transfer printing. (A) The first of three common methods for transfer printing, additive transfer involves placing ink on the stamp which is then transferred to the substrate. (B) Subtractive transfer is the opposite process, whereby the ink is placed on the substrate and selectively removed by the stamp. (C) Deterministic assembly uses a stamp to selectively transfer preexisting structures from one substrate to another. [265] John Wiley & Sons. Copyright © 2012 WILEY-VCH Verlag GmbH & Co. KGaA, Weinheim.

restrictions in the generation of complex interwoven hierarchical, three-dimensional material architectures.

**3.4.3. Colloidal self-assembly and directed-assembly approaches.** While conventional micro- and nanofabrication processes, soft lithography, and transfer printing have been highly successful, they have inherent limitations with respect to creating arbitrary three-dimensional geometries. A family of processes with the potential to address these limitations relies on directed self-assembly processes, which involve pre-existing, rationally designed building blocks that assemble to form the desired material, or at least parts thereof [270]. There have been impressive advances in these techniques over the past two decades, resulting in the creation of self-assembled functional materials that possess a wide variety of optical, chemical, mechanical, and dynamic properties. When describing a specific self-assembly process there are a number of defining characteristics, such as the size, geometry, and material composition of the building blocks, the environment in which those building blocks are placed, the physical phenomena causing them to self-assemble, and the type of initial and boundary conditions applied to the system.

Colloidal self-assembly perhaps represents the most heavily studied synthetic self-assembly process, which has

led to many inspiring insights into possible strategies for controlling material structures at the nano- and microscale. In general, the building blocks in colloidal assembly are nano- or microscale particles of a well-controlled shape and size. In their simplest form the colloids are spherical and have no specific chemical functionality. Fabrication approaches relying on colloidal self-assembly have tremendous potential for the design of complex hierarchical structures on surfaces and in three-dimensional volumes using simple building blocks, which is discussed comprehensively in recent reviews [271–273]. In the context of this review, we will focus on a selection of exemplary processes and strategies that have employed colloidal assembly for the design of optical materials.

A wide variety of approaches have been proposed to assemble colloidal particles by taking advantage of their chemical and physical interactions (figure 26(A)). Direct deposition methods, such as gravitational sedimentation, evaporation-induced assembly techniques, and electrostatic deposition, allow for the formation of colloidal monolayers and three-dimensional colloidal structures directly on the substrate, while liquid interface-mediated approaches allow for the formation of colloidal monolayers and multilayers that then are transferred to the substrate [272, 274].



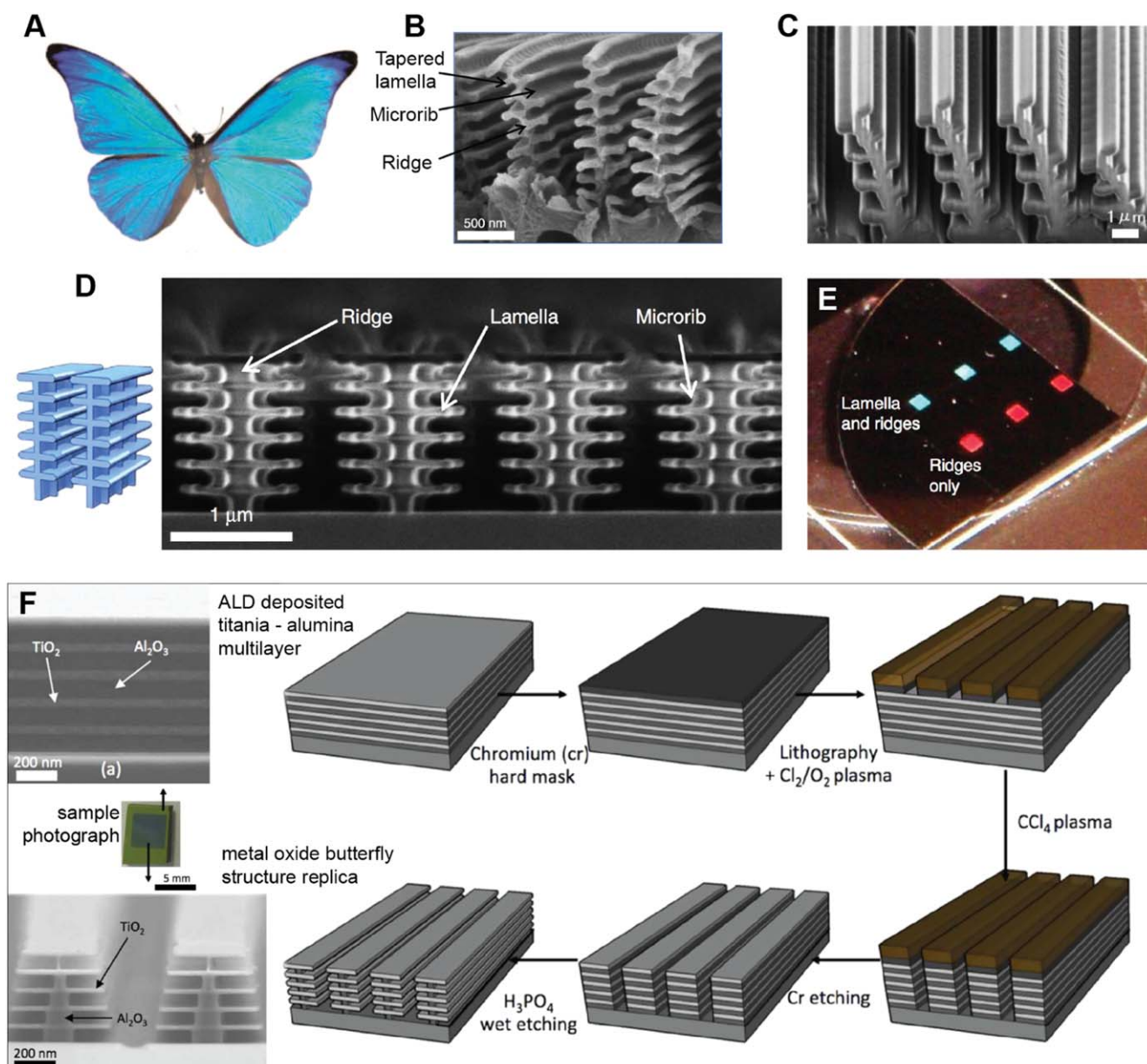


**Figure 25.** Microfabricated replicas of the *Morpho* butterfly's wing structures. (A) Photo of a *Morpho* butterfly. (B) Scanning electron micrograph of the nanostructures on the butterfly's wing scales. Features of the scale morphology, such as ridges, microribs, and lamellae, are marked (scale 500 nm). (C) Small-area replica of the butterfly's structure formed from diamond-like carbon by using a focused ion beam—chemical vapor deposition technique (scale 1  $\mu\text{m}$ ). (D) A more recent synthetic analog of the butterfly structure formed in photoresist materials (poly(methyl methacrylate) and a copolymer of methyl methacrylate methacrylic acid) through a combination of electron beam lithography and selective removal of the copolymer using a binary solvent (scale 1  $\mu\text{m}$ ). (E) Photograph of the patterned areas, which measure 4  $\text{mm}^2$ . (F) A replica of the *Morpho* structure formed from metal oxides (titania and alumina) using a combination of atomic layer deposition (ALD), photolithography, plasma-enabled anisotropic reactive ion etching and wet etching (scale: SEM images 200 nm; sample photograph 5 mm). The structures in (D)–(F) are used for vapor sensing. (A) and (C) Reproduced from [267]. Copyright (c) 2005 The Japan Society of Applied Physics. All rights reserved. (B), (D) and (E) Reprinted by permission from Springer Nature: Nature, Nature Communications [268], 2015. (F) Reproduced from [269]. © IOP Publishing Ltd. All rights reserved.

The capacities of colloidal self-assembly to create unique three-dimensional, hierarchical architectures can be greatly expanded by using carefully designed anisotropic and chemically modified building blocks [282–284] (figure 26(B)). For instance, manipulation of the particle shapes to create discs, spheres with cavities, or cuboids can direct the self-assembly process towards creating unique structures [285, 286] (figure 27). In another example,

microspheres are transformed into hollow spheres, providing different physical characteristics for the bulk crystal [287]. More exotic shapes, such as nanoscale octapods, can also be self-assembled into complex architectures [288]. The particles' assembly behavior can be manipulated by tailoring their internal composition and morphology. This is demonstrated in temperature-responsive microgel particles that change their size in response to thermal stimuli and can thereby assume

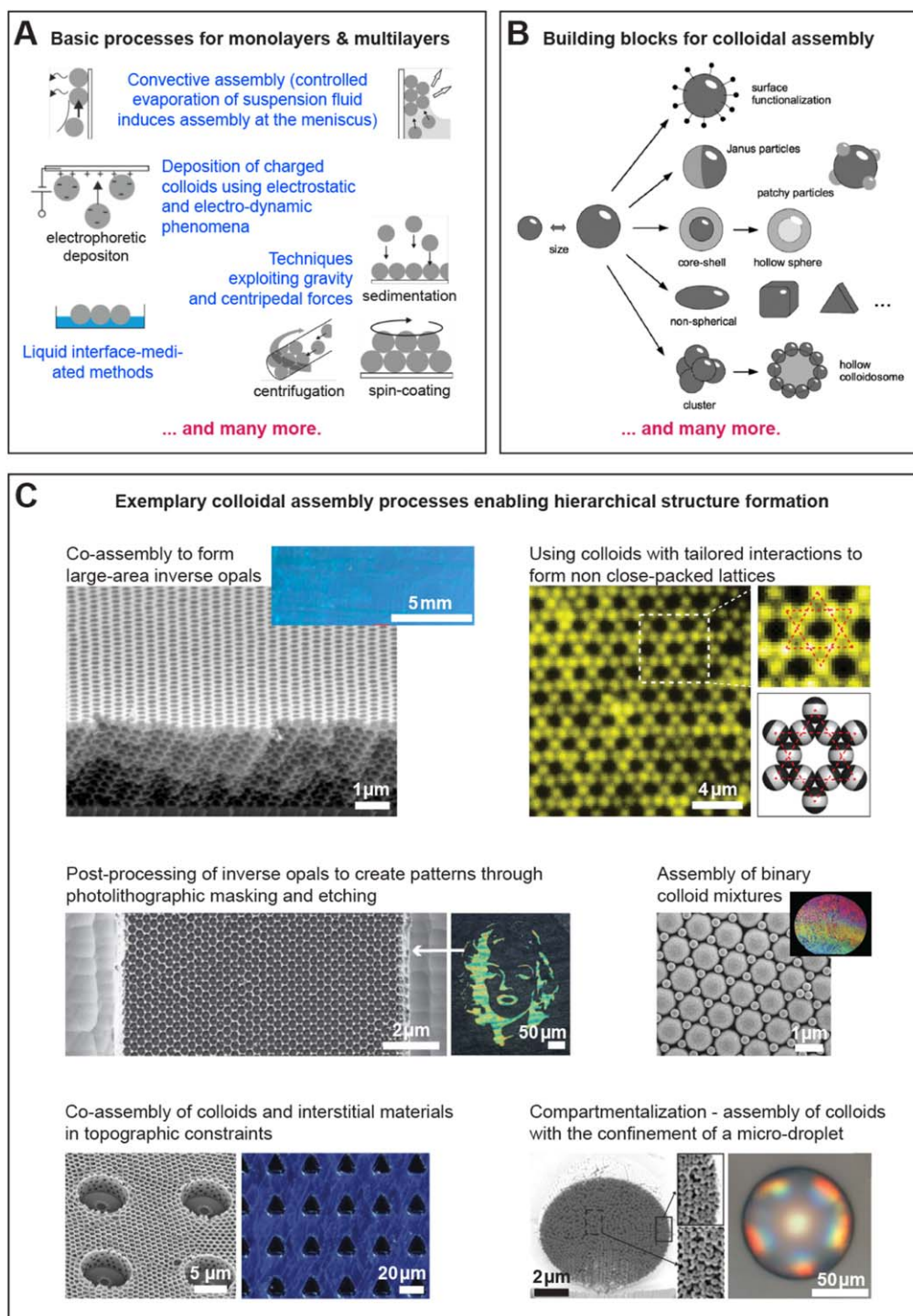


**Figure 26.** Colloidal self-assembly processes. (A) Selection of processes used to form colloidal monolayers and multilayers. (B) Tailoring properties of the building blocks to modify their self-assembly behavior and the functionality of the final structures. (C) A selection of strategies to direct assembly of colloids for forming hierarchical architectures. (A) and (B) Reprinted with permission from [275]. Copyright (2015) American Chemical Society. ((C) bottom left) [280] John Wiley & Sons. © 2012 WILEY-VCH Verlag GmbH & Co. KGaA, Weinheim. ((C) bottom right) Reproduced with permission from [281]. ((C) middle left) [278] John Wiley & Sons. © 2015 WILEY-VCH Verlag GmbH & Co. KGaA, Weinheim. ((C) middle right) [279] John Wiley & Sons. © 2011 WILEY-VCH Verlag GmbH & Co. KGaA, Weinheim. ((C) top left) Reproduced with permission from [276]. ((C) top right) Reprinted by permission from Springer Nature: Nature, Nature [277], 2011.

different colloidal arrangements [289]. Alternatively, core-shell particle designs with a hard core and a soft elastomeric shell enable the creation of soft, stretchable opals whose photonic properties vary with strain [290, 291]. Another good

example of advanced building block design are spherical Janus particles with hemispheres possessing different optical and magnetic properties that can be oriented by applying an external magnetic field [292], as shown in figure 28.



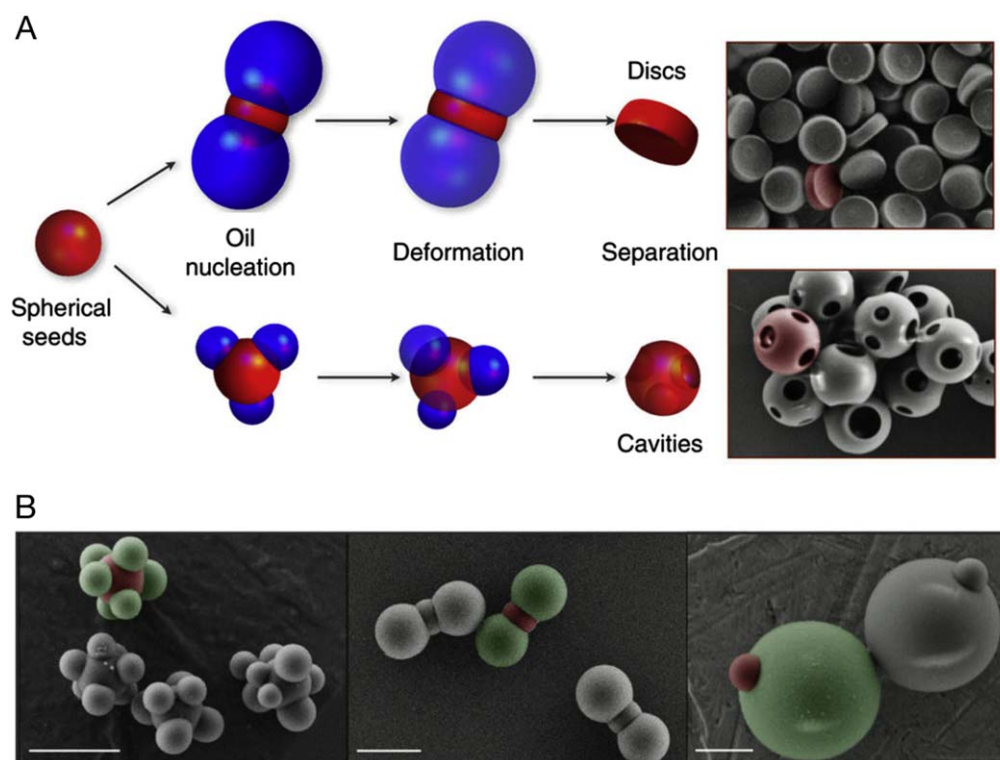


**Figure 27.** Designing colloidal particles. (A) Two example processes for creating shaped colloids. An oil of 3-methacryloxypropyl trimethoxysilane (TPM) oligomers, shown here in blue, undergoes induced nucleation on the surface of solid polystyrene (PS) spheres, shown here in red. Adding small amounts of toluene liquefies the PS spheres, allowing both the PS and TPM to deform due to surface tension until they reach an equilibrium geometry. At this point, either or both of the liquid PS and TPM can be polymerized to create solid colloidal particles, or instead completely dissolved by toluene and ethanol respectively. Shown here are solid PS discs and spheres with multiple cavities, with the TPM removed. (B) SEM images showing additional colloidal particles (scale  $2\ \mu\text{m}$ ). In this case both the PS, shown here in red, and the TPM, shown here in green, are present, demonstrating more complex geometries. Reprinted by permission from Springer Nature: Nature, Nature Communications [283], 2013.

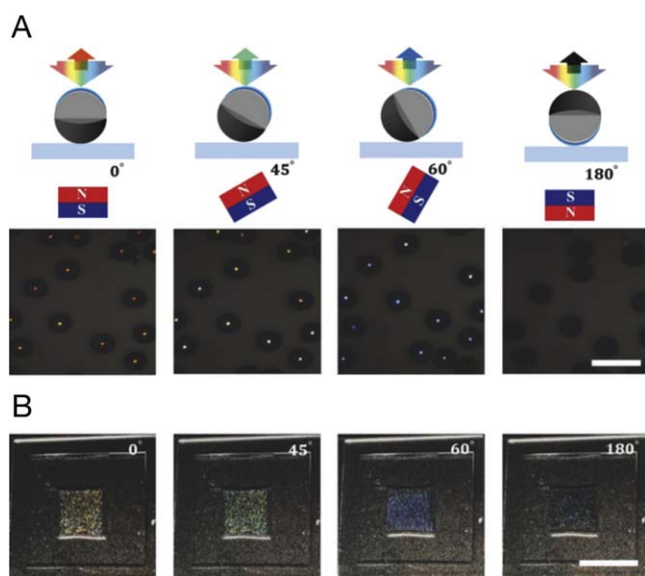


**Figure 28.** Magneto-responsive Janus particles. (A) Diagram of the Janus particles showing how their reflected color changes with orientation, which in turn changes with an applied external magnetic field. Below are corresponding optical microscope images of the particles (scale  $200\ \mu\text{m}$ ). (B) Photographs of a larger number of particles, showing that the color change is dependent on particle orientations (scale  $1\ \text{cm}$ ). [292] John Wiley & Sons. © 2017 WILEY-VCH Verlag GmbH & Co. KGaA, Weinheim.

An intriguing strategy relies on designing the particles' surface chemistry to feature distinct attractive patches, which modify particle attraction and repulsion depending on their relative orientation. Such particles have for instance been used to form non-close-packed Kagome lattices [277] (figure 26(C)). Simulations show that entropy associated with the patchy colloid's unique rotational and vibrational modes plays a fundamental role in stabilizing open lattices [294]. Using microspheres with a polydisperse size distribution for colloidal assembly can lead to a significant increase in the structural complexity of the resulting crystal [295]. It has also been proposed that highly specific interactions between colloidal particles can be designed by attaching strands of DNA to colloidal particles [296] (figure 29).

A common approach to capitalize on colloidal assembly for the design of functional materials consists of using the colloidal structures after assembly as a template for the desired materials to infiltrate into the interstitial spaces. Subsequent removal of the colloids leaves behind an inverse opal structure of the desired material with interconnected voids that under appropriate conditions can be infiltrated with a wide range of fluids to enable various optical sensing applications [297–299]. The inverse opal-based biosensor presented as an example in section 2.3.1 relies on this two-step structure formation and infiltration approach before



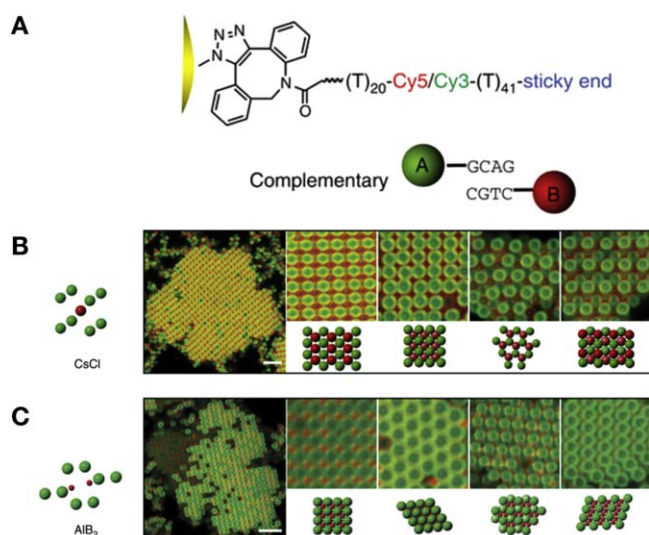


**Figure 29.** Crystallization of DNA-coated colloids. (A) Illustration showing the structure of the DNA-coated colloidal particles. At the top is the general structure, consisting of a colloidal particle attached to 61 thymine (T) bases, separated by either a red Cy5 or green Cy3 fluorescent dye molecule, and a four base sticky end. Each particle has roughly one DNA strand per 27 nm<sup>2</sup> of surface area. Below are two specific structures: 'A' particles have green dye and a guanine-cytosine-adenine-guanine (GCAG) sticky end, while 'B' particles have red dye and a complementary cytosine-guanine-thymine-cytosine (CGTC) sticky end. (B) Combining 1 μm sized A particles with 1 μm sized B particles results in a lattice isostructural to caesium chloride (scale 5 μm). On the right are confocal fluorescence images showing the resultant colloidal crystals. 110, 100, 111, and 211 lattice planes are shown from left to right. (C) Combining 1 μm sized A particles with 0.54 μm sized B particles results in a lattice isostructural to aluminum boride (scale 5 μm). 100, 001, 111, and 101 lattice planes are shown from left to right. Reprinted by permission from Springer Nature: Nature, Nature Communications [293], 2015.

colloid removal to form a regular porous architecture in silk fibroin, which can be modified bio-chemically to achieve specific sensing functionality [117, 300].

Self-assembly processes strongly depend on the environment in which building blocks assemble to form a specific structure. Controlling chemical and physical parameters such as the composition of the fluid medium, temperature, humidity, solvent concentration, and the incorporation of additives can greatly influence the assembly dynamics, ultimately affecting the composition, structure, long-range order, and area coverage of the formed colloidal structures [301] (figure 26(C)). In this context, co-assembly is an elegant strategy to form functional colloidal architectures. This approach relies on using suitable chemical precursors in the aqueous colloidal suspension to achieve simultaneous assembly of colloids with a desired material phase in the interstitial spaces in a one-step procedure [276]. This alleviates the need for subsequent back-infiltration. Subsequent removal of the colloids allows for the creation of inverse opal structures, which feature a connected network of mono-disperse, orderly arranged voids. Colloidal co-assembly has several advantages compared to common colloidal assembly and infiltration procedures: (1) it combines assembly of colloids and matrix phase in a single step. (2)

Compared to backfilling methods, the crack density in formed films is greatly reduced and the uniformity of the interstitial material is significantly increased, which are key requirements for scaling up the manufacturing process. (3) The presence of the matrix phase precursor material can affect the assembly kinetics to allow for the formation of large-area, single crystal orientation colloidal crystal architectures in a scalable process. (4) Co-assembly also enables the sequential deposition of layers with a hierarchy of different colloid sizes on curved surfaces prior to colloid removal.

The assembly of colloids can be directed by topographically modifying the substrate on which the assembly occurs to control the structural outcome. Topographical patterns with structural features smaller than the colloid particles' size and with comparable period have been shown to influence the orientation of the colloidal crystal, analogous to epitaxial growth of atomic crystals and minerals [302, 303]. Correct choice of the nano-scale substrate patterns onto which the colloids are assembled allows the formation of large-scale crystals with minimal defect density [304]. Microscale surface patterns with periods exceeding the colloid size can be used to impose specific structural arrangements, orientations, domain sizes, extent of disorder, and defect locations on the forming crystal [280] (figure 26(C)). Similar colloidal particle localization effects can also be achieved by patterning a flat substrate with regions of different wettability [305]. Another approach combines colloidal self-assembly with soft lithography; by creating a mold of the surface of a colloidal crystal, stretching it, and using that as a template for a subsequent colloidal self-assembly step, it is possible to obtain a variety of novel crystal structures [306] (figure 30).

Structural confinement in three dimensions can be imposed by assembling colloids within micro- and macro-scale droplets to control the resulting structures. This approach has been used to generate ordered and disordered spherical colloidal superstructures formed within microfluidic devices [281, 307] (figure 26(C)), colloidal domes by inkjet printing [308], and donut-shaped pellets by drop-casting [309]. It is worth pointing out that in these examples the appropriate design of the assembling colloids and the control of the reaction kinetics allows creation of colloidal architectures with varying degree of order. Similar concepts also work for materials that can be considered 'colloidal' on a smaller length-scale; for instance, cellulose nanocrystals assemble into regular cholesteric structures within microscale droplet confinements [310].

Physical interactions between the assembling colloids and the medium can be used to direct the assembly, for instance by placing simple colloidal particles with no inherent functionality in a ferrofluid and applying a magnetic field (figure 31). In this case, the magnetic field directs the fluid, which in turn confines the location of the particles [311].

Alternatively, magnetic fields can be used to align and order colloids formed from superparamagnetic nanocrystal clusters that are suspended in a photocurable resin-rich solvent. Applying a magnetic field induces formation of chains of the paramagnetic colloids. The strength of the magnetic field determines the distance between individual

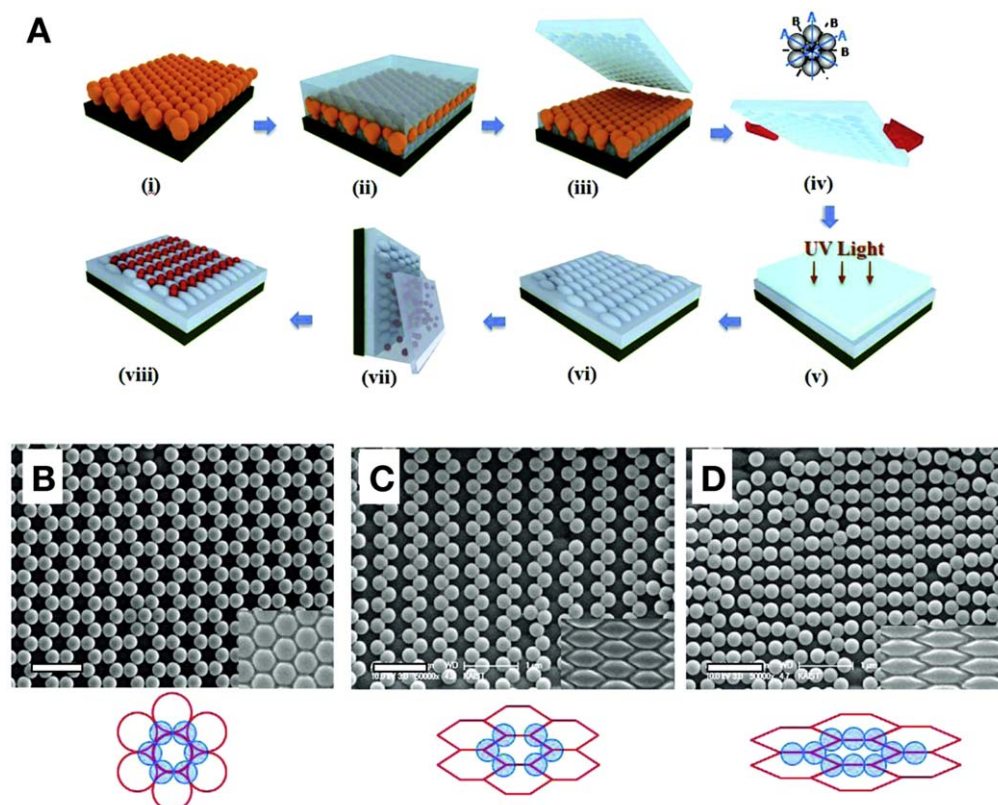


**Figure 30.** Combining soft lithography with colloidal self-assembly. (A) Illustration showing the creation of a PDMS mold based upon a colloidal crystal, followed by stretching (i)–(iv). The stretched mold is then used to create a cast, by UV polymerization of an applied acrylate solution (v). This cast is used as the bottom layer for subsequent binary colloidal crystal growth (vi)–(viii). (B) An SEM image showing an example binary colloidal crystal fabricated by the above method. In this case the mold was not stretched, resulting in a standard structure. The inset image shows the underlying cast, while the illustration below shows the crystal lattice. (C) In this case, the mold was stretched by 150% along the B axis. (D) In this case, the mold was stretched by 200% along the B axis. (Scale for all:  $1\ \mu\text{m}$ .) Reprinted with permission from [306]. Copyright (2010) American Chemical Society.

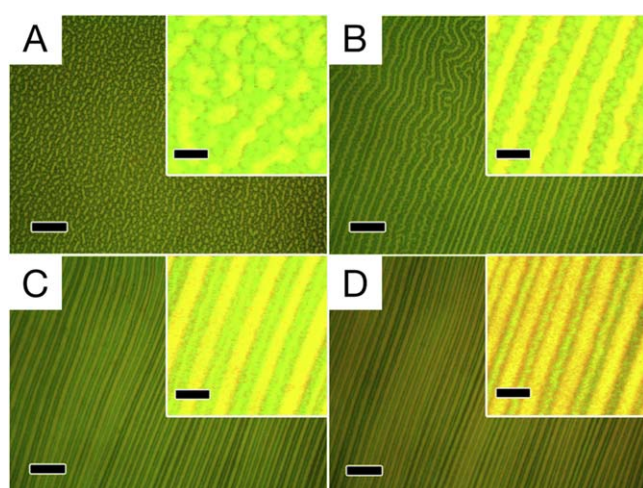


**Figure 31.** Magnetic assembly of photonic crystal structures. A series of optical microscope images, showing the formation of photonic structures as an increasing magnetic field from (A) to (D) is applied to a ferrofluid containing dispersed 185 nm polystyrene beads (scale  $20\ \mu\text{m}$ ). Insets are enlarged versions of their corresponding images (scale  $5\ \mu\text{m}$ ). Reprinted with permission from [311]. Copyright (2010) American Chemical Society.

colloids, which in turn determines the wavelength of the light they diffract. The structures formed under an applied field can then be fixed in place within a small region of the material, by applying spatially patterned ultraviolet radiation [312] (figure 32). This approach is used to create structural color bar codes in individual microparticles for applications in multiplexed bioassays [313]. Another elegant study showed that colloids could be directed in their assembly using an optically induced electrical field [314].

Post-processing of an already assembled colloidal crystal is another strategy to create hierarchical material architectures. Anisotropic morphologies of inverse opal structures can be achieved through controlled thermal treatment following inverse opal formation by co-assembly [315]. Additionally, two photon polymerization can be used for post-processing colloidal crystals to create cavities and waveguides [316]. Photolithography can be used to create superstructures within a colloidal crystal [278] (figure 26(C)), and reactive ion etching of hollow sphere colloidal crystals can produce complex 3D shapes [317]. The silk inverse opal example presented in section 2.3.1 demonstrates an alternative approach to the multi-scale patterning of photonic materials after assembly [109]. The silk inverse opal



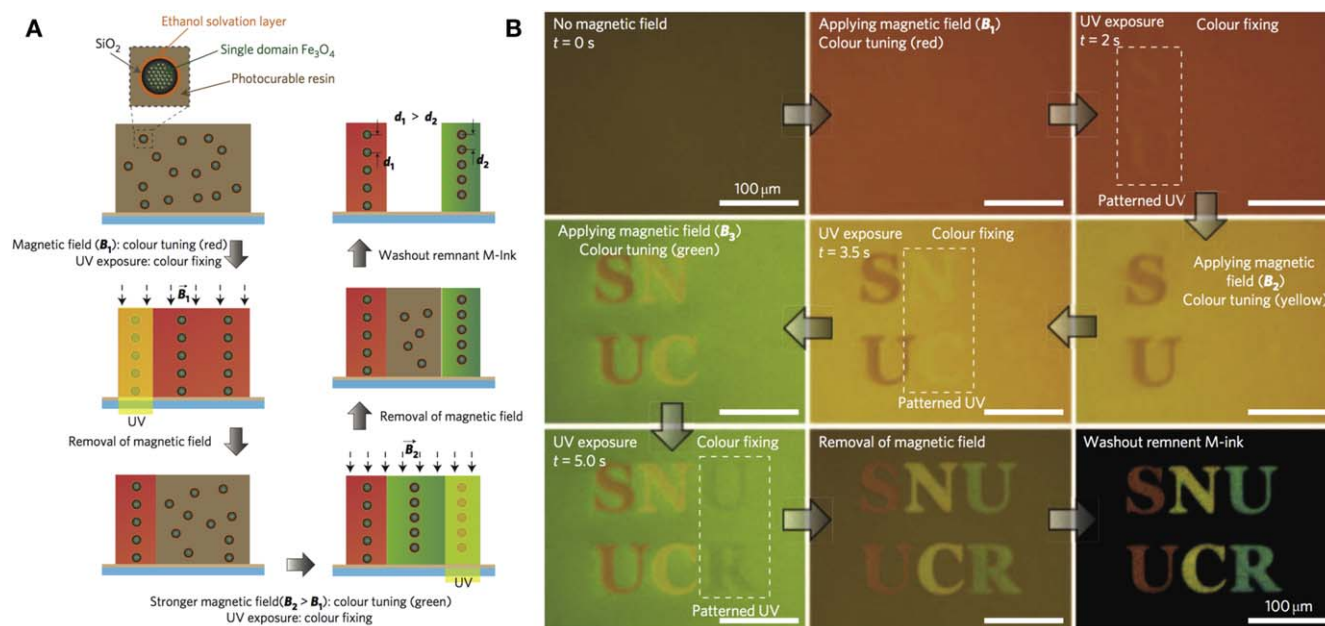


**Figure 32.** Magnetically tunable structural color printing. (A) Diagram showing the printing process. Firstly, a magnetic field is applied to the material, aligning the colloidal nanocrystals (CNCs) in order to generate structural color. Secondly, spatially selective UV exposure fixes the resin in a specific region of the material, locking the CNCs in place. Next, adjusting the strength of the magnetic field changes the color in the remainder of the material, allowing subsequent fixation steps to preserve different colors. Finally, the remainder of the material can be washed out. (B) Optical microscope images showing the printing process in action, including elapsed time at multiple steps. Reprinted by permission from Springer Nature: Nature, Nature Photonics [312], 2009.

can undergo conformational changes in response to a variety of stimuli, including exposure to water vapor and UV light. The study effectively combines pattern control on the molecular scale achieved through controlling conformational changes in the silk, on the nanoscale via colloidal assembly, and micro- and macroscale through spatially selective exposure to light or water vapor. The resulting photonic materials have a controllable color palette spanning almost the entire visible spectral range. This approach beautifully demonstrates how carefully chosen combinations of stimuli-responsive, reconfigurable material constituents, multi-scale assembly strategies, and conventional patterning techniques can lead to the exquisite control of hierarchical material architectures needed to tailor the material's functionality. Formed colloidal structures can also be transferred post-assembly to desired surfaces and materials using a variety of techniques. For instance, transfer printing onto voile fabrics can attach patches of colloidal crystals onto a deformable fabric substrate [318].

**3.4.4. Molecular self-assembly: block co-polymers, DNA-constructs and other biopolymers for structure formation.** In parallel with the development of colloidal assembly processes for advanced material design, efforts centered on the self-assembly of molecular-scale building blocks have received significant scientific interest in recent decades, with potential to create novel photonic materials and devices [319–322]. Block copolymers are particularly versatile for the controlled design of a wide variety of nano-scale material structures [323, 324] (figure 33). An example of the use of block copolymers to form structurally colored filaments used in 3D printing was discussed in section 2.3.3. Another rather complex organic polymeric

material, DNA, has received immense interest in the scientific community over the last decade for its potential to enable the controlled formation of complex hierarchical nano- and microscale material architectures [325]. Finally, other biopolymers, such as cellulose, might have intrinsically favorable molecular interactions that enable the formation of structures with desirable optical properties [326].

The structures that form during the self-assembly of block co-polymers are highly dependent on the morphological characteristics of, and the interactions between, the molecular building blocks. Common parameters that chemists and material scientists have been able to control well are the number of chemically distinct blocks and their respective lengths, the block arrangement in linear or more complicated sequences, and the chemical interactions between blocks. This leads to an incredibly rich design space, which in principle allows for an enormous range of molecular architectures with minimal surface area between the distinct co-polymer building blocks, including layered morphologies [327], perforated lamella, cylindrical structures, bicontinuous gyroid networks [331], and spherical phases of the minority block(s) in the majority block phase [332] (figure 33(A)).

A versatile set of techniques has been developed over the last three decades providing control over specific aspects of block copolymer self-assembly and the resulting material structures [333].

Block copolymers are extensively used for lithographic pattern generation. The pattern period is determined by the polymers' characteristics (such as block length and interaction parameter). Block copolymers enable unique lithographic patterning, and often the polymer pattern provides a template



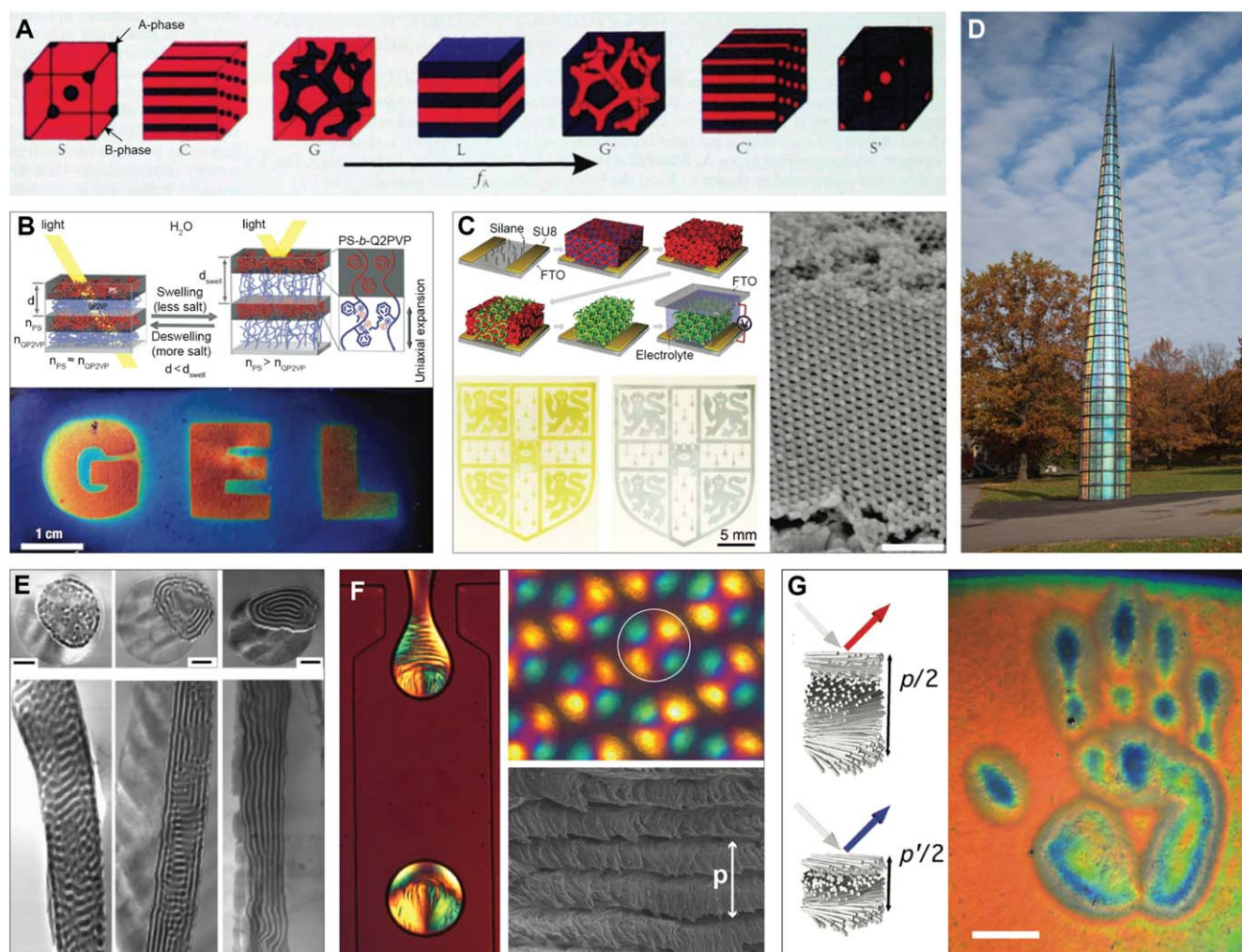


**Figure 33.** Self-assembly of block copolymers and biopolymers. (A) Phase separation morphologies in di-block copolymers.  $f_A$ —ratio of length of block A (black) to overall polymer chain length. (B) Lamellar architecture formed from a polystyrene-*b*-quaternized poly(2-vinyl pyridine) block copolymer. The poly(2-vinyl pyridine) block (P2VP) can be swollen and collapsed by varying the solvent's ion concentration. Schematic diagram of the layered structure and its color tuning that can be achieved through swelling of the P2VP block, which leads to a decrease in refractive index ( $n_{P2VP}$ ) and an increase in layer thickness ( $d_{P2VP}$ ). The photograph shows color adjustment throughout the visible spectral range; different degrees of cross-linking allow to create distinctly colored areas in the gel. (C) Block copolymers are used as templates for electrochromic materials. The schematic shows the process: surface preparation with silanes and photomask, block copolymer microphase separation, selective removal of one phase, electrodeposition of vanadium pentoxide ( $V_2O_5$ ) in the areas not covered by the photomask, and finally removal of the second block phase and assembly of the complete device. The photographs show the electrochromic switching of the  $V_2O_5$  between bluish gray reduced and the yellow-green oxidized state. The scanning electron micrograph reveals the regular ( $V_2O_5$ ) gyroid structure. (D) The Needle Woman on the Cornell University Arts Quad in 2014. The iridescent panels are produced through a scalable block copolymer self-assembly process. This artwork resulted from a collaboration between the research group of Professor U Wiesner, artist Kimsooja, and architect J Chong. (E) Assembly of block copolymer morphologies within the confinement of electro-spun microfibers. (F) Assembly of helicoidal cellulose architectures in microscale droplets using microfluidics. Droplet size is  $\approx 140 \mu\text{m}$ . Polarization microscopy reveals a pronounced Maltese cross-like pattern, which indicates radial ordering of the cellulose nanocrystals. A scanning electron micrograph shows the helicoidal architecture of the cellulose nanocrystals ( $p$ —pitch). (G) A pressure-responsive cellulose photonic film. Compression induces a reduction of the helicoidal structure's pitch and corresponding color variation (scale 4 cm). (A) Reprinted from [323], with the permission of AIP Publishing. (B) Reprinted by permission from Springer Nature: Nature, Nature Materials [327], 2007. (C) [328] John Wiley & Sons. Copyright © 2012 WILEY-VCH Verlag GmbH & Co. KGaA, Weinheim. (D) Used with permission from J. Kosky, Cornell University Photography. (E) [329] John Wiley & Sons. © 2006 WILEY-VCH Verlag GmbH & Co. KGaA, Weinheim. (F) Reprinted with permission from [310]. Copyright (2016) American Chemical Society. (G) Reproduced from [330]. CC BY 4.0.

that then is populated with the desired inorganic or organic functional materials via conventional microfabrication procedures such as selective etching and deposition in the resulting voids [334]. In contrast to conventional pattern generation, which is often confined to planar patterns, block copolymer

templating can achieve three-dimensional material architectures with desirable optical functionality [335–337]. In turn, comparable to templated colloidal assembly, block copolymer structure formation can be influenced by topological patterns created with conventional microfabrication approaches, by

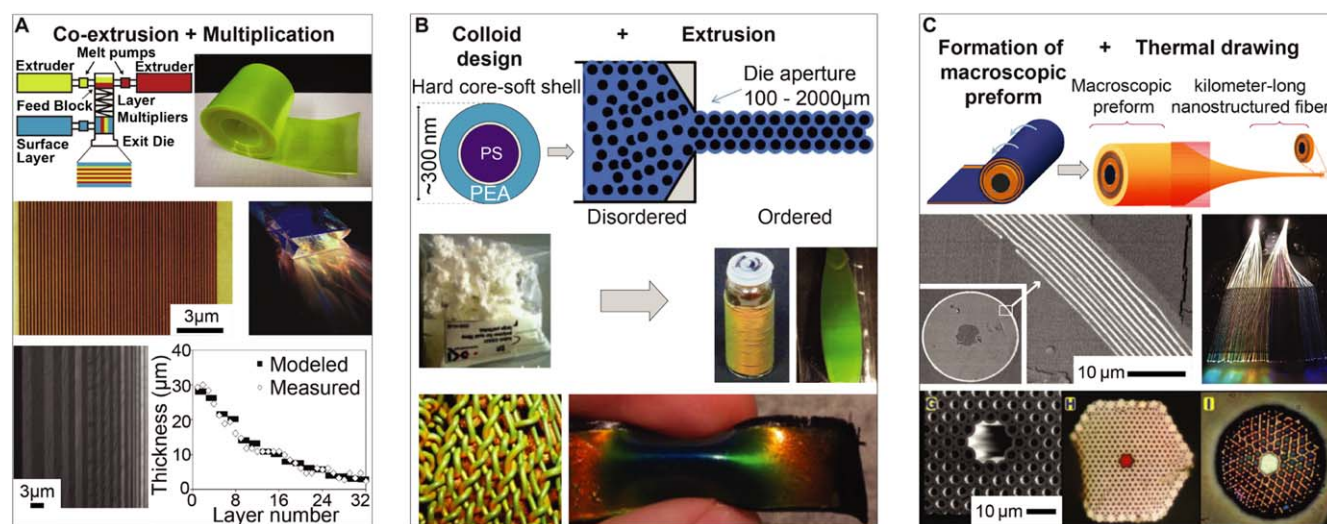


**Figure 34.** Coextrusion and thermal drawing of nanostructured materials. (A) Coextrusion and multiplication of two or more optically distinct polymer layers. Using special dyes the layers can be multiplied by factors of two for each dye stage, while the individual layers get thinner and thinner. A coextrusion and layer multiplication setup is shown schematically in the top figure, next to a multilayered film on a roll, which is used for high capacity optical data storage. The second row shows a coextruded giant birefringent multilayer stack imaged with atomic force microscopy and a photograph of light guided through that structure. The image in the bottom row shows a coextruded multilayer with gradually varying layer thicknesses; the layer thickness variation is graphed to the right. (B) Extrusion of colloidal particles with a soft shell. Colloids are formed from a hard polystyrene (PS) core and a soft polyethylacrylate (PEA) shell. During extrusion at around 150 °C the colloids form ordered iridescent opal structures. The colloidal precursor material shown in the second row can be formed into 3D photonic crystal fibers or sheets. Fibers can then be woven into more complex architectures, as shown in the third row. The material is deformable and changes its color when a strain is applied. (C) Thermal drawing of macroscopic preforms to form nanostructured photonic fibers. A preform can be formed by rolling and thermally consolidating individual structural elements; it is then drawn down from ten's of centimeters of diameter to ten's of micrometers. The second row shows a scanning electron micrograph of a drawn fiber with a multilayer cladding (Scale bar 10  $\mu\text{m}$ , inset 100  $\mu\text{m}$ ). The photograph in the second row on the right shows a textile woven from thermally drawn multilayer-clad polymer fibers, which guide and scatter light. The bottom row shows a selection of 2D photonic fiber designs produced by thermal drawing. ((A) bottom) Reprinted with permission from [351]. Copyright (2010) American Chemical Society. ((A) middle) From [345]. Reprinted with permission from AAAS. ((A) top) [343] John Wiley & Sons. Copyright © 2012 WILEY-VCH Verlag GmbH & Co. KGaA, Weinheim. ((B) middle left and bottom right) [355] John Wiley & Sons. © 2013 Society of Chemical Industry. ((B) top, bottom left and middle right) Reproduced with permission from [354], OSA. ((C) bottom) From [359]. Reprinted with permission from AAAS. ((C) middle left) From [357]. Reprinted with permission from AAAS. ((C) middle right) Reproduced with permission from [358], OSA. ((C) top) [356] John Wiley & Sons. Copyright © 2006 WILEY-VCH Verlag GmbH & Co. KGaA, Weinheim.

chemically-patterned templates [338], or by assembling the block copolymers within the confinement of electro-spun fibers [329, 339] (figures 33(E), (F)). The morphology of block copolymers can also be controlled electrostatically by varying the charge of the polymer blocks, which tailors the interactions between blocks during assembly and greatly expands the available structure design space [340]. Most importantly, block copolymers can be used to form structurally colored, iridescent films in scalable manufacturing procedures, as recently demonstrated by researchers and artists at Cornell who created the Needle Woman, an art installation over 10 m high, assembled from iridescent block copolymer-coated panels [341] (figure 33(D)).

DNA-mediated assembly of optical materials is another promising strategy for forming structures with a programmed nano- or even microscale morphology [325]. This intriguing approach is based on the principle that the complex interactions between DNA nucleotides can be harnessed to program a specific folding and assembly behavior by carefully controlling the assembling DNA's nucleotide sequence. Although small throughput hampers the scalability

of this approach, and although the nucleotide sequence requires careful design and testing, DNA assembly represents an exciting strategy that could potentially change the way how we control material formation processes from the bottom-up. By combining DNA with other components, such as nanoparticles and colloids, functional building blocks can be programmed to exhibit specific interactions with other building blocks. These strategies bear promise for a wide variety of applications, including the design of novel optical materials [342, 343]. DNA is not the only biopolymer known to show interesting assembly behavior. Other readily available biopolymers—such as cellulose, the most abundant biopolymer on earth—have great potential for nano- and microscale structure control. Analogous to the cellulose-based photonic structures found in tropical fruits [28, 31], synthetic cellulose films can adopt a helicoidal nanoscale architecture by self-assembly of the constituent cellulose nanocrystals into chiral nematic liquid crystalline phases; these are preserved in the dry cellulose structures [326, 344]. An interesting strategy to control arrangement of the helicoidal structures and to impose hierarchy is to assemble cellulose nanocrystal



structures within the confinement of microdroplets, similar to colloidal assembly [310] (figure 33(F)).

**3.4.5. Forced micro-assembly: coextrusion and thermal drawing of macroscopic architectures to micro- and nanoscale dimensions.** A discussion of micro- and nanoscale structure assembly would be incomplete without addressing two techniques that are widely employed in industrial manufacturing settings: co-extrusion and thermal drawing (continuous structure formation processes). For several decades, forced co-extrusion processes have been very successfully employed to form layered photonic materials [345, 346–350]. In this technique, two or more polymers with appropriate thermal and rheological properties are co-extruded through a set of layer-multiplying extrusion dies. This allows for the formation of Bragg stacks—layered photonic crystals with several tens to thousands of layers—with layer thicknesses ranging from a few tens of nanometers to several micrometers, thereby providing a high degree of control over the Bragg stack configuration (figure 34(A)). Smart design of the extrusion dies allows for the creation of controlled graded variations in layer thickness across the multilayer stack, which allows for fine control of the material's optical performance, as well as the optimization of its mechanical properties [351]. Depending on the extrusion die, layered 1D photonic morphologies of different shapes and also 2D photonic morphologies can be extruded. Block copolymer self-assembly can be combined with forced coextrusion to form materials with multiple periodicities across different length scales, thereby greatly expanding the complexities of realizable hierarchical architectures [352].

Other functional materials can be incorporated into the co-extrusion process to enable advanced optical materials, such as multilayer films that can be used for high capacity optical data storage [353]. By using thermoplastic elastomers, photonic materials with dynamically tunable optical response can be realized [349]. Furthermore, fibers and sheets with three-dimensional photonic structures can be extruded using tailor-made colloidal particles with hard cores and soft shells of different refractive indices [360–363] (figure 34(B)). This approach has several advantages: (1) the soft shell of the colloids imparts the material with the ability to deform in response to mechanical stimuli, which in turn induces a variation in the material's coloration. (2) Variations in the design of the colloidal particles leads to different structural periods and hence different material colors. (3) The amount of ordering in the colloidal structures of the stretchable photonic material can be tailored during manufacture, allowing for adjustment of the material's optical appearance. (4) Most importantly, extrusion—an industrially well-established process—allows for high throughput manufacture.

Thermal drawing, the same technique applied to form optical fibers, is another high throughput approach to continuously form photonic structures with nanoscale periodicity [357, 359, 364, 365] (figure 34(C)). Here a macroscopic preform, such as a layered stack of polymer sheets or a stack of glass capillaries, is first consolidated

thermally and then drawn down to microscale dimensions in one or more drawing steps. This process can produce photonic fiber structures with one-, two-, and even three-dimensional structures with controllable periodicity [366]. These fibers can then in turn be used to form photonic materials, for instance by weaving or other commonly applied textile manufacturing approaches [358].

**3.4.6. Additive manufacture—printing in two and three dimensions.** Additive manufacturing—a term that is often used to describe industrial 3D printing—encompasses a broad variety of techniques that rely on building up complex material structures ‘bit by bit’, i.e. the structure is formed from individually deposited units of material. These techniques are very useful in controlling ‘what’ (material, building block, functional component) ‘goes where’ (location within the formed structure). Here, we include and discuss several notable techniques under the umbrella of additive manufacturing. In particular, we will elaborate on the utility of 3D printing of structurally colored materials, direct write lithography, and jet printing, for forming materials with interesting optical properties.

The 3D-printed material discussed in section 2.3.3 is an example of utilizing structurally colored materials in additive manufacturing to achieve color in macroscopic structures. This approach is characterized by the temporal separation of structure formation by self-assembly on the nanoscale and the shaping of the nanostructured material on the micro- and macroscale [125]. Presumably, with the appropriate 3D printing equipment, structurally colored materials with feature resolution of around one micrometer could be achievable with this technique [367]. Another strategy that combines self-assembly and additive manufacturing is the modification of block copolymer layers with inkjet printing [368]. Here, a block copolymer is first cast into thin films, where it self-assembles into a lamellar architecture, thus forming a multilayer reflector. Subsequently, selective spatial application of a crosslinking agent using a modified inkjet printer limits the swelling thickness in specific regions, which in turn defines the wavelength of reflected light in that sample area. This can be reversed by the application of an uncrosslinking agent.

On even smaller length scales, photonic crystal geometries and other optical elements can be formed by direct laser writing, a technique that employs multiphoton absorption processes for photo-crosslinking polymers with diffraction-limited resolution [369–371]. The creation of a chiral beam splitter with gyroid photonic structures similar to the ones found in butterfly wing scales represents a beautiful demonstration of the capabilities of direct-write lithography for photonic device design [372] (figure 35(A)). Another example is the design of multicomponent microscale objectives on optical fibers and imaging sensors using two-photon direct laser writing [369] (figure 35(B)). Direct-write techniques provide opportunities for prototyping on the nano- and microscale with a large variety of material systems and



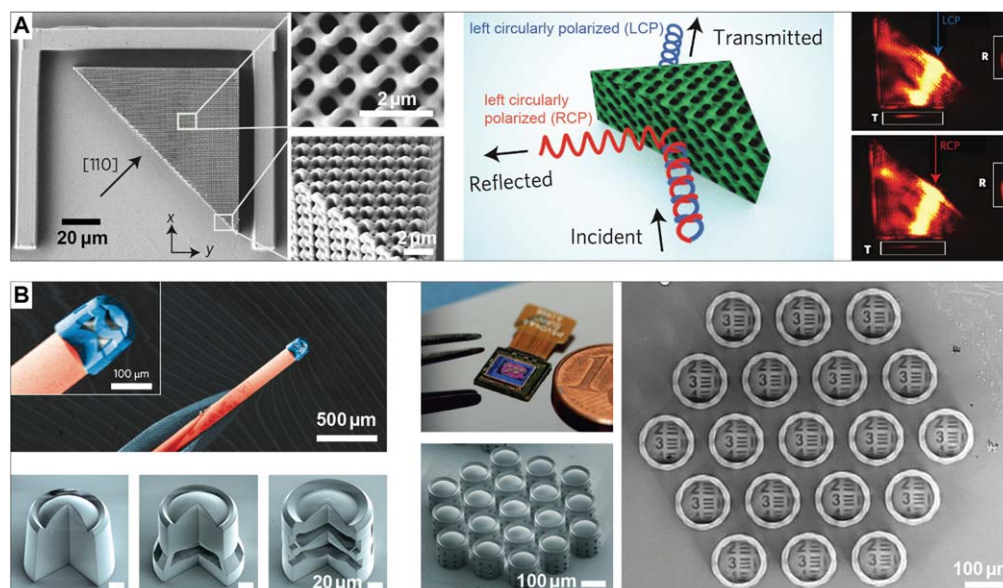


**Figure 35.** Direct laser writing of optical materials and devices. (A) A miniature chiral beam splitter consisting of a gyroid photonic crystal produced by direct laser writing. The scanning electron micrographs show the device and two zooms focused at its center and one corner. The schematic shows the working principle: the periodic chiral gyroid architecture can reflect circularly polarized light of one handedness, while transmitting the other. This is experimentally demonstrated in the images on the right: left circularly polarized (LCP) light of 1615 nm wavelength is preferentially transmitted, while right circularly polarized (RCP) light is mostly reflected. (B) Miniature multi-lens objectives produced with two-photon direct laser writing. The false-colored scanning electron micrograph shows a lens attached to the end of an optical fiber. The images on the bottom-left show different objective designs with one, two, and three lens elements. The images on the right show an array of objectives directly fabricated on a CMOS image sensor together with a test pattern visualized through the lens array. (A) Reprinted by permission from Springer Nature: Nature, Nature Photonics [372], 2013. (B) Reprinted by permission from Springer Nature: Nature, Nature Photonics [369], 2016.

desired structures for targeting a diverse range of applications. One shortcoming of the technique might be limitations to its scaling potential due to the sequential writing nature, although these limitations might be addressed through clever technology design involving multi-beam approaches [373], or the utilization of direct writing to form master patterns that can then be replicated in soft, polymeric materials hundreds of times [374].

In nature, many of the assembly processes involved in hierarchical material structure formation occur in parallel. Similarly, additive manufacturing approaches have great potential to define material structure on the macro- and microscale, while enabling nano-scale pattern assembly through simultaneously occurring self-assembly processes. The confinement of the self-assembling building blocks to small material volumes provide useful bounds on the forming structures, defect density, and orientation similar to the compartmentalization that plays a crucial role in the formation of biological photonic structures within cells and scales, as discussed earlier. For example, inkjet printing can be used to arrange colloidal particles in a variety of photonic patterns [104, 375, 376], as shown in figure 36. Similar techniques have been used as the basis for anti-counterfeiting methods [377, 378], creating spherical colloidal crystals [379], and photonic crystal domes for wide-angle viewing displays [380]. Inkjet printing has also been used to directly print colloidal photonic architectures on flexible, topographically complex fabrics [381].

Many different parameters influence the accuracy and resolution of inkjet printing, including surface wetting,

droplet impact and spreading, droplet coalescence, and process dynamics; if these and other parameters are well-controlled, printing resolution of a few micrometers should be achievable [382], defining the microscale compartments of ink, in which building blocks can self-assemble.

**3.4.7. Formation of dynamic optical materials.** A huge variety of dynamic optical materials have been proposed over the last two decades [100, 298, 383–386], many of which rely on the synthetic processing strategies discussed above. Below, we discuss a few cases and provide examples with interesting aspects regarding the involved material formation processes.

Tuning strategies employed in synthetic responsive photonic materials can rely on a variety of effects (figure 37(A)). Here, we focus on two particular phenomena, which are closely related to the biological strategies for color tuning: (1) the reversible deformation of the material's nano- and microstructure to vary its spectral response, and (2) a controlled change in refractive index contrast or absorption strength in porous photonic architectures by exchanging the medium within the pores.

The first strategy relying on reversible deformation of the material structure is primarily implemented through the use of soft materials, which can be processed with a wide range of structure formation processes, many of which have been discussed above. Soft material structures deform in response to mechanical stimuli, providing a predictable variation in optical response (figures 37(B)–(D)) [291, 387, 389, 390]. Alternatively, soft materials can be swollen with the

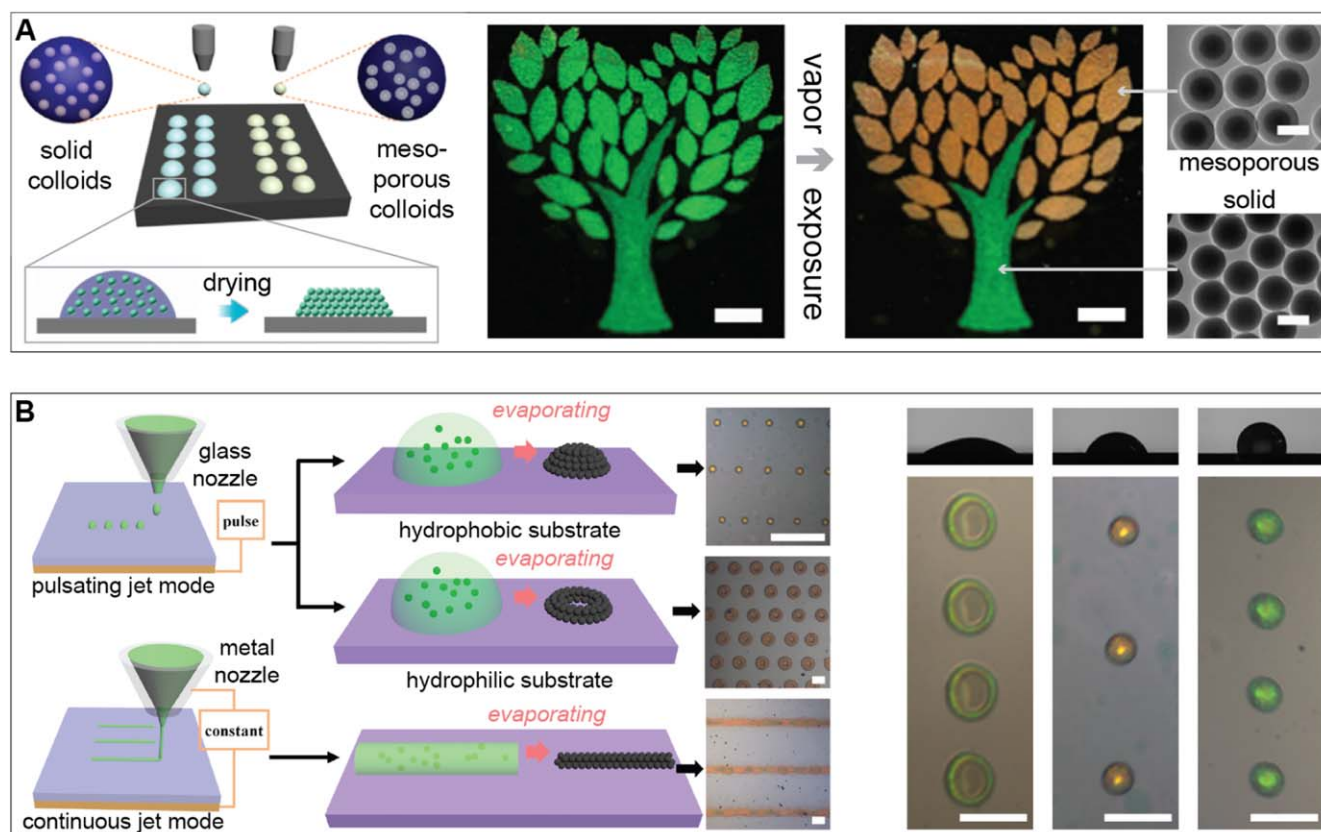


**Figure 36.** Inkjet printing of photonic crystals. (A) Inkjet printing allows for the localized deposition of suspensions with different colloidal species that assemble within the confinement of dispensed droplets. Inkjet printing provides structure control on scales upwards of  $10\ \mu\text{m}$ ; within the drying droplets photonic crystals form by self-assembly. Here, two colloidal species—one solid and one mesoporous—are assembled in the tree pattern. Absorption of solvent vapor within the mesoporous colloids leads to a change in refractive index, which induces a color shift that can be used for vapor sensing (scale:  $200\ \mu\text{m}$  in the photographs,  $200\ \text{nm}$  in the transmission electron micrographs). (B) Electrohydrodynamic inkjet printing of colloidal crystals with varying morphology using different deposition modes (pulsed and continuous) on substrates with tailored wettability. The diagram shows the deposition of a colloidal suspension to create dot patterns or continuous lines. The micrographs in the top-right corner show the droplet morphology on substrates with varying wettability; below optical micrographs of the resulting colloidal crystals are displayed (scale for all in (B) is  $100\ \mu\text{m}$ ). (A) Reprinted with permission from [104]. Copyright (2014) American Chemical Society. (B) Reprinted with permission from [376]. Copyright (2017) American Chemical Society.

appropriate solvents (figure 33(B)), reconfigure in response to temperature variations [391], change configuration in magnetic and electric fields [392, 393], or even react to light exposure [394]. In many cases, a deformation of the material's structure coincides with a change in refractive index, which is particularly evident in the case of tuning strategies that rely on swelling [327].

One recent example of a pressure-responsive soft photonic material cunningly exploits the self-assembly of a cellulose derivative into ordered helicoidal structures in a cholesteric liquid-crystalline phase, which reflects circularly polarized light of specific wavelengths that are determined by the structure's pitch [330] (figure 33(G)). Exerting pressure on the material leads to a change in pitch and a corresponding variation in color. Given that cellulose is the most abundant biopolymer on earth and that the fabrication of this material consists in letting self-assembly take its course between two polymer sheets, this approach promises to be easily scalable to industrial manufacture. The formation of cellulose-based hydrogels that can respond to solvents, pH, or temperature

represents another interesting strategy to make use of this abundant biopolymer [395].

Another example of an optical material responsive to mechanical stimuli are color-tunable photonic fibers (figure 37(B)). These fibers can change color throughout the whole visible range in response to strains between a few to over a hundred percent. They are formed in a somewhat exotic manufacturing process comprised of standard thin-film formation via spin-coating, and subsequent rolling of the thin elastomer films that are stabilized on a water surface onto an elastomeric core fiber [387]. Alternatively, layer-by-layer deposition of self-assembling bilayers has yielded soft, hydrogel-based photonic crystals [396].

A versatile strategy to alter a material's optical appearance is to reversibly vary the light absorption within the material temporally and spatially. This can for instance be achieved elegantly with electro-chromic materials formed from nickel oxide and assembled into nano-scale gyroid architectures [336, 397]. The material is fabricated by first forming a block copolymer template via self-assembly and



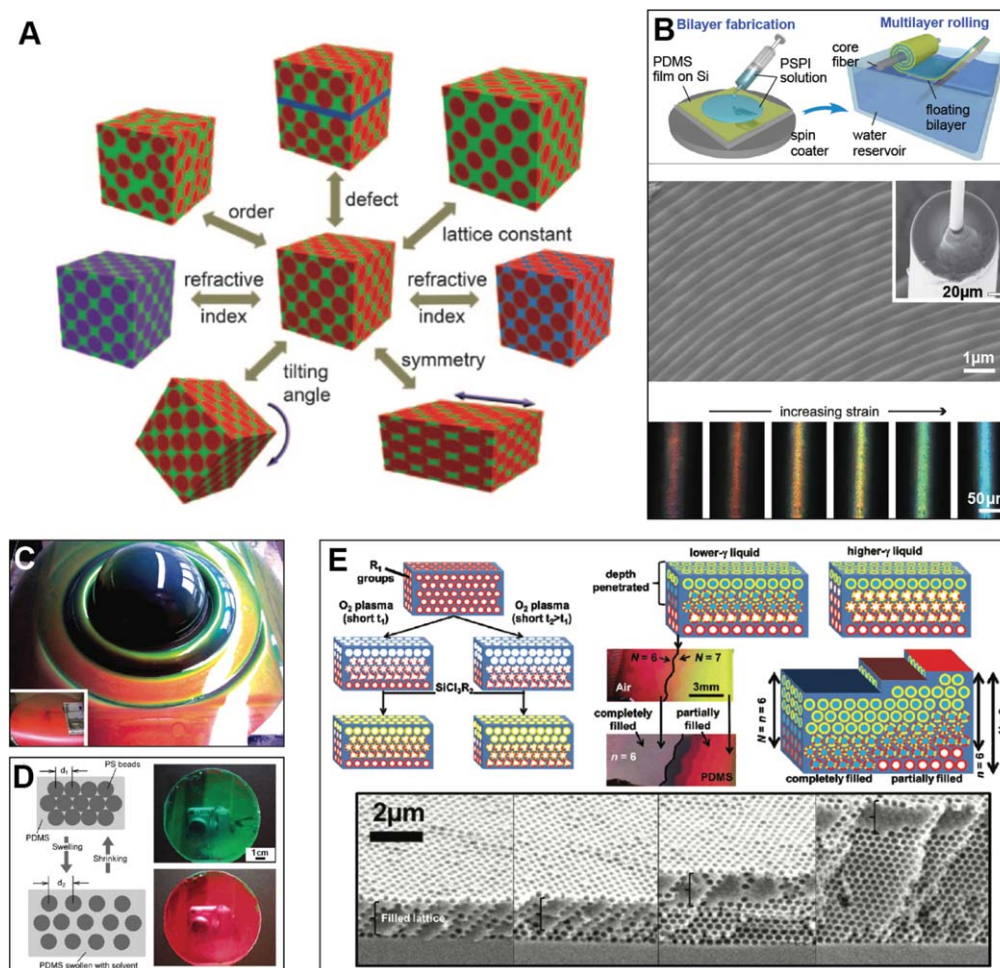


**Figure 37.** Materials with tunable structural color. (A) Illustration of the variables that can be varied to change the color of tunable photonic materials. (B) Stretch-tunable photonic fibers, formed by spin-coating a thin bilayer of elastomers with different optical density, which is then rolled onto an elastic core fiber. The scanning electron micrograph shows the fibers' multilayer cladding. The fibers change color when stretched. (C) A deformed sheet of stretchy elastomeric opal formed from hard core-soft shell colloids; the bottom-right inset show the undeformed sheet. (D) Swelling and de-swelling of an opal structure to tune its color. (E) Color tuning in inverse opals by selective infiltration with fluids and cross-linkable polymers. The sketch on the top left shows the procedure of modifying an inverse opal with silanized surfaces by timed plasma-exposure. The exposure degrades the silane layer, which alters the pores' wetting behavior. The sketch on the top right and photos in the center insets show how partial wetting of this structure results in a variation in color. The scanning electron micrographs show inverse opals with different layer number partially filled with a polymer. (A) [384] John Wiley & Sons. Copyright © 2011 WILEY-VCH Verlag GmbH & Co. KGaA, Weinheim. (B) [387] John Wiley & Sons. © 2013 WILEY-VCH Verlag GmbH & Co. KGaA, Weinheim. (C) Reprinted with permission from [291]. Copyright (2007) American Chemical Society. (D) Reprinted with permission from [388]. Copyright (2003) American Chemical Society. (E) Reprinted with permission from [297]. Copyright (2012) American Chemical Society.

then selective etching and replacement of the block copolymer phases with the desired functional material, which in this particular case involved electro-deposition.

Alternatively, the replacement of a medium infiltrating a porous photonic architecture can be employed to change the material's optical signature (figure 37(E)) [297]. This concept is widely applied in opal and inverse opal photonic materials produced via a wide variety of processes that combine self-assembly with other microfabrication approaches, and has also been used in for vapor sensing with butterfly-inspired hierarchical microstructures formed by electron beam lithography processes [268].

Chemists, material scientists, physicists, and engineers have conceived a broad variety of processes to tailor

material structures from the nano- to the macroscale, in order to achieve a wide range of functions. Advanced nano- and microfabrication techniques applied to semiconductor components and soft materials have been used to produce structurally colored materials. In parallel, directed assembly strategies have evolved to the point where molecular and nanoscale colloidal building blocks can be assembled into structures with desired regularity and periods that are appropriate for the interference and diffraction effects required for structural colors. Many processes combine top-down with bottom-up strategies to realize hierarchical material architectures that exploit synergistic combinations of absorption, fluorescence, interference, diffraction, and geometrical optics to achieve unique optical responses.



## 4. Conclusions and perspectives

The nano- and microscale structure of a material is a critical factor in defining its function. Processes that reliably produce these structures are therefore essential for enabling the correct performance of a biological or synthetic material. Many parallels exist between biological and synthetic structure formation principles, but there are also fundamental differences between processes evolved in nature and approaches conceived by humans.

### 4.1. Insights to be gained from comparing biological and artificial structure formation processes

The reader may have found that the scope of the biological process section slightly differs from the one in the synthetic process section. In the biological section, we described exemplary processes phenomenologically, tying in hypotheses about process dynamics and underlying principles, provided any exist. However, most formation processes for structurally colored materials are yet to be deciphered, leaving us with the longing for more specific details to be discovered. In the synthetic process section, conversely, we point out exemplary processes that can be utilized to make particular material architectures. In a sense, these different scopes reflect an interesting contrast in the field of structural coloration. On one hand, the study of material-forming processes in biology prioritizes a deeper understanding—that is, it is aimed at describing biological structure formation processes and the resulting outcomes in qualitative and quantitative ways. On the other hand, the study of synthetic structure formation processes is focused on understanding a process sufficiently well to reliably implement and control it—in other words, mastering the application of physical and chemical principles to realize a specific material structure. These two aspects perhaps represent two sides of one coin: knowledge about the parameters (such as material constituents, their physical and chemical interactions, and their temporal and spatial occurrence) that enable a biological structure formation process on the one side, and the ability to control all relevant parameters in a synthetic process to systematically alter the structural outcomes on the other. Taken together, these two sides should allow us to broaden the realm of processes that, in principle, could be part of the human materials processing library (given that we can observe them in nature) and to develop mastery over these processes to significantly enlarge our repertoire of available material structures and functionalities.

**4.1.1. Process contexts and conditions.** Both synthetic and natural processes control the location of the final structure's material constituents, using auxiliary materials for support and additional infrastructure for manipulating and regulating these materials. However, the conditions for biological and synthetic processes are starkly different. Many biological systems will regulate their temperature and pH [398], which often are necessary for optimal enzyme function. On the other hand, synthetic processes may operate on various different

temperature conditions (often in temperature ranges that are prohibitive for most or all known organisms) to create favorable conditions for material shaping and conversion during different process stages. Conversely, biological processes that create structurally colored materials operate in 'messy' environments, which involve a multitude of elements and processes unrelated to the structurally colored material, while synthetic processes are often tailored for relatively pristine environments and carefully controlled material constituents. The 'messiness' in biological processes in part might result from the organisms' need to ensure multiple functions within the same material. Thus, the optical appearance is usually not the only performance criterion that the material formed by the organism has to satisfy; mechanical robustness, interfacial interactions, heat, and nutrient transport characteristics might be other relevant metrics. In synthetic processes we still largely optimize for one property. There may be lessons to be learned from messy biological processes regarding the efficient integration and co-optimization of a multitude of functions on the materials level.

Furthermore, physical phenomena underlying the formation of any particular biological photonic structure impose constraints on the practically achievable system parameters and tolerances, such as structural resolution, structural regularity, and short- and long-range order. Studying the processes underlying the formation of biological systems with desirable parameters and tolerances could teach us valuable lessons for the synthetic or even bio-sourced manufacture of novel optical components.

**4.1.2. Process principles.** Biological organisms employ a few remarkable approaches to robustly handle material formation processes in the complex conditions that they work in. The first strategy is compartmentalization. All cells have a plasma membrane that helps define a barrier between the intracellular and extracellular regions. Moreover, the interior of the cell itself is subdivided by various membranes, such as the iridophore lamellae that contain reflectin separate from the material in the rest of the cell. A second strategy is intracellular transport. A whole host of methods exist to provide shipping from one point to another within the cell, including (but certainly not limited to) reaction-diffusion, microtubule transport, transport via the Golgi apparatus, and targeting molecules. Both compartmentalization and intracellular transport contribute to a third, broader strategy—the spatially and temporally distributed availability of material constituents. Although further material shaping may be achieved by directed self-assembly, the local availability of molecules contributes substantially to material structure formation.

The state of parameters and boundary conditions are also key differences between 'messy' biological systems and the 'clean' environment of synthetic approaches. Humans often use processes designed to operate close to an equilibrium, but biology operates at non-equilibrium to achieve many transient

phenomena. In addition, parameters in synthetic manufacturing tend to be defined globally, while a cell may control the local parameters, such as manipulating water or protein content. In addition, boundary conditions in synthetic systems are often static, while a hallmark of the growth of biological systems is their continuously changing boundary conditions.

The scale of manufacturing is also another key distinction. Since the reaction chamber for many biological processes is limited at least to the cell, the size of the cell is a rough upper bound for individual photonic elements—an important exception being materials secreted to form shells, feathers or hairs with internal structure. Synthetic approaches do not have the size limitation of the cell, and instead are limited by their ability to reliably regulate the sizes and order of features in the structurally colored element; often, this allows larger individual material products. It is ironic, however, that synthetic techniques generally require larger infrastructure and equipment to create morphologies with finer resolution.

Both synthetic and biological approaches tend to have limited scalability in terms of their throughput. In synthetic approaches, this is due to both limitations of size and the time required to organize precise morphologies (although the scale of this time varies greatly depending on the technique). Biological organisms, for their part, must balance all the other life-sustaining activities as well as procure the molecular substance to create the structurally colored material.

Hierarchical materials offer a tantalizing opportunity for exploration, since they often rely on the interplay of multiple processes. Biological, structurally colored materials tend to have a high degree of hierarchy. In human-made materials, we are still exploring how to enable and control different degrees of hierarchy in a fashion that optimizes the material's functionality [399]. Hierarchical biological structures in general appear to arise from the highly interdependent relationship between form, microstructure, and the processes occurring during their growth [205]. In synthetic systems, hierarchy is often brought about by using relatively distinct processes to impose the required periodicity at each desired length scale, often in a sequential fashion. Further opportunities in functional material hierarchy may lie in achieving more efficient integration of multiple processes, perhaps by better understanding, emulating, and accelerating biological growth processes.

**4.1.3. Making synthetic fabrication methods (even) better.** A valid method to overcome limitations on throughput in any particular structure formation process is to run many instances of this process in parallel, a strategy used in biological and synthetic materials alike. In biology, this is often seen in the formation of more or less identical structures within multiple cells, which is the case in the formation of thousands of scales on wings of butterflies and moths. This parallelization is enabled by the genetic information carried by cells; one of the decisive drivers of structure formation processes are the genes. It is therefore paramount to understand the interplay of different individual genes and the genetic circuits that contain the code for and initiate the structure formation within or around a cell. However, genes and all the materials

expressed are undoubtedly subject to the laws of chemistry and physics, hence there is a second important component to understanding structure formation: the physical and chemical interactions between the material's components, once their expression has been initiated by genetic pathways [400].

To frame the situation with the words of Helen Ghiradella, one of the leading experts on structure formation in butterfly scales: 'little work has been done on the reasons for this kind of patterning, but it is an article of faith that those reasons do exist; biological systems do not expend energy and information on trivial pursuits. We need to know how the animal codes and interprets the genetic information to specify lamellae, microribs, laminae, and lattices. While studies to date on scale formation are far from conclusive, they do suggest that at least some of the construction is the result of simple physical and mechanical processes (e.g. elastic buckling, surface tension, etc.) acting on the impressionable cuticle as it forms' [15]. What mechanical effects, transport phenomena, and chemical relations are involved in the formation of these intriguingly complex structures and how are these phenomena guided through appropriate spatial and temporal control of material expression by the genes?

In an article on the color-producing nanostructures in bird feathers about a decade ago, Richard Prum, a leading authority on the formation of photonic elements in feathers, asks the following questions: 'how do these color-producing nanostructures develop? What physical and biological mechanisms do organisms use to construct arrays of quasi-ordered and highly periodic nanostructures?' before concluding that '... surprisingly, these fundamental questions have been little studied' [222]. While these views and questions on structure formation in butterflies and birds have motivated different efforts to reveal the underlying principles, as discussed in section 3.3, they are still valid today.

Another important angle is added by a question posed by Joanna Aizenberg and Peter Fratzl in the lead article of an *Advanced Materials* special issue on biological and biomimetic materials in 2009: 'how do we reformulate biological designs in man-made structures and create bioinspired advanced materials that are structurally and functionally optimized, that can build themselves, repair themselves and evolve?' This line of thinking might also entrain the following questions: can we utilize insights about the formation processes to establish very different material systems that support analogous physical and chemical interactions to form better synthetic materials? In the interim, could some of the biological machineries be employed to form desirable nano- and microstructures?

While there are a great many variations in the processes that organisms employ to form their functional material structures—most of which remain to be fully understood—the laws of physics and chemistry apply to all of them. This implies that perhaps we should expect some convergence of the strategies employed by related and non-related organisms to form materials with similar architecture. Understanding the formation of the generic scale structures in *Vanessa cardui* might open the door to revealing the process parameter modifications that are necessary to tweak the base scale blue-

print for forming the *Morpho* butterflies' elaborate scale ridges. The formation of spines of seashells occurring due to evolving mechanical interactions of the soft mantle and the already deposited hard shell might hold parallels to the processes that lead to the spatially-selective chitin expression on the butterfly wing scale membrane during formation of intricately patterned ridges and cross-ribs. Likewise, the helicoidal cellulose architectures in structurally colored tropical fruit and the cholesteric liquid-crystal-like cuticle morphologies of some brightly reflecting beetles might share common traits in their formation processes. Moreover, the current state of the literature suggests that a vast proportion of biological coloration structures are formed in template-molding and controlled self-assembly processes, acting on newly expressed material, which is often brought to the appropriate location in an additive fashion. So, while structure formation processes are complex and challenging to study, insights obtained from one organism might help us to decipher another organism's approach to forming similar structures. Understanding the details of these broader themes in structure formation processes across living organisms could lead to insights regarding the synthetic manufacture of optical materials.

In synthetic materials development, the chemist or material scientist is the driving force that chooses the material constituents, and conceives of processes to tailor the material composition and morphology to achieve a desired outcome. Human manufacturing has become particularly adept at manipulating a truly broad set of substances that are employable for structurally colored materials (as opposed to the more restricted set of biological material classes). One area of particular success has been the tailoring of the 'building block' for self-assembly (such as block copolymers, colloids, and DNA-mediated approaches). As a consequence of having a desired material with particular performance attributes as the prescribed goal, human-designed synthetic processes usually rely on controlled conditions and strict sequences of procedural steps that might have arisen from an iterative optimization scenario.

By contrast, natural organisms merely follow a genetically imposed program; this program has evolved under the harsh scrutiny of any random mutation's benefits for the organism in its strive to survive, mate, and compete for limited resources in its environment. Biological evolutionary processes run on timescales that are incompatible with the timespan of a human life and by no means should we follow nature's approach to randomly modify, scrutinize, and reject material solutions ... unless it can be done on a much shorter timescale. Computational efforts for evolutionary materials design with a specific objective and a clear metric for performance evaluation could implement this approach to be run on faster timescales and to provide guidance to chemists and materials designers in vast and difficult to screen parameter spaces, before attempting to synthesize a new material [401].

A complimentary strategy in the development of synthetic processes is to regard the study of nature's structure formation principles as establishing useful principles and

good starting parameters within often dauntingly large parameter spaces. To this end, we should comply with a philosophy that was recommended for biomimetic approaches that target the realization of specific material structures [205]: for biomimetic process design to make a positive difference in manufacturing it is very important to know the boundary conditions and constraints under which the organism has implemented the target process. In addition, we should aim to understand the processes' influence on the resulting material performance. Consequently, biomimetic approaches for process design in general necessitate two efforts, which do not necessarily have to occur in sequence: (1) we have to gain a quantitative understanding of the processes occurring in nature and elucidate strategies to control them. (2) We have to implement them in synthetic material systems. A hybrid approach could be to hijack and utilize biological formation processes to form structured materials of interest to humans. If successful we might reconcile some of the differences between biological growth and synthetic fabrication, which could enable the design of materials and devices with unprecedented functionality.

#### 4.2. Opportunities in bioinspired process design

A common practically employed definition of bioinspiration appears to be 'taking a cue—any cue—from biology'. However, it might be prudent to be careful with the usage of the term 'bioinspiration' for it to keep a useful meaning. Surely most readers would agree that it would be too far-fetched to say the proverbial apple 'bioinspired' Newton's ideas about gravity. Parallels between a natural and a synthetic system should be obvious and there should be something to be gained on the synthetic side, when taking inspiration from a natural system. And there is much to be gained: considering the discussion above, the human toolbox of materials and device manufacturing processes could likely be significantly expanded with better understanding and emulation of the principles and processes underlying biological structure formation. It seems prudent, therefore, to explore the possibilities for new and improved processes.

The bio-optics community has a history of mimicking the *morphology* of biological structurally colored materials, yet often through *methods* and *processes* that are distinctly different from the structure formation principles in the biological counterpart. Different materials, and ultimately different functional objectives are just part of the reason for these differences; another significant reason is the lack of understanding of the biological processes that enable the formation of the target structure, which is necessary to conceive of strategies for replicating these processes. We believe that in this community and in other fields, one major opportunity lies in improving the implementation of scalable, cost-efficient processes to produce bioinspired nanostructured materials by implementing and emulating the underlying biological structure formation principles and processes. As an example, self-assembly strategies continue to be a vibrant, promising area of active research in human fabrication. If we understand better how self-assembly is directed in biological processes to



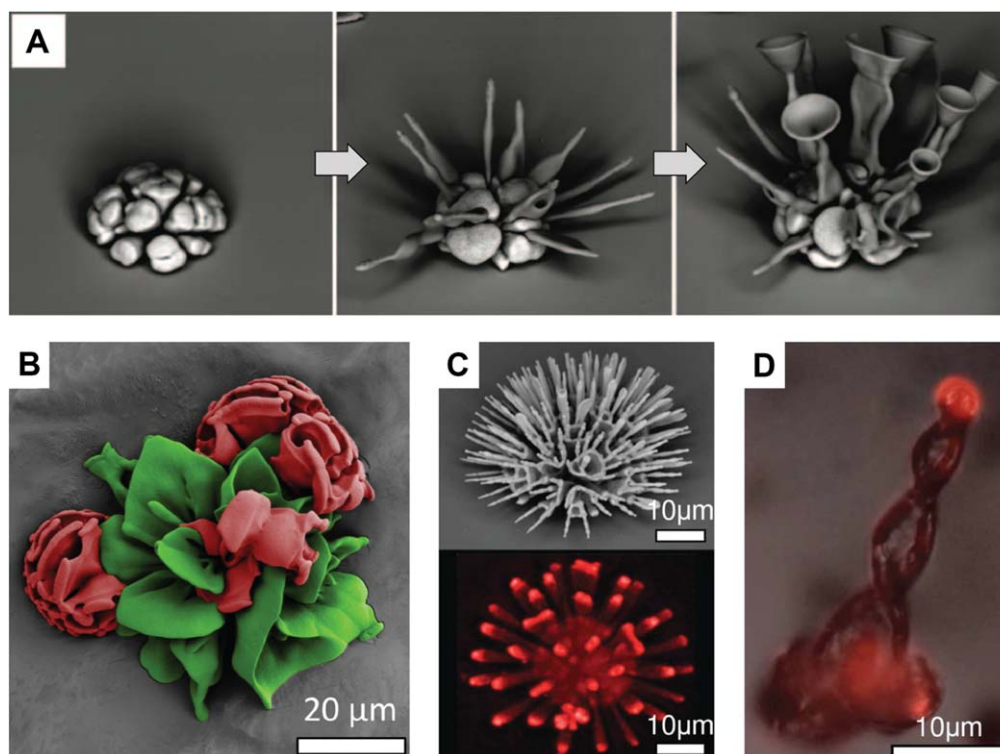


**Figure 38.** Rational design and synthetic growth of hierarchically assembled multimaterial microarchitectures with tailored functionality. (A) Scanning electron micrographs of a microstructure composed of barium carbonate, strontium carbonate and silica grown in three steps by varying the conditions in the growth medium and controlling carbon dioxide supply. (B) False color scanning electron micrograph of a carbonate-silica microstructure; the colors mark different deliberately induced growth regimes. The resemblance with biological growth forms is stunning. (C) and (D) Given the transparency and relatively high refractive index of carbonate materials, these structures can be used as optical elements. (C) A coral equipped with posts can function as a beamsplitter. (D) A helical structure guiding light and releasing it at its tip. (A) From [402]. Reprinted with permission from AAAS. (B) to (D) From [403]. Reprinted with permission from AAAS.

enable robust and reliable structural outcomes, we can hope to implement much of that insight in synthetic self-assembly strategies to advance functional materials design. To this end, the physics underlying the phase separation processes that appear to occur during the development of the keratin structures in colorful bird feathers are worth exploring further. Additionally, the role of membranes involved in the formation of morphologies that exhibit structural color could represent an interesting area of research. Our understanding of the physics of membrane interactions in controlling micro- and nanostructures is still limited; moreover, to our knowledge, the use of membranes is a barely explored area for the artificial fabrication of structural color.

Recent research has emphasized the potential of exploiting complex interplays between reaction and diffusion in co-precipitating mineral species for microstructure formation with a degree of control over the resulting structural outcomes that equals nature's abilities, without involving any biological components [402, 403] (figure 38). This work provides an inspiring example of how a deeper understanding of an inorganic model system might elucidate phenomena that occur during biological structure formation and moreover provide the theoretical framework for controlling the synthetic creation of functional microstructures.

While biomimicry emulates biology, biotechnology directly incorporates biological processes to exploit material production [6]. One approach, already industrialized in other fields, could lie in genetic modification. This would require a significant improvement in our minimal understanding of the genes behind structural color [149], but some organisms (such as butterflies) can be induced to express structural color phenotypes by both selective breeding and genetic modification [149, 404]. Another biotechnological approach is to incorporate a biological product in the overall fabrication process. Using biological structures as templates allows for close replication of the biological structures [405–407]. Alternatively, biological products can be used as components in the final structure [408].

Many species in nature have evolved the ability to form material morphologies that enable structural colors and a variety of other optical phenomena. Independently of nature, scientists and engineers have conceived a wide breadth of techniques to form synthetic optical materials. While these materials in many cases exploit very similar optical effects, they might have been formed by completely different processes. In this review, we aimed to identify similarities between biological and synthetic structure formation principles and to elucidate fundamental differences. We believe that further interdisciplinary study of biological growth and

synthetic production offers significant potential to improve the fabrication of structurally colored materials (and, by proxy, other functional materials). Nature continues to hold mysteries regarding biological growth processes, involving temporal and spatial integration of molecular synthesis, the role that physical and chemical phenomena play in implementing or even initiating hierarchical structure formation, and the deployment of functional materials. A deeper understanding of biological structure formation principles will allow us to conceive useful strategies to implement useful aspects of biological processes in synthetic process analogs. This will allow increased precision in controlling ‘what goes where’ on all relevant length scales using a wide range of material constituents with specific desirable properties, such as softness, stimuli-response, reconfigurability, and the ability to self-heal. Ultimately, this should enable us to produce many of the bioinspired materials with desirable functional attributes that are already reported in the literature but with cost-efficiency and at industrial scales.

## 5. Creative commons attributions

- Akos Harka, CC BY, [https://en.wikipedia.org/wiki/Alburnus#/media/File:Alburnus\\_alburnus\\_Hungary.jpg](https://en.wikipedia.org/wiki/Alburnus#/media/File:Alburnus_alburnus_Hungary.jpg)
- Anaxibia, CC BY-SA, [https://en.wikipedia.org/wiki/Teinopalpus\\_imperialis#/media/File:Teinopalpus\\_imperialis\\_verso.JPG](https://en.wikipedia.org/wiki/Teinopalpus_imperialis#/media/File:Teinopalpus_imperialis_verso.JPG)
- Arddu, CC BY, [https://commons.wikimedia.org/wiki/File:Green\\_Peafowl,\\_Hanoi.jpg#/media/File:Green\\_Peafowl,\\_Hanoi.jpg](https://commons.wikimedia.org/wiki/File:Green_Peafowl,_Hanoi.jpg#/media/File:Green_Peafowl,_Hanoi.jpg)
- Edouard Hue, CC BY-SA, [https://commons.wikimedia.org/wiki/File:UR1\\_insectes\\_de\\_1](https://commons.wikimedia.org/wiki/File:UR1_insectes_de_1)
- Esculapio, CC BY-SA, [https://en.wikipedia.org/wiki/Ophrys\\_speculum#/media/File:Ophrys\\_ciliata\\_zingaro\\_038.jpg](https://en.wikipedia.org/wiki/Ophrys_speculum#/media/File:Ophrys_ciliata_zingaro_038.jpg)
- Frank van de Putte, CC-BY, [https://commons.wikimedia.org/wiki/File:Floronia\\_bucculenta.jpg](https://commons.wikimedia.org/wiki/File:Floronia_bucculenta.jpg)
- Gregory Phillips, CC BY-SA, [https://commons.wikimedia.org/wiki/File:Morpho\\_menelaus.png](https://commons.wikimedia.org/wiki/File:Morpho_menelaus.png)
- H. Krisp, CC BY, [https://en.wikipedia.org/wiki/Neon\\_tetra#/media/File:Neonsalmler\\_Paracheirodon\\_innesi.jpg](https://en.wikipedia.org/wiki/Neon_tetra#/media/File:Neonsalmler_Paracheirodon_innesi.jpg)
- Jatin Sindhu, CC BY-SA, [https://en.wikipedia.org/wiki/Peafowl#/media/File:Peacock\\_Plumage.jpg](https://en.wikipedia.org/wiki/Peafowl#/media/File:Peacock_Plumage.jpg)
- Lorenzo Cortese and Silvia Vignolini, CC BY, <http://www.cam.ac.uk/research/news/the-beetles-white-album>
- Matt Sabbath, CC BY, [https://commons.wikimedia.org/wiki/File:Mandrillus\\_sphinx\\_portrait.jpg#/media/File:Mandrillus\\_sphinx\\_portrait.jpg](https://commons.wikimedia.org/wiki/File:Mandrillus_sphinx_portrait.jpg#/media/File:Mandrillus_sphinx_portrait.jpg)
- Morkelsker, CC BY, [https://commons.wikimedia.org/wiki/File:Poecilotheria\\_metallica.JPG](https://commons.wikimedia.org/wiki/File:Poecilotheria_metallica.JPG)
- Quartl, CC BY, [https://commons.wikimedia.org/wiki/File:Ara\\_ararauna\\_qt3.jpg](https://commons.wikimedia.org/wiki/File:Ara_ararauna_qt3.jpg)
- Robert Young, CC BY, [https://commons.wikimedia.org/wiki/File:Mandrill\\_at\\_Singapore\\_Zoo.jpg#/media/File:Mandrill\\_at\\_Singapore\\_Zoo.jpg](https://commons.wikimedia.org/wiki/File:Mandrill_at_Singapore_Zoo.jpg#/media/File:Mandrill_at_Singapore_Zoo.jpg)
- Sarah and Iain, CC BY, [https://commons.wikimedia.org/wiki/File:Toco\\_toucan\\_Parque\\_das\\_Aves.jpg#/media/File:Toco\\_toucan\\_Parque\\_das\\_Aves.jpg](https://commons.wikimedia.org/wiki/File:Toco_toucan_Parque_das_Aves.jpg#/media/File:Toco_toucan_Parque_das_Aves.jpg)
- Silke Baron, CC BY, [https://en.wikipedia.org/wiki/Mantis\\_shrimp#/media/File:Odontodactylus\\_Scyllarus.jpg](https://en.wikipedia.org/wiki/Mantis_shrimp#/media/File:Odontodactylus_Scyllarus.jpg)
- Vítězslav Maňák, CC BY-SA, [https://commons.wikimedia.org/wiki/File:Calophrys\\_rubi\\_SLU.JPG#/media/File:Calophrys\\_rubi\\_SLU.JPG](https://commons.wikimedia.org/wiki/File:Calophrys_rubi_SLU.JPG#/media/File:Calophrys_rubi_SLU.JPG)

## ORCID iDs

Anthony McDougal  <https://orcid.org/0000-0002-9980-4193>

Mathias Kolle  <https://orcid.org/0000-0001-7395-8824>

## References

- [1] Committee on Biomolecular Materials and Processes, National Research Council 2008 *Inspired by Biology: From Molecules to Materials to Machines* (Washington, DC.: National Academies Press) (<https://doi.org/10.17226/12159>)
- [2] Biró L P and Vigneron J P 2011 Photonic nanoarchitectures in butterflies and beetles: valuable sources for bioinspiration *Laser Photon. Rev.* **5** 27–51
- [3] Greanya V 2015 *Bioinspired Photonics: Optical Structures and Systems Inspired by Nature* (Boca Raton, FL: CRC Press) (<https://doi.org/10.1201/b18516>)
- [4] Tadeipalli S, Slocik J M, Gupta M K, Naik R R and Singamaneni S 2017 Bio-optics and bio-inspired optical materials *Chem. Rev.* **117** 12705–63
- [5] Newton I 1730 *Opticks: or, a Treatise of the Reflections, Refractions, Inflections and Colours of Light* (London: William Innys)
- [6] Parker A R and Townley H E 2007 Biomimetics of photonic nanostructures *Nat. Nanotechnol.* **2** 347–53
- [7] Saito A 2011 Material design and structural color inspired by biomimetic approach *Sci. Technol. Adv. Mater.* **12** 064709
- [8] Luke S M and Vukusic P 2011 An introduction to biomimetic photonic design *Europhys. News* **42** 20–3
- [9] Fudouzi H 2011 Tunable structural color in organisms and photonic materials for design of bioinspired materials *Sci. Technol. Adv. Mater.* **12** 064704
- [10] Zhao Y, Xie Z, Gu H, Zhu C and Gu Z 2012 Bio-inspired variable structural color materials *Chem. Soc. Rev.* **41** 3297
- [11] Liu F, Dong B and Liu X 2012 Bio-inspired photonic structures: prototypes, fabrications and devices *Optical Devices in Communication and Computation* ed P Xi (Rijeka: InTech) (<https://doi.org/10.5772/50199>)
- [12] Yu K, Fan T, Lou S and Zhang D 2013 Biomimetic optical materials: integration of nature's design for manipulation of light *Prog. Mater. Sci.* **58** 825–73
- [13] Fu Y, Tippetts C A, Donev E U and Lopez R 2016 Structural colors: from natural to artificial systems *WIREs Nanomed. Nanobiotechnol.* **8** 758–75
- [14] Wu L, He J, Shang W, Deng T, Gu J, Su H, Liu Q, Zhang W and Zhang D 2016 Optical functional materials inspired by biology *Adv. Opt. Mater.* **4** 195–224

- [15] Ghiradella H 1991 Light and color on the wing: Structural colors in butterflies and moths *Appl. Opt.* **30** 3492
- [16] Srinivasarao M 1999 Nano-optics in the biological world: beetles, butterflies, birds, and moths *Chem. Rev.* **99** 1935–62
- [17] Parker A R 2000 515 million years of structural colour *J. Opt. A: Pure Appl. Opt.* **2** R15
- [18] Vukusic P and Sambles J R 2003 Photonic structures in biology *Nature* **424** 852–5
- [19] Parker A R 2004 A vision for natural photonics *Phil. Trans. R. Soc. A* **362** 2709–20
- [20] Kinoshita S 2008 *Structural Colors in the Realm of Nature* (Singapore: World Scientific) (<https://doi.org/10.1142/6496>)
- [21] Seago A E, Brady P, Vigneron J-P and Schultz T D 2009 Gold bugs and beyond: a review of iridescence and structural colour mechanisms in beetles (Coleoptera) *J. R. Soc. Interface* **6** S165–84
- [22] Johnsen S 2012 *The Optics of Life* (Princeton, NJ: Princeton University Press)
- [23] Kolle M and Steiner U 2012 Structural color in animals *Encyclopedia of Nanotechnology* ed B Bhushan (Berlin: Springer) pp 2514–27
- [24] Dushkina N and Lakhtakia A 2013 Structural colors *Engineered Biomimicry* (Amsterdam: Elsevier) pp 267–303
- [25] Sun J, Bhushan B and Tong J 2013 Structural coloration in nature *RSC Adv.* **3** 14862
- [26] Kientz B, Luke S, Vukusic P, Péteri R, Beaudry C, Renault T, Simon D, Mignot T and Rosenfeld E 2016 A unique self-organization of bacterial sub-communities creates iridescence in cellulophaga lytica colony biofilms *Sci. Rep.* **6** 19906
- [27] Thomas K R, Kolle M, Whitney H M, Glover B J and Steiner U 2010 Function of blue iridescence in tropical understorey plants *J. R. Soc. Interface* **7** 1699–707
- [28] Vignolini S, Rudall P J, Rowland A V, Reed A, Moyroud E, Faden R B, Baumberg J J, Glover B J and Steiner U 2012 Pointillist structural color in Pollia fruit *Proc. Natl Acad. Sci.* **109** 15712–5
- [29] Jacobs M, Lopez-Garcia M, Phrathep O-P, Lawson T, Oulton R and Whitney H M 2016 Photonic multilayer structure of Begonia chloroplasts enhances photosynthetic efficiency *Nat. Plants* **2** 16162
- [30] Vignolini S, Moyroud E, Hingant T, Banks H, Rudall P J, Steiner U and Glover B J 2015 The flower of Hibiscus trionum is both visibly and measurably iridescent *New Phytologist* **205** 97–101
- [31] Vignolini S, Gregory T, Kolle M, Lethbridge A, Moyroud E, Steiner U, Glover B J, Vukusic P and Rudall P J 2016 Structural colour from helicoidal cell-wall architecture in fruits of Margaritaria nobilis *J. R. Soc. Interface* **13** 20160645
- [32] Li L, Kolle S, Weaver J C, Ortiz C, Aizenberg J and Kolle M 2015 A highly conspicuous mineralized composite photonic architecture in the translucent shell of the blue-rayed limpet *Nat. Commun.* **6** 6322
- [33] Stavenga D G, Otto J C and Wilts B D 2016 Splendid coloration of the peacock spider Maratus splendens *J. R. Soc. Interface* **13** 20160437
- [34] Burrelli M, Cortese L, Pattelli L, Kolle M, Vukusic P, Wiersma D S, Steiner U and Vignolini S 2014 Bright-white beetle scales optimise multiple scattering of light *Sci. Rep.* **4** srep06075
- [35] Kolle M and Steiner U 2012 Structural color in animals *Encyclopedia of Nanotechnology* ed B Bhushan (Berlin: Springer) pp 2514–27
- [36] Kinoshita S, Yoshioka S and Miyazaki J 2008 Physics of structural colors *Rep. Prog. Phys.* **71** 076401
- [37] Arwin H, Magnusson R, Landin J and Järrendahl K 2012 Chirality-induced polarization effects in the cuticle of scarab beetles: 100 years after Michelson *Phil. Mag.* **92** 1583–99
- [38] Amir A and Vukusic P 2013 Elucidating the stop bands of structurally colored systems through recursion *Am. J. Phys.* **81** 253–7
- [39] Yoshioka S, Fujita H, Kinoshita S and Matsuhana B 2013 Alignment of crystal orientations of the multi-domain photonic crystals in Parides sesostris wing scales *J. R. Soc. Interface* **11** 20131029
- [40] Ghiradella H 1994 Structure of butterfly scales: patterning in an insect cuticle *Microsc. Res. Tech.* **27** 429–38
- [41] Pouya C, Stavenga D G and Vukusic P 2011 Discovery of ordered and quasi-ordered photonic crystal structures in the scales of the beetle Eupholus magnificus *Opt. Express* **19** 11355–64
- [42] Kinoshita S and Yoshioka S 2005 Structural colors in nature: the role of regularity and irregularity in the structure *ChemPhysChem* **6** 1442–59
- [43] Vukusic P, Sambles J R, Lawrence C R and Wootton R J 1999 Quantified interference and diffraction in single Morpho butterfly scales *Proc. R. Soc. B* **266** 1403–11
- [44] Jordan T M, Partridge J C and Roberts N W 2012 Non-polarizing broadband multilayer reflectors in fish *Nat. Photon.* **6** 759–63
- [45] Prum R O and Torres R 2003 Structural colouration of avian skin: convergent evolution of coherently scattering dermal collagen arrays *J. Exp. Biol.* **206** 2409–29
- [46] Dufresne E R, Noh H, Saranathan V, Mochrie S G J, Cao H and Prum R O 2009 Self-assembly of amorphous biophotonic nanostructures by phase separation *Soft Matter* **5** 1792–5
- [47] Vigneron J P, Rassart M, Vértessy Z, Kertész K, Sarrazin M, Biró L P, Ertz D and Lousse V 2005 Optical structure and function of the white filamentary hair covering the edelweiss bracts *Phys. Rev. E* **71** 011906
- [48] Vukusic P, Hallam B and Noyes J 2007 Brilliant whiteness in ultrathin beetle scales *Science* **315** 348
- [49] Luke S M, Hallam B T and Vukusic P 2010 Structural optimization for broadband scattering in several ultra-thin white beetle scales *Appl. Opt.* **49** 4246–54
- [50] Mäthger L M *et al* 2013 Bright white scattering from protein spheres in color changing, flexible cuttlefish skin *Adv. Funct. Mater.* **23** 3980–9
- [51] Bell G R R, Mäthger L M, Gao M, Senft S L, Kuzirian A M, Kattawar G W and Hanlon R T 2014 Diffuse white structural coloration from multilayer reflectors in a squid *Adv. Mater.* **26** 4352–6
- [52] Ghiradella H T and Butler M W 2009 Many variations on a few themes: a broader look at development of iridescent scales (and feathers) *J. R. Soc. Interface* **6** S243–S251
- [53] Schmitz H 1994 Thermal characterization of butterfly wings: I. Absorption in relation to different color, surface structure and basking type *J. Therm. Biol.* **19** 403–12
- [54] Srygley R B and Thomas A L R 2002 Unconventional lift-generating mechanisms in free-flying butterflies *Nature* **420** 660–4
- [55] Biró L P *et al* 2003 Role of photonic-crystal-type structures in the thermal regulation of a Lycaenid butterfly sister species pair *Phys. Rev. E* **67**
- [56] Zheng Y, Gao X and Jiang L 2007 Directional adhesion of superhydrophobic butterfly wings *Soft Matter* **3** 178–82
- [57] Morehouse N I and Rutowski R L 2010 In the eyes of the beholders: female choice and avian predation risk associated with an exaggerated male butterfly color *Am. Nat.* **176** 768–84
- [58] Doucet S M and Meadows M G 2009 Iridescence: a functional perspective *J. R. Soc. Interface* **6** S115–32
- [59] Siddique R H, Gomard G and Hölscher H 2015 The role of random nanostructures for the omnidirectional anti-reflection properties of the glasswing butterfly *Nat. Commun.* **6** 6909



- [60] Ghiradella H 1998 Hairs, bristles and scales *Microscopic Anatomy of Invertebrates (Insecta)* ed F W Harrison and M Locke vol 11A (New York: Wiley) pp 257–87
- [61] Yoshioka S and Kinoshita S 2006 Structural or pigmentary? Origin of the distinctive white stripe on the blue wing of a morpho butterfly *Proc. R. Soc. B* **273** 129–34
- [62] Mille C, Tyrode E C and Corkery R W 2013 3D titania photonic crystals replicated from gyroid structures in butterfly wing scales: approaching full band gaps at visible wavelengths *RSC Adv.* **3** 3109
- [63] Kolle M 2011 *Photonic Structures Inspired by Nature* (Berlin: Springer) (<https://doi.org/10.1007/978-3-642-15169-9>)
- [64] England G, Kolle M, Kim P, Khan M, Muñoz P, Mazur E and Aizenberg J 2014 Bioinspired micrograting arrays mimicking the reverse color diffraction elements evolved by the butterfly *Pierella luna* *Proc. Natl Acad. Sci.* **111** 15630–4
- [65] Kinoshita S, Yoshioka S and Kawagoe K 2002 Mechanisms of structural colour in the morpho butterfly: cooperation of regularity and irregularity in an iridescent scale *Proc. R. Soc. B* **269** 1417–21
- [66] Saito A, Yonezawa M, Murase J, Juodkazis S, Mizeikis V, Akai-Kasaya M and Kuwahara Y 2011 Numerical analysis on the optical role of nano-randomness on the morpho butterfly's scale *J. Nanosci. Nanotechnol.* **11** 2785–92
- [67] Yoshioka S and Kinoshita S 2007 Polarization-sensitive color mixing in the wing of the madagascan sunset moth *Opt. Express* **15** 2691–701
- [68] Yoshioka S, Nakano T, Nozue Y and Kinoshita S 2008 Coloration using higher order optical interference in the wing pattern of the Madagascan sunset moth *J. R. Soc. Interface* **5** 457–64
- [69] Vukusic P, Sambles J R and Lawrence C R 2000 Structural colour: colour mixing in wing scales of a butterfly *Nature* **404** 457
- [70] Vukusic P, Sambles R, Lawrence C and Wakely G 2001 Sculpted-multilayer optical effects in two species of *Papilio* butterfly *Appl. Opt.* **40** 1116–25
- [71] Michielsen K and Stavenga D G 2008 Gyroid cuticular structures in butterfly wing scales: biological photonic crystals *J. R. Soc. Interface* **5** 85–94
- [72] Saranathan V, Osuji C O, Mochrie S G J, Noh H, Narayanan S, Sandy A, Dufresne E R and Prum R O 2010 Structure, function, and self-assembly of single network gyroid (I4132) photonic crystals in butterfly wing scales *Proc. Natl Acad. Sci.* **107** 11676–81
- [73] Saba M, Wilts B D, Hielscher J and Schröder-Turk G E 2014 Absence of circular polarisation in reflections of butterfly wing scales with Chiral Gyroid structure *Mater. Today: Proc.* **1** 193–208
- [74] Winter B, Butz B, Dieker C, Schröder-Turk G E, Mecke K and Spiecker E 2015 Coexistence of both gyroid chiralities in individual butterfly wing scales of *Callophrys rubi* *Proc. Natl Acad. Sci.* **112** 12911–6
- [75] Wilts B D, Zubiri B A, Klatt M A, Butz B, Fischer M G, Kelly S T, Spiecker E, Steiner U and Schröder-Turk G E 2017 Butterfly gyroid nanostructures as a time-frozen glimpse of intracellular membrane development *Sci. Adv.* **3** e1603119
- [76] Prum R O, Torres R H, Williamson S and Dyck J 1998 Coherent light scattering by blue feather barbs *Nature* **396** 28–9
- [77] Shawkey M D, Morehouse N I and Vukusic P 2009 A protean palette: colour materials and mixing in birds and butterflies *J. R. Soc. Interface* **6** S221–31
- [78] Noh H, Liew S F, Saranathan V, Mochrie S G J, Prum R O, Dufresne E R and Cao H 2010 How noniridescent colors are generated by quasi-ordered structures of bird feathers *Adv. Mater.* **22** 2871–80
- [79] Saranathan V, Forster J D, Noh H, Liew S-F, Mochrie S G J, Cao H, Dufresne E R and Prum R O 2012 Structure and optical function of amorphous photonic nanostructures from avian feather barbs: a comparative small angle x-ray scattering (SAXS) analysis of 230 bird species *J. R. Soc. Interface* **9** 2563–80
- [80] Cooper K M, Hanlon R T and Budelmann B U 1990 Physiological color change in squid iridophores *Cell Tissue Res.* **259** 3–14
- [81] Mäthger L M and Hanlon R T 2007 Malleable skin coloration in cephalopods: selective reflectance, transmission and absorbance of light by chromatophores and iridophores *Cell Tissue Res.* **329** 179
- [82] Mäthger L M, Denton E J, Marshall N J and Hanlon R T 2009 Mechanisms and behavioural functions of structural coloration in cephalopods *J. R. Soc. Interface* **6** S149–63
- [83] Wardill T J, Gonzalez-Bellido P T, Crook R J and Hanlon R T 2012 Neural control of tuneable skin iridescence in squid *Proc. R. Soc. B* **279** 4243–52
- [84] Kramer R M, Crookes-Goodson W J and Naik R R 2007 The self-organizing properties of squid reflectin protein *Nat. Mater.* **6** 533–8
- [85] DeMartini D G, Izumi M, Weaver A T, Pandolfi E and Morse D E 2015 Structures, organization, and function of reflectin proteins in dynamically tunable reflective cells *J. Biol. Chem.* **290** 15238–49
- [86] Teyssier J, Saenko S V, van der Marel D and Milinkovitch M C 2015 Photonic crystals cause active colour change in chameleons *Nat. Commun.* **6** 7368
- [87] Klemm D, Heublein B, Fink H-P and Bohn A 2005 Cellulose: fascinating biopolymer and sustainable raw material *Angew. Chem. Int. Ed.* **44** 3358–93
- [88] Grimann M and Fuhrmann-Lieker T 2015 Biological photonic crystals *Organic and Hybrid Photonic Crystals* ed D Comoretto (Berlin: Springer) pp 57–74
- [89] Levy-Lior A, Shimoni E, Schwartz O, Gavish-Regev E, Oron D, Oxford G, Weiner S and Addadi L 2010 Guanine-based biogenic photonic-crystal arrays in fish and spiders *Adv. Funct. Mater.* **20** 320–9
- [90] Jordan T M, Partridge J C and Roberts N W 2012 Non-polarizing broadband multilayer reflectors in fish *Nat. Photon.* **6** 759–63
- [91] Gur D, Leshem B, Pierantoni M, Farstey V, Oron D, Weiner S and Addadi L 2015 Structural basis for the brilliant colors of the sapphirinid copepods *J. Am. Chem. Soc.* **137** 8408–11
- [92] Shawkey M D and Hill G E 2005 Carotenoids need structural colours to shine *Biol. Lett.* **1** 121–4
- [93] Prum R O and Torres R H 2004 Structural colouration of mammalian skin: convergent evolution of coherently scattering dermal collagen arrays *J. Exp. Biol.* **207** 2157–72
- [94] DeMartini D G, Krogstad D V and Morse D E 2013 Membrane invaginations facilitate reversible water flux driving tunable iridescence in a dynamic biophotonic system *Proc. Natl Acad. Sci.* **110** 2552–6
- [95] Sharma V, Crne M, Park J O and Srinivasarao M 2009 Structural origin of circularly polarized iridescence in jeweled beetles *Science* **325** 449–51
- [96] Parker A R, Welch V L, Driver D and Martini N 2003 Structural colour: opal analogue discovered in a weevil *Nature* **426** 786–7
- [97] Welch V, Lousse V, Deparis O, Parker A and Vigneron J P 2007 Orange reflection from a three-dimensional photonic crystal in the scales of the weevil *pachyrhynchus congestus pavonius* (curculionidae) *Phys. Rev. E* **75** 041919
- [98] Galusha J W, Richey L R, Jorgensen M R, Gardner J S and Bartl M H 2010 Study of natural photonic crystals in beetle scales and their conversion into inorganic structures via a sol-gel bio-templating route *J. Mater. Chem.* **20** 1277–84

- [99] Pursiainen O L, Baumberg J J, Winkler H, Viel B, Spahn P and Ruhl T 2007 Nanoparticle-tuned structural color from polymer opals *Opt. Express* **15** 9553–61
- [100] Aguirre C I, Reguera E and Stein A 2010 Tunable colors in opals and inverse opal photonic crystals *Adv. Funct. Mater.* **20** 2565–78
- [101] Hatton B, Mishchenko L, Davis S, Sandhage K H and Aizenberg J 2010 Assembly of large-area, highly ordered, crack-free inverse opal films *Proc. Natl Acad. Sci.* **107** 10354–9
- [102] Cong H, Yu B, Tang J, Li Z and Liu X 2013 Current status and future developments in preparation and application of colloidal crystals *Chem. Soc. Rev.* **42** 7774–800
- [103] Takeoka Y, Yoshioka S, Teshima M, Takano A, Harun-Ur-Rashid M and Seki T 2013 Structurally coloured secondary particles composed of black and white colloidal particles *Sci. Rep.* **3** 2371
- [104] Bai L, Xie Z, Wang W, Yuan C, Zhao Y, Mu Z, Zhong Q and Gu Z 2014 Bio-inspired vapor-responsive colloidal photonic crystal patterns by inkjet printing *ACS Nano* **8** 11094–100
- [105] Park J-G, Kim S-H, Magkiriadou S, Choi T M, Kim Y-S and Manoharan V N 2014 Full-spectrum photonic pigments with non-iridescent structural colors through colloidal assembly *Angew. Chem. Int. Ed.* **53** 2899–903
- [106] Vogel N, Utech S, England G T, Shirman T, Phillips K R, Koay N, Burgess I B, Kolle M, Weitz D A and Aizenberg J 2015 Color from hierarchy: diverse optical properties of micron-sized spherical colloidal assemblies *Proc. Natl Acad. Sci.* **112** 10845–50
- [107] Phillips K R, England G T, Sunny S, Shirman E, Shirman T, Vogel N and Aizenberg J 2016 A colloidoscope of colloid-based porous materials and their uses *Chem. Soc. Rev.* **45** 281–322
- [108] Waterhouse G and Waterland M R 2007 Opal and inverse opal photonic crystals: fabrication and characterization *Polyhedron* **26** 356–68
- [109] Wang Y, Aurelio D, Li W, Tseng P, Zheng Z, Li M, Kaplan D L, Liscidini M and Omenetto F G 2017 Modulation of multiscale 3d lattices through conformational control: painting silk inverse opals with water and light *Adv. Mater.* **29** 1702769
- [110] Omenetto F G and Kaplan D L 2010 New opportunities for an ancient material *Science* **329** 528–31
- [111] Tao H, Kaplan D L and Omenetto F G 2012 Silk materials—a road to sustainable high technology *Adv. Mater.* **24** 2824–37
- [112] Lawrence B D, Cronin-Golomb M, Georgakoudi I, Kaplan D L and Omenetto F G 2008 Bioactive silk protein biomaterial systems for optical devices *Biomacromolecules* **9** 1214–20
- [113] Amsden J J, Perry H, Boriskina S V, Gopinath A, Kaplan D L, Negro L D and Omenetto F G 2009 Spectral analysis of induced color change on periodically nanopatterned silk films *Opt. Express* **17** 21271–9
- [114] Caixeiro S, Gaio M, Marelli B, Omenetto F G and Sapienza R 2016 Silk-based biocompatible random lasing *Adv. Opt. Mater.* **4** 998–1003
- [115] Hu X, Shmelev K, Sun L, Gil E-S, Park S-H, Cebe P and Kaplan D L 2011 Regulation of silk material structure by temperature-controlled water vapor annealing *Biomacromolecules* **12** 1686–96
- [116] Shao J, Zheng J, Liu J and Carr C M 2005 Fourier transform Raman and Fourier transform infrared spectroscopy studies of silk fibroin *J. Appl. Polym. Sci.* **96** 1999–2004
- [117] Burke K A, Brenckle M A, Kaplan D L and Omenetto F G 2016 Evaluation of the spectral response of functionalized silk inverse opals as colorimetric immunosensors *ACS Appl. Mater. Interfaces* **8** 16218–26
- [118] Van Kessel P F, Hornbeck L J, Meier R E and Douglass M R 1998 A MEMS-based projection display *Proc. IEEE* **86** 1687–704
- [119] Noell W, Clerc P A, Dellmann L, Guldemann B, Herzig H P, Manzardo O, Marxer C R, Weible K J, Dandliker R and de Rooij N 2002 Applications of SOI-based optical MEMS *IEEE J. Sel. Top. Quantum Electron.* **8** 148–54
- [120] Solgaard O, Godil A A, Howe R T, Lee L P, Peter Y A and Zappe H 2014 Optical MEMS: from micromirrors to complex systems *J. Microelectromech. Syst.* **23** 517–38
- [121] Hornbeck L J 1983 128 × 128 deformable mirror device *IEEE Trans. Electron Devices* **30** 539–45
- [122] Dudley D, Duncan W M and Slaughter J 2003 Emerging digital micromirror device (DMD) applications *Proc. SPIE* **4985** pp 14–25
- [123] Hong J *et al* 2015 Continuous color reflective displays using interferometric absorption *Optica* **2** 589–97
- [124] Chan E K, Chang T, Fung T-C, Hong J, Kim C, Ma J, Pan Y, Wang S-G and Wen B 2017 Continuous color reflective display fabricated in integrated MEMS-and-TFT-on-Glass process *J. Microelectromech. Syst.* **26** 143–57
- [125] Boyle B M, French T A, Pearson R M, McCarthy B G and Miyake G M 2017 Structural color for additive manufacturing: 3d-printed photonic crystals from block copolymers *ACS Nano* **11** 3052–8
- [126] Crick F 1958 On protein synthesis *Symp. of the Society for Experimental Biology* vol 12, pp 138–63
- [127] Crick F 1970 Central dogma of molecular biology *Nature* **227** 227561a0
- [128] Lodish H, Berk A, Kaiser C A, Krieger M, Bretscher A, Ploegh H, Amon A and Martin K C 2016 *Molecular Cell Biology* 8th edn (New York: W. H. Freeman)
- [129] Reck-Peterson S L, Yildiz A, Carter A P, Gennerich A, Zhang N and Vale R D 2006 Single-molecule analysis of dynein processivity and stepping behavior *Cell* **126** 335–48
- [130] Vale R D 2000 The way things move: looking under the hood of molecular motor proteins *Science* **288** 88–95
- [131] Grishchuk E L, Molodtsov M I, Ataullakhanov F I and McIntosh J R 2005 Force production by disassembling microtubules *Nature* **438** 384–8
- [132] Kieliszewski M J and Lampion D T A 1994 Extensin: repetitive motifs, functional sites, post-translational codes, and phylogeny *Plant J.* **5** 157–72
- [133] Wang B, Yang W, McKittrick J and Meyers M A 2016 Keratin: structure, mechanical properties, occurrence in biological organisms, and efforts at bioinspiration *Prog. Mater. Sci.* **76** 229–318
- [134] Rogers G E 1969 The structure and biochemistry of keratin *The Biological Basis of Medicine* ed E E Bittar and N Bittar vol 6 (New York: Academic) pp 21–57
- [135] Luzio J P, Pryor P R and Bright N A 2007 Lysosomes: fusion and function *Nat. Rev. Mol. Cell Biol.* **8** 622
- [136] Xu H and Ren D 2015 Lysosomal physiology *Annu. Rev. Physiol.* **77** 57–80
- [137] Thelen A M and Zoncu R 2017 Emerging roles for the lysosome in lipid metabolism *Trends Cell Biol.* **27** 833–50
- [138] Gorb S N, Kesel A and Berger J 2000 Microsculpture of the wing surface in odonata: evidence for cuticular wax covering *Arthropod Struct. Dev.* **29** 129–35
- [139] Trzeciak T M and Vukusic P 2009 Photonic crystal fiber in the polychaete worm *Pherusa* sp *Phys. Rev. E* **80** 061908
- [140] Prum R O and Williamson S 2001 Theory of the growth and evolution of feather shape *J. Exp. Zoology* **291** 30–57
- [141] Mallavarapu A and Mitchison T 1999 Regulated actin cytoskeleton assembly at filopodium tips controls their extension and retraction *J. Cell Biol.* **146** 1097–106

- [142] Pollard T D and Borisy G G 2003 Cellular motility driven by assembly and disassembly of actin filaments *Cell* **112** 453–65
- [143] Locke M 1961 Pore canals and related structures in insect cuticle *J. Biophys. Biochem. Cytology* **10** 589–618
- [144] Saranathan V, Seago A E, Sandy A, Narayanan S, Mochrie S G J, Dufresne E R, Cao H, Osuji C O and Prum R O 2015 Structural diversity of arthropod biophotonic nanostructures spans amphiphilic phase-space *Nano Lett.* **15** 3735–42
- [145] Semper C 1857 Über die bildung der flügel, schuppen und haare bei den lepidopteren *Zeitschr. F. Wiss. Zool* **8** 326–39
- [146] Landois H 1871 Beiträge zur entwicklungsgeschichte des schmetterlingsflügel in der raupen und puppe *Zeits. Wiss. Zool.*, *bd* **21** 305–16
- [147] Galant R, Skeath J B, Paddock S, Lewis D L and Carroll S B 1998 Expression pattern of a butterfly achaete-scute homolog reveals the homology of butterfly wing scales and insect sensory bristles *Curr. Biol.* **8** 807–13
- [148] Dinwiddie A, Null R, Pizzano M, Chuong L, Leigh Krup A, Ee Tan H and Patel N H 2014 Dynamics of F-actin prefigure the structure of butterfly wing scales *Dev. Biol.* **392** 404–18
- [149] Zhang L, Mazo-Vargas A and Reed R D 2017 Single master regulatory gene coordinates the evolution and development of butterfly color and iridescence *Proc. Natl Acad. Sci.* **114** 10707–12
- [150] Köhler W 1932 Die entwicklung der flügel bei der mehlmotte ephestia kühniella zeller, mit besonderer Berücksichtigung des zeichnungsmusters *Z. Morphologie Ökologie Tiere* **24** 582–681
- [151] Stossberg M 1938 Die zellvorgänge bei der entwicklung der flügel-schuppen von ephestia kühniella *Z. Z. Morphologie Ökologie Tiere* **34** 173–206
- [152] Overton J 1966 Microtubules and microfibrils in morphogenesis of the scale cells of ephestia kühniella *J. Cell Biol.* **29** 293–305
- [153] Nijhout H F 1980 Ontogeny of the color pattern on the wings of *Precis coenia* (Lepidoptera: Nymphalidae) *Dev. Biol.* **80** 275–88
- [154] Ghiradella H 1989 Structure and development of iridescent butterfly scales: lattices and laminae *J. Morphol.* **202** 69–88
- [155] James D G 1987 Effects of temperature and photoperiod on the development of *Vanessa kershawi* McCoy and *Junonia villida* Godart (Lepidoptera: Nymphalidae) *Aust. J. Entomology* **26** 289–92
- [156] Muzzarelli R A A 2011 Chitin nanostructures in living organisms *Topics in Geobiology* ed N S Gupta vol 34 (Berlin: Springer) pp 1–34
- [157] Merzendorfer H and Zimoch L 2003 Chitin metabolism in insects: structure, function and regulation of chitin synthases and chitinases *J. Exp. Biol.* **206** 4393–412
- [158] Merzendorfer H 2005 Insect chitin synthases: a review *J. Comparative Physiol. B* **176** 1–15
- [159] Ghiradella H 1974 Development of ultraviolet-reflecting butterfly scales: how to make an interference filter *J. Morphol.* **142** 395–409
- [160] Onelli O D, van de Kamp T, Skepper J N, Powell J, dos Santos Rolo T, Baumbach T and Vignolini S 2017 Development of structural colour in leaf beetles *Sci. Rep.* **7** 1373
- [161] Locke M and Huie P 1979 Apolysis and the turnover of plasma membrane plaques during cuticle formation in an insect *Tissue Cell* **11** 277–91
- [162] Chapman R F 2012 *The Insects: Structure and Function* 5th edn (Cambridge: Cambridge University Press)
- [163] Neville A C 1963 Daily growth layers for determining the age of grasshopper populations *Oikos* **14** 1–8
- [164] Bereiter-Hahn J, Gedeon Matoltsy A and Richards K S 1984 *Biology of the Integument* (Berlin: Springer) (<https://doi.org/10.1007/978-3-642-51593-4>)
- [165] Neville A C 1975 *Biology of the Arthropod Cuticle* (Berlin: Springer) (<https://doi.org/10.1007/978-3-642-80910-1>)
- [166] Lenau T and Barfoed M 2008 Colours and metallic sheen in beetle shells—a biomimetic search for material structuring principles causing light interference *Adv. Eng. Mater.* **10** 299–314
- [167] Carter I E, Weir K, McCall M W and Parker A R 2016 Variation in the circularly polarized light reflection of Lomaptera (Scarabaeidae) beetles *J. R. Soc. Interface* **13** 20160015
- [168] McAuslane H J and King K 2000 *Larger Canna Leafroller, Calpodex ethlius (Stoll)* (Hesperiidae: Insecta: Lepidoptera) (<https://edis.ifas.ufl.edu/in289>)
- [169] Maeno K and Tanaka S 2008 A reddish-brown mutant in the desert locust, *Schistocerca gregaria* *Appl. Entomol. Zool.* **43** 497–502
- [170] Amador G J, Endlein T and Sitti M 2017 Soiled adhesive pads shear clean by slipping: a robust self-cleaning mechanism in climbing beetles *J. R. Soc. Interface* **14** 20170134
- [171] Weiner S and Addadi L 2011 Crystallization pathways in biomineralization *Annu. Rev. Mater. Res.* **41** 21–40
- [172] Chateigner D, Hedegaard C and Wenk H R 2000 Mollusc shell microstructures and crystallographic textures *J. Struct. Geol.* **22** 1723–35
- [173] Chirat R, Moulton D E and Goriely A 2013 Mechanical basis of morphogenesis and convergent evolution of spiny seashells *Proc. Natl Acad. Sci.* **110** 6015–20
- [174] Moulton D E, Goriely A and Chirat R 2012 Mechanical growth and morphogenesis of seashells *J. Theor. Biol.* **311** 69–79
- [175] Seitz K-A 1987 *Excretory Organs, In Ecophysiology of Spiders* (Berlin: Springer) pp 239–48
- [176] Palmer B A, Taylor G J, Brumfeld V, Gur D, Shemesh M, Elad N, Osherov A, Oron D, Weiner S and Addadi L 2017 The image-forming mirror in the eye of the scallop *Science* **358** 1172–5
- [177] Li B, Cao Y-P, Feng X-Q and Gao H 2012 Mechanics of morphological instabilities and surface wrinkling in soft materials: a review *Soft Matter* **8** 5728–45
- [178] Eskandari M and Kuhl E 2015 Systems biology and mechanics of growth *Wiley Interdiscip. Rev.: Syst. Biol. Med.* **7** 401–12
- [179] Bowden N, Brittain S, Evans A G, Hutchinson J W and Whitesides G M 1998 Spontaneous formation of ordered structures in thin films of metals supported on an elastomeric polymer *Nature* **393** 146
- [180] Jiang H, Khang D-Y, Song J, Sun Y, Huang Y and Rogers J A 2007 Finite deformation mechanics in buckled thin films on compliant supports *Proc. Natl Acad. Sci.* **104** 15607–12
- [181] Cerda E and Mahadevan L 2003 Geometry and physics of wrinkling *Phys. Rev. Lett.* **90** 074302
- [182] Kourounioti R L A, Band L R, Fozard J A, Hampstead A, Lovrics A, Moyroud E, Vignolini S, King J R, Jensen O E and Glover B J 2013 Buckling as an origin of ordered cuticular patterns in flower petals *J. R. Soc. Interface* **10** 20120847
- [183] Whitney H M, Kolle M, Andrew P, Chittka L, Steiner U and Glover B J 2009 Floral iridescence, produced by diffractive optics, acts as a cue for animal pollinators *Science* **323** 130–3
- [184] Glover B J and Whitney H M 2010 Structural colour and iridescence in plants: the poorly studied relations of pigment colour *Ann. Bot.* **105** 505–11



- [185] Narayanan B, Gilmer G H, Tao J, De Yoreo J J and Ciobanu C V 2014 Self-assembly of collagen on flat surfaces: the interplay of collagen–collagen and collagen–substrate interactions *Langmuir* **30** 1343–50
- [186] Fessler J H 1974 Self-assembly of collagen *J. Supramolecular Struct.* **2** 99–102
- [187] Hartgerink J D, Beniash E and Stupp S I 2001 Self-assembly and mineralization of peptide-amphiphile nanofibers *Science* **294** 1684–8
- [188] Welch V, Vigneron J P, Lousse V and Parker A 2006 Optical properties of the iridescent organ of the comb-jellyfish *Beroë cucumis* (Ctenophora) *Phys. Rev. E* **73** 041916
- [189] Guillermo-Ferreira R, Bispo P C, Appel E, Kovalev A and Gorb S N 2015 Mechanism of the wing colouration in the dragonfly *Zenithoptera lanei* (Odonata: Libellulidae) and its role in intraspecific communication *J. Insect Physiol.* **81** 129–36
- [190] Guillermo-Ferreira R, Appel E, Urban P, Bispo P C and Gorb S N 2017 The unusual tracheal system within the wing membrane of a dragonfly *Biol. Lett.* **13** 20160960
- [191] Zi J, Yu X, Li Y, Hu X, Xu C, Wang X, Liu X and Fu R 2003 Coloration strategies in peacock feathers *Proc. Natl Acad. Sci.* **100** 12576–8
- [192] Fratzl P 2003 Cellulose and collagen: from fibres to tissues *Curr. Opin. Colloid Interface Sci.* **8** 32–9
- [193] Singla V and Reiter J F 2006 The primary cilium as the cell antenna: signaling at a sensory organelle *Science* **313** 629–33
- [194] Alvarez-Buylla A, García-Verdugo J M, Mateo A S and Merchant-Larios H 1998 Primary neural precursors and intermitotic nuclear migration in the ventricular zone of adult canaries *J. Neurosci.* **18** 1020–37
- [195] Anderson R G W 1972 The three-dimensional structure of the basal body from the rhesus monkey oviduct *J. Cell Biol.* **54** 246–65
- [196] Preble A M, Giddings T H and Dutcher S K 2001 Extragenic bypass suppressors of mutations in the essential gene BLD2 promote assembly of basal bodies with abnormal microtubules in *Chlamydomonas reinhardtii* *Genetics* **157** 163–81
- [197] Prum R O 1999 Development and evolutionary origin of feathers *J. Exp. Zoology* **285** 291–306
- [198] Durrer H and Villiger W 1967 Bildung der schillerstruktur beim glanzstar *Z. Zellforschung Mikrosk. Anatomie* **81** 445–56
- [199] Parker A R, McPhedran R C, McKenzie D R, Botten L C and Nicorovici N-A P 2001 Aphroditeas iridescence *Nature* **409** 36
- [200] Singer A, Boucheron L, Dietze S H, Jensen K E, Vine D, McNulty I, Dufresne E R, Prum R O, Mochrie S G J and Shpyrko O G 2016 Domain morphology, boundaries, and topological defects in biophotonic gyroid nanostructures of butterfly wing scales *Sci. Adv.* **2** e1600149
- [201] Simonis P and Vigneron J P 2011 Structural color produced by a three-dimensional photonic polycrystal in the scales of a longhorn beetle: *pseudomyagrus waterhousei* (Coleoptera: Cerambycidae) *Phys. Rev. E* **83** 011908
- [202] Hallam B T, Hiorns A G and Vukusic P 2009 Developing optical efficiency through optimized coating structure: biomimetic inspiration from white beetles *Appl. Opt.* **48** 3243–9
- [203] Mäthger L M *et al* 2013 Bright white scattering from protein spheres in color changing, flexible cuttlefish skin *Adv. Funct. Mater.* **23** 3980–9
- [204] Bell G R R, Mäthger L M, Gao M, Senft S L, Kuzirian A M, Kattawar G W and Hanlon R T 2014 Diffuse white structural coloration from multilayer reflectors in a squid *Adv. Mater.* **26** 4352–6
- [205] Fratzl P and Weinkamer R 2007 Nature's hierarchical materials *Prog. Mater. Sci.* **52** 1263–334
- [206] Weaver J C *et al* 2007 Hierarchical assembly of the siliceous skeletal lattice of the hexactinellid sponge *euplectella aspergillum* *J. Struct. Biol.* **158** 93–106
- [207] Wegst U G K, Bai H, Saiz E, Tomsia A P and Ritchie R O 2015 Bioinspired structural materials *Nat. Mater.* **14** 23–36
- [208] Watson G S, Watson J A and Cribb B W 2017 Diversity of cuticular micro- and nanostructures on insects: properties, functions, and potential applications *Annu. Rev. Entomology* **62** 185–205
- [209] Fuhrmann T, Landwehr S, El Rharbi-Kucki M and Sumper M 2004 Diatoms as living photonic crystals *Appl. Phys. B* **78** 257–60
- [210] Noyes J, Sumper M and Vukusic P 2008 Light manipulation in a marine diatom *J. Mater. Res.* **23** 3229–35
- [211] De Stefano L, Rea I, Rendina I, De Stefano M and Moretti L 2007 Lensless light focusing with the centric marine diatom *Coscinodiscus walesii* *Opt. Express* **15** 18082–8
- [212] Wang Y, Cai J, Jiang Y, Jiang X and Zhang D 2013 Preparation of biosilica structures from frustules of diatoms and their applications: current state and perspectives *Appl. Microbiol. Biotechnol.* **97** 453–60
- [213] Tesson B and Hildebrand M 2010 Extensive and intimate association of the cytoskeleton with forming silica in diatoms: control over patterning on the meso- and micro-scale *PLoS One* **5** e14300
- [214] Scheffel A, Poulsen N, Shian S and Kröger N 2011 Nanopatterned protein microrings from a diatom that direct silica morphogenesis *Proc. Natl Acad. Sci.* **108** 3175–80
- [215] Kotzsch A, Pawolski D, Milentyev A, Shevchenko A, Scheffel A, Poulsen N, Shevchenko A and Kröger N 2015 Biochemical composition and assembly of biosilica-associated insoluble organic matrices from the diatom *thalassiosira pseudonana* *J. Biol. Chem.* **291** 4982–97
- [216] Hildebrand M and Lerch S J L 2015 Diatom silica biomineralization: parallel development of approaches and understanding *Semin. Cell Dev. Biol.* **46** 27–35
- [217] Yu M, Wu P, Widelitz R B and Chuong C-M 2002 The morphogenesis of feathers *Nature* **420** 308–12
- [218] Yu M, Yue Z, Wu P, Wu D-Y, Mayer J-A, Medina M, Widelitz R B, Jiang T-X and Chuong C-M 2004 The developmental biology of feather follicles *Int. J. Dev. Biol.* **8** 181–91
- [219] Yue Z, Jiang T-X, Widelitz R B and Chuong C-M 2005 Mapping stem cell activities in the feather follicle *Nature* **438** 1026–9
- [220] Chen C-F, Foley J, Tang P-C, Li A, Jiang T X, Wu P, Widelitz R B and Chuong C M 2015 Development, regeneration, and evolution of feathers *Annu. Rev. Animal Biosci.* **3** 169–95
- [221] Li A, Figueroa S, Jiang T-X, Wu P, Widelitz R, Nie Q and Chuong C-M 2017 Diverse feather shape evolution enabled by coupling anisotropic signalling modules with self-organizing branching programme *Nat. Commun.* **8** ncomms14139
- [222] Prum R O, Dufresne E R, Quinn T and Waters K 2009 Development of colour-producing  $\beta$ -keratin nanostructures in avian feather barbs *J. R. Soc. Interface* **6** S253–65
- [223] Lucas A M and Stettenheim P R (ed) 1972 *Avian Anatomy: Integument (Agriculture Handbook/United States Department of Agriculture vol 362)* (Washington, D.C.: Avian Anatomy Project)
- [224] Widelitz R B, Veltmaat J M, Mayer J A, Foley J and Chuong C-M 2007 Mammary glands and feathers: Comparing two skin appendages which help define novel classes during vertebrate evolution *Semin. Cell Dev. Biol.* **18** 255–66
- [225] Takenaka M and Hashimoto T 1992 Scattering studies of self-assembling processes of polymer blends in spinodal decomposition. II. Temperature dependence *J. Chem. Phys.* **96** 6177–90

- [226] Jones R A L 2002 *Soft Condensed Matter* vol 6 (Oxford: Oxford University Press)
- [227] Gur D, Palmer B A, Leshem B, Oron D, Fratzl P, Weiner S and Addadi L 2015 The mechanism of color change in the neon tetra fish: a light-induced tunable photonic crystal array *Angew. Chem. Int. Ed.* **54** 12426–30
- [228] Vigneron J P *et al* 2007 Switchable reflector in the panamanian tortoise beetle charidotella egregia (chrysomelidae: cassidinae) *Phys. Rev. E* **76** 031907
- [229] Arnold J M 1967 Organellenogenesis of the cephalopod iridophore: cytomembranes in development *J. Ultrastructure Res.* **20** 410–21
- [230] Tao A R, DeMartini D G, Izumi M, Sweeney A M, Holt A L and Morse D E 2010 The role of protein assembly in dynamically tunable bio-optical tissues *Biomaterials* **31** 793–801
- [231] Andouche A, Bassaglia Y, Baratte S and Bonnaud L 2013 Reflectin genes and development of iridophore patterns in *Sepia officinalis* embryos (Mollusca, Cephalopoda) *Dev. Dyn.* **242** 560–71
- [232] Guan Z *et al* 2017 Origin of the reflectin gene and hierarchical assembly of its protein *Curr. Biol.* **27** 2833–2842.e6
- [233] Levenson R, Bracken C, Bush N and Morse D E 2016 Cyclable condensation and hierarchical assembly of metastable reflectin proteins, the drivers of tunable biophotonics *J. Biol. Chem.* **291** 4058–68
- [234] Messenger J B 2001 Cephalopod chromatophores: neurobiology and natural history *Biol. Rev.* **76** 473–528
- [235] Gonzalez-Bellido P T, Wardill T J, Buresch K C, Ulmer K M and Hanlon R T 2014 Expression of squid iridescence depends on environmental luminance and peripheral ganglion control *J. Exp. Biol.* **217** 850–8
- [236] Mouchet S R, Van Hooijdonk E, Welch V L, Louette P, Colomer J-F, Su B-L and Deparis O 2016 Liquid-induced colour change in a beetle: The concept of a photonic cell *Sci. Rep.* **6** 19322
- [237] Wunderlin J and Kropf C 2013 *Rapid Colour Change in Spiders, In Spider Ecophysiology* (Berlin: Springer) pp 361–70
- [238] Aimi M F, Rao M P, MacDonald N C, Zuruzi A S and Bothman D P 2004 High-aspect-ratio bulk micromachining of titanium *Nat. Mater.* **3** 103–5
- [239] Zandi K, Belanger J A and Peter Y A 2012 Design and demonstration of an in-plane silicon-on-insulator optical MEMS fabry-Pérot-based accelerometer integrated with channel waveguides *J. Microelectromech. Syst.* **21** 1464–70
- [240] Cox J A, Dobson D C, Ohnstein T R and Zook J D 1998 Optical performance of high-aspect LIGA gratings II *Opt. Eng.* **37** 2878–85
- [241] Umbers K D L, Fabricant S A, Gawryszewski F M, Seago A E and Herberstein M E 2014 Reversible colour change in Arthropoda *Biol. Rev.* **9** 820–48
- [242] Kasukawa H and Oshima N 1987 Divisionistic generation of skin hue and the change of shade in the scalychick damselfish, pomacentrus lepidogenys *Pigment Cell Res.* **1** 152–7
- [243] Goda M and Fujii R 1998 The blue coloration of the common surgeonfish, paracanthurus hepatus: II. Color revelation and color changes *Zoological Sci.* **15** 323–33
- [244] Taylor J D and Hadley M E 1970 Chromatophores and color change in the lizard, *textit{Anolis carolinensis}* *Z. für Zellforschung Mikrosk. Anatomie* **104** 282–94
- [245] Phan L, Kautz R, Arulmoli J, Kim I H, Le D T T, Shenk M A, Pathak M M, Flanagan L A, Tombola F and Gorodetsky A A 2016 Reflectin as a material for neural stem cell growth *ACS Appl. Mater. Interfaces* **8** 278–84
- [246] Cui Z 2008 *Nanofabrication* (New York: Springer)
- [247] Peercy P S 2000 The drive to miniaturization *Nature* **406** 1023–6
- [248] Muller R S 2000 MEMS: Quo vadis in century XXI? *Microelectron. Eng.* **53** 47–54
- [249] Pan T and Wang W 2011 From cleanroom to desktop: emerging micro-nanofabrication technology for biomedical applications *Ann Biomed Eng* **39** 600–20
- [250] Sackmann E K, Fulton A L and Beebe D J 2014 The present and future role of microfluidics in biomedical research *Nature* **507** 181–9
- [251] Monat C, Domachuk P and Eggleton B J 2007 Integrated optofluidics: a new river of light *Nat. Photon.* **1** 106–14
- [252] Samiei E, Tabrizian M and Hoorfar M 2016 A review of digital microfluidics as portable platforms for lab-on a-chip applications *Lab on a Chip* **16** 2376–96
- [253] Truby R L and Lewis J A 2016 Printing soft matter in three dimensions *Nature* **540** 371–8
- [254] Judy J W 2001 Microelectromechanical systems (MEMS): fabrication, design and applications *Smart Mater. Struct.* **10** 1115
- [255] Becker H and Gärtner C 2008 Polymer microfabrication technologies for microfluidic systems *Anal. Bioanalytical Chem.* **390** 89–111
- [256] Kovacs G T A, Maluf N I and Petersen K E 1998 Bulk micromachining of silicon *Proc. IEEE* **86** 1536–51
- [257] Bustillo J M, Howe R T and Muller R S 1998 Surface micromachining for microelectromechanical systems *Proc. IEEE* **86** 1552–74
- [258] Muller R S and Lau K Y 1998 Surface-micromachined microoptical elements and systems *Proc. IEEE* **86** 1705–20
- [259] Malek C K and Saile V 2004 Applications of LIGA technology to precision manufacturing of high-aspect-ratio micro-components and -systems: a review *Microelectron. J.* **35** 131–43
- [260] Franssila S 2010 *Introduction to Microfabrication* (New York: Wiley)
- [261] Ziaie B, Baldi A and Atashbar M Z 2010 Introduction to micro-/nanofabrication *In Springer Handbook of Nanotechnology* (Berlin: Springer) pp 231–69
- [262] Quake S R and Scherer A 2000 From micro-to nanofabrication with soft materials *Science* **290** 1536–40
- [263] Kumar A and Whitesides G M 1993 Features of gold having micrometer to centimeter dimensions can be formed through a combination of stamping with an elastomeric stamp and an alkanethiol ‘ink’ followed by chemical etching *Appl. Phys. Lett.* **63** 2002–4
- [264] Qin D, Xia Y and Whitesides G M 2010 Soft lithography for micro- and nanoscale patterning *Nat. Protocols* **5** 491–502
- [265] Carlson A, Bowen A M, Huang Y, Nuzzo R G and Rogers J A 2012 Transfer printing techniques for materials assembly and micro/nanodevice fabrication *Adv. Mater.* **24** 5284–318
- [266] Rogers J A and Nuzzo R G 2005 Recent progress in soft lithography *Mater. Today* **8** 50–6
- [267] Watanabe K, Hoshino T, Kanda K, Haruyama Y and Matsui S 2004 Brilliant blue observation from a Morpho-butterfly-scale quasi-structure *Japan. J. Appl. Phys.* **44** L48
- [268] Potyrailo R A *et al* 2015 Towards outperforming conventional sensor arrays with fabricated individual photonic vapour sensors inspired by Morpho butterflies *Nat. Commun.* **6** 7959
- [269] Poncelet O, Tallier G, Mouchet S R, Crahay A, Rasson J, Kotipalli R, Deparis O and Francis L A 2016 Vapour sensitivity of an ALD hierarchical photonic structure inspired by morpho *Bioinsp. Biomim.* **11** 036011
- [270] Whitesides G M and Grzybowski B 2002 Self-assembly at all scales *Science* **295** 2418–21
- [271] von Freymann G, Kitaev V, Lotsch B V and Ozin G A 2013 Bottom-up assembly of photonic crystals *Chem. Soc. Rev.* **42** 2528–54

- [272] Vogel N, Retsch M, Fustin C-A, del Campo A and Jonas U 2015 Advances in colloidal assembly: the design of structure and hierarchy in two and three dimensions *Chem. Rev.* **115** 6265–311
- [273] Phillips K R, England G T, Sunny S, Shirman E, Shirman T, Vogel N and Aizenberg J 2016 A colloidoscope of colloid-based porous materials and their uses *Chem. Soc. Rev.* **45** 281–322
- [274] Yan Q, Yu J, Cai Z and Zhao X S 2011 Colloidal photonic crystals: fabrication and applications *Hierarchically Structured Porous Materials* ed B Su, S Sanchez and X Yang (New York: Wiley) pp 531–76
- [275] Vogel N, Retsch M, Fustin C-A, del Campo A and Jonas U 2015 Advances in colloidal assembly: the design of structure and hierarchy in two and three dimensions *Chem. Rev.* **115** 6265–311
- [276] Hatton B, Mishchenko L, Davis S, Sandhage K H and Aizenberg J 2010 Assembly of large-area, highly ordered, crack-free inverse opal films *Proc. Natl Acad. Sci.* **107** 10354–9
- [277] Chen Q, Bae S C and Granick S 2011 Directed self-assembly of a colloidal Kagome lattice *Nature* **469** 381–4
- [278] Schaffner M, England G, Kolle M, Aizenberg J and Vogel N 2015 Combining bottom-up self-assembly with top-down microfabrication to create hierarchical inverse opals with high structural order *Small* **11** 4334–40
- [279] Vogel N, de Viguerie L, Jonas U, Weiss C K and Landfester K 2011 Wafer-scale fabrication of ordered binary colloidal monolayers with adjustable stoichiometries *Adv. Funct. Mater.* **21** 3064–73
- [280] Mishchenko L, Hatton B, Kolle M and Aizenberg J 2012 Patterning hierarchy in direct and inverse opal crystals *Small* **8** 1904–11
- [281] Vogel N, Utech S, England G T, Shirman T, Phillips K R, Koay N, Burgess I B, Kolle M, Weitz D A and Aizenberg J 2015 Color from hierarchy: diverse optical properties of micron-sized spherical colloidal assemblies *Proc. Natl Acad. Sci.* **112** 10845–50
- [282] Glotzer S C and Solomon M J 2007 Anisotropy of building blocks and their assembly into complex structures *Nat. Mater.* **6** 557–62
- [283] Sacanna S, Korpics M, Rodriguez K, Colón-Meléndez L, Kim S-H, Pine D J and Yi G-R 2013 Shaping colloids for self-assembly *Nat. Commun.* **4** 1688
- [284] Gerth M and Voets I K 2017 Molecular control over colloidal assembly *Chem. Commun.* **53** 4414–28
- [285] Sun Y and Xia Y 2002 Shape-controlled synthesis of gold and silver nanoparticles *Science* **298** 2176–9
- [286] Sacanna S and Pine D J 2011 Shape-anisotropic colloids: building blocks for complex assemblies *Curr. Opin. Colloid Interface Sci.* **16** 96–105
- [287] Lv H, Lin Q, Zhang K, Yu K, Yao T, Zhang X, Zhang J and Yang B 2008 Facile fabrication of monodisperse polymer hollow spheres *Langmuir* **24** 13736–41
- [288] Miszta K *et al* 2011 Hierarchical self-assembly of suspended branched colloidal nanocrystals into superlattice structures *Nat. Mater.* **10** 872–6
- [289] Yunker P J, Chen K, Gratale M D, Lohr M A, Still T and Yodh A G 2014 Physics in ordered and disordered colloidal matter composed of poly(N-isopropylacrylamide) microgel particles *Rep. Prog. Phys.* **77** 056601
- [290] Pursiainen O L J, Baumberg J J, Ryan K, Bauer J, Winkler H, Viel B and Ruhl T 2005 Compact strain-sensitive flexible photonic crystals for sensors *Appl. Phys. Lett.* **87** 101902
- [291] Viel B, Ruhl T and Hellmann G P 2007 Reversible deformation of opal elastomers *Chem. Mater.* **19** 5673–9
- [292] Lee S Y, Choi J, Jeong J-R, Shin J H and Kim S-H 2017 Magnetoresponsive photonic microspheres with structural color gradient *Adv. Mater.* **29** 1605450
- [293] Wang Y, Wang Y, Zheng X, Ducrot É, Yodh J S, Weck M and Pine D J 2015 Crystallization of DNA-coated colloids *Nat. Commun.* **6** 7253
- [294] Mao X, Chen Q and Granick S 2013 Entropy favours open colloidal lattices *Nat. Mater.* **12** 217–22
- [295] Cabane B, Li J, Artzner F, Botet R, Labbez C, Bareigts G, Sztucki M and Goehring L 2016 Hiding in plain view: colloidal self-assembly from polydisperse populations *Phys. Rev. Lett.* **116**
- [296] Rogers W B, Shih W M and Manoharan V N 2016 Using DNA to program the self-assembly of colloidal nanoparticles and microparticles *Nat. Rev. Mater.* **1** 16008
- [297] Burgess I B, Koay N, Raymond K P, Kolle M, Lonçar M and Aizenberg J 2012 Wetting in color: colorimetric differentiation of organic liquids with high selectivity *ACS Nano* **6** 1427–37
- [298] Burgess I B, Lonçar M and Aizenberg J 2013 Structural colour in colourimetric sensors and indicators *J. Mater. Chem. C* **1** 6075
- [299] Inan H, Poyraz M, Inci F, Lifson M A, Baday M, Cunningham B T and Demirci U 2017 Photonic crystals: emerging biosensors and their promise for point-of-care applications *Chem. Soc. Rev.* **46** 366–88
- [300] Kim S, Mitropoulos A N, Spitzberg J D, Tao H, Kaplan D L and Omenetto F G 2012 Silk inverse opals *Nat. Photon.* **6** 818–23
- [301] Stein A and Schrodner R C 2001 Colloidal crystal templating of three-dimensionally ordered macroporous solids: materials for photonics and beyond *Curr. Opin. Solid State Mater. Sci.* **5** 553–64
- [302] van Blaaderen A, Ruel R and Wiltzius P 1997 Template-directed colloidal crystallization *Nature* **385** 321
- [303] Hoogenboom J P, van Langen-Suurling A K, Romijn J and van Blaaderen A 2003 Hard-sphere crystals with hcp and non-close-packed structure grown by colloidal epitaxy *Phys. Rev. Lett.* **90**
- [304] Jensen K E, Pennachio D, Recht D, Weitz D A and Spaepen F 2013 Rapid growth of large, defect-free colloidal crystals *Soft Matter* **9** 320–8
- [305] Fan F and Stebe K J 2004 Assembly of colloidal particles by evaporation on surfaces with patterned hydrophobicity *Langmuir* **20** 3062–7
- [306] Choi H K, Im S H and Park O O 2010 Fabrication of unconventional colloidal self-assembled structures *Langmuir* **26** 12500–4
- [307] Park J-G, Kim S-H, Magkiriadou S, Choi T M, Kim Y-S and Manoharan V N 2014 Full-spectrum photonic pigments with non-iridescent structural colors through colloidal assembly *Angew. Chem. Int. Ed.* **53** 2899–903
- [308] Kim S-H, Kim S-H and Yang S-M 2009 Patterned polymeric domes with 3d and 2d embedded colloidal crystals using photocurable emulsion droplets *Adv. Mater.* **21** 3771–5
- [309] Kawamura A, Kohri M, Morimoto G, Nannichi Y, Taniguchi T and Kishikawa K 2016 Full-color biomimetic photonic materials with iridescent and non-iridescent structural colors *Sci Rep* **6** 33984
- [310] Parker R M, Frka-Petesic B, Guidetti G, Kamita G, Consani G, Abell C and Vignolini S 2016 Hierarchical self-assembly of cellulose nanocrystals in a confined geometry *ACS Nano* **10** 8443–9
- [311] He L, Hu Y, Kim H, Ge J, Kwon S and Yin Y 2010 Magnetic assembly of nonmagnetic particles into photonic crystal structures *Nano Lett.* **10** 4708–14
- [312] Kim H, Ge J, Kim J, Choi S-E, Lee H, Lee H, Park W, Yin Y and Kwon S 2009 Structural colour printing using a magnetically tunable and lithographically fixable photonic crystal *Nat. Photon.* **3** 534–40



- [313] Lee H, Kim J, Kim H, Kim J and Kwon S 2010 Colour-barcode magnetic microparticles for multiplexed bioassays *Nat. Mater.* **9** 745–9
- [314] Hwang H, Park Y-H and Park J-K 2009 Optoelectrofluidic control of colloidal assembly in an optically induced electric field *Langmuir* **25** 6010–4
- [315] Phillips K R, Vogel N, Hu Y, Kolle M, Perry C C and Aizenberg J 2014 Tunable anisotropy in inverse opals and emerging optical properties *Chem. Mater.* **26** 1622–8
- [316] Rinne S A, García-Santamaría F and Braun P V 2008 Embedded cavities and waveguides in three-dimensional silicon photonic crystals *Nat. Photon.* **2** 52–6
- [317] Zhong K, Li J, Van Cleuvenbergen S and Clays K 2016 Direct fabrication of complex 3d hierarchical nanostructures by reactive ion etching of hollow sphere colloidal crystals *Nanoscale* **8** 15845–9
- [318] Meng Y, Tang B, Ju B, Wu S and Zhang S 2017 Multiple colors output on voile through 3d colloidal crystals with robust mechanical properties *ACS Appl. Mater. Interfaces* **9** 3024–9
- [319] Edrington A C, Urbas A M, DeRege P, Chen C X, Swager T M, Hadjichristidis N, Xenidou M, Fetters L J, Joannopoulos J D and Fink Y 2001 Polymer-based photonic crystals *Adv. Mater.* **13** 421–5
- [320] Parviz B A, Ryan D and Whitesides G M 2003 Using self-assembly for the fabrication of nano-scale electronic and photonic devices *IEEE Trans. Adv. Packag.* **6** 233–41
- [321] Stefik M, Guldin S, Vignolini S, Wiesner U and Steiner U 2015 Block copolymer self-assembly for nanophotonics *Chem. Soc. Rev.* **44** 5076–91
- [322] Dolan J A, Wilts B D, Vignolini S, Baumberg J J, Steiner U and Wilkinson T D 2015 Optical properties of gyroid structured materials: from photonic crystals to metamaterials *Adv. Opt. Mater.* **3** 12–32
- [323] Bates F S and Fredrickson G H 1999 Block copolymers—designer soft materials *Phys. Today* **52** 32–8
- [324] Ross C A, Berggren K K, Cheng J Y, Jung Y S and Chang J-B 2014 Three-dimensional nanofabrication by block copolymer self-assembly *Adv. Mater.* **26** 4386–96
- [325] Rothmund P W K 2006 Folding DNA to create nanoscale shapes and patterns *Nature* **440** 297–302
- [326] Dumanli A G, Kamita G, Landman J, van der Kooij H, Glover B J, Baumberg J J, Steiner U and Vignolini S 2014 Controlled, bio-inspired self-assembly of cellulose-based chiral reflectors *Adv. Opt. Mater.* **2** 646–50
- [327] Kang Y, Walish J J, Gorishnyy T and Thomas E L 2007 Broad-wavelength-range chemically tunable block-copolymer photonic gels *Nat. Mater.* **6** 957–60
- [328] Scherer M R J, Li L, Cunha P M S, Scherman O A and Steiner U 2012 Enhanced electrochromism in gyroid-structured vanadium pentoxide *Adv. Mater.* **24** 1217–21
- [329] Kalra V, Mendez S, Lee J H, Nguyen H, Marquez M and Joo Y L 2006 Confined assembly in coaxially electrospun block copolymer fibers *Adv. Mater.* **18** 3299–303
- [330] Kamita G, Frka-Petescic B, Allard A, Dargaud M, King K, Dumanli A G and Vignolini S 2016 Biocompatible and sustainable optical strain sensors for large-area applications *Adv. Opt. Mater.* **4** 1950–4
- [331] Hajduk D A, Harper P E, Gruner S M, Honeker C C, Kim G, Thomas E L and Fetters L J 1994 The gyroid: a new equilibrium morphology in weakly segregated diblock copolymers *Macromolecules* **27** 4063–75
- [332] Thomas E L, Anderson D M, Henkee C S and Hoffman D 1988 Periodic area-minimizing surfaces in block copolymers *Nature* **334** 598
- [333] Park C, Yoon J and Thomas E L 2003 Enabling nanotechnology with self assembled block copolymer patterns *Polymer* **44** 6725–60
- [334] Bates C M, Maher M J, Janes D W, Ellison C J and Willson C G 2014 Block copolymer lithography *Macromolecules* **47** 2–12
- [335] Vignolini S, Yufa N A, Cunha P S, Guldin S, Rushkin I, Stefik M, Hur K, Wiesner U, Baumberg J J and Steiner U 2012 A 3d optical metamaterial made by self-assembly *Adv. Mater.* **24** OP23–OP27
- [336] Scherer M R J and Steiner U 2013 Efficient electrochromic devices made from 3d nanotubular gyroid networks *Nano Lett.* **13** 3005–10
- [337] Dehmel R, Nicolas A, Scherer M R J and Steiner U 2015 3d nanostructured conjugated polymers for optical applications *Adv. Funct. Mater.* **25** 6900–5
- [338] Cheng J Y, Ross C A, Smith H I and Thomas E L 2006 Templated self-assembly of block copolymers: top-down helps bottom-up *Adv. Mater.* **18** 2505–21
- [339] Ma M, Krikorian V, Yu J H, Thomas E L and Rutledge G C 2006 Electrospun polymer nanofibers with internal periodic structure obtained by microphase separation of cylindrically confined block copolymers *Nano Lett.* **6** 2969–72
- [340] Sing C E, Zwanikken J W and Olvera de la Cruz M 2014 Electrostatic control of block copolymer morphology *Nat. Mater.* **13** 694–8
- [341] Aloï D 2015 Art series highlights creative discovery in ‘A Needle Woman’ *Cornell Chronicle*
- [342] Su W, Bonnard V and Burley G A 2011 DNA-templated photonic arrays and assemblies: design principles and future opportunities *Chem. Eur. J.* **17** 7982–91
- [343] Lan X and Wang Q 2014 DNA-programmed self-assembly of photonic nanoarchitectures *NPG Asia Mater.* **6** e97
- [344] Revol J-F, Bradford H, Giasson J, Marchessault R H and Gray D G 1992 Helicoidal self-ordering of cellulose microfibrils in aqueous suspension *Int. J. Biol. Macromolecules* **14** 170–2
- [345] Weber M F, Stover C A, Gilbert L R, Nevitt T J and Ouderkirk A J 2000 Giant birefringent optics in multilayer polymer mirrors *Science* **287** 2451–6
- [346] Alfrey T, Gurnee E F and Schrenk W J 1969 Physical optics of iridescent multilayered plastic films *Polym. Eng. Sci.* **9** 400–4
- [347] Radford J A, Alfrey T and Schrenk W J 1973 Reflectivity of iridescent coextruded multilayered plastic films *Polym. Eng. Sci.* **13** 216–21
- [348] Shirk J S, Pong R G S, Flom S R, Hiltner A and Baer E 2005 Nanostructured polymeric nonlinear photonic materials for optical limiting *Defense Applications of Nanomaterials* ed A W Miziolek, S P Karna, J M Mauro and R A Vaia vol 891 (Washington, DC: American Chemical Society) pp 254–64
- [349] Kazmierczak T, Song H, Hiltner A and Baer E 2007 Polymeric one-dimensional photonic crystals by continuous coextrusion *Macromol. Rapid Commun.* **28** 2210–6
- [350] Ponting M, Hiltner A and Baer E 2010 Polymer nanostructures by forced assembly: process, structure, and properties *Macromol. Symp.* **294** 19–32
- [351] Ponting M, Burt T M, Korley L T J, Andrews J, Hiltner A and Baer E 2010 Gradient multilayer films by forced assembly coextrusion *Ind. Eng. Chem. Res.* **49** 12111–8
- [352] Burt T M, Monemian S, Jordan A M and Korley L T J 2013 Thin film confinement of a spherical block copolymer via forced assembly co-extrusion *Soft Matter* **9** 4381–5
- [353] Ryan C *et al* 2012 Roll-to-roll fabrication of multilayer films for high capacity optical data storage *Adv. Mater.* **24** 5222–6
- [354] Finlayson C E, Goddard C, Papachristodoulou E, Snoswell D R E, Kontogeorgos A, Spahn P, Hellmann G P, Hess O and Baumberg J J 2011 Ordering in stretch-tunable polymeric opal fibers *Opt. Express* **19** 3144–54
- [355] Finlayson C E and Baumberg J J 2013 Polymer opals as novel photonic materials: polymer opals as novel photonic materials *Polym. Int.* **62** 1403–7

- [356] Bayindir M, Abouraddy A F, Arnold J, Joannopoulos J D and Fink Y 2006 Thermal-sensing fiber devices by multimaterial codrawing *Adv. Mater.* **18** 845–9
- [357] Hart S D, Maskaly G R, Temelkuran B, Prideaux P H, Joannopoulos J D and Fink Y 2002 External reflection from omnidirectional dielectric mirror fibers *Science* **296** 510–3
- [358] Gauvreau B, Guo N, Schicker K, Stoeffler K, Boismenu F, Ajji A, Wingfield R, Dubois C and Skorobogatiy M 2008 Color-changing and color-tunable photonic bandgap fiber textiles *Opt. Express* **16** 15677–93
- [359] Russell P 2003 Photonic crystal fibers *Science* **299** 358–62
- [360] Ruhl T, Spahn P and Hellmann G P 2003 Artificial opals prepared by melt compression *Polymer* **44** 7625–34
- [361] Finlayson C E, Spahn P, Snoswell D R E, Yates G, Kontogeorgos A, Haines A I, Hellmann G P and Baumberg J J 2011 3d bulk ordering in macroscopic solid opaline films by edge-induced rotational shearing *Adv. Mater.* **23** 1540–4
- [362] Schäfer C G, Winter T, Heidt S, Dietz C, Ding T, Baumberg J J and Gallei M 2015 Smart polymer inverse-opal photonic crystal films by melt-shear organization for hybrid core-shell architectures *J. Mater. Chem. C* **3** 2204–14
- [363] Zhao Q *et al* 2016 Large-scale ordering of nanoparticles using viscoelastic shear processing *Nat. Commun.* **7** 11661
- [364] Knight J C 2003 Photonic crystal fibres *Nature* **424** 847–51
- [365] Abouraddy A F, Bayindir M, Benoit G, Hart S D, Kuriki K, Orf N, Shapira O, Sorin F, Temelkuran B and Fink Y 2007 Towards multimaterial multifunctional fibres that see, hear, sense and communicate *Nat. Mater.* **6** 336–47
- [366] Bayindir M, Abouraddy A F, Shapira O, Viens J, Saygin-Hinczewski D, Sorin F, Arnold J, Joannopoulos J D and Fink Y 2006 Kilometer-long ordered nanophotonic devices by preform-to-fiber fabrication *IEEE J. Sel. Top. Quantum Electron.* **12** 1202–13
- [367] Gratson G M, Xu M and Lewis J A 2004 Microperiodic structures: direct writing of three-dimensional webs *Nature* **428** 386–386
- [368] Kang H S *et al* 2017 Printable and rewritable full block copolymer structural color *Adv. Mater.* **29** 1700084
- [369] Gissibl T, Thiele S, Herkommer A and Giessen H 2016 Two-photon direct laser writing of ultracompact multi-lens objectives *Nat. Photon.* **10** 554
- [370] Serbin J, Ovsianikov A and Chichkov B 2004 Fabrication of woodpile structures by two-photon polymerization and investigation of their optical properties *Opt. Express* **12** 5221–8
- [371] von Freymann G, Ledermann A, Thiel M, Staude I, Essig S, Busch K and Wegener M 2010 Three-dimensional nanostructures for photonics *Adv. Funct. Mater.* **20** 1038–52
- [372] Turner M D, Saba M, Zhang Q, Cumming B P, Schröder-Turk G E and Gu M 2013 Miniature chiral beamsplitter based on gyroid photonic crystals *Nat. Photon.* **7** 801–5
- [373] Maruo S and Fourkas J T 2008 Recent progress in multiphoton microfabrication *Laser Photon. Rev.* **2** 100–11
- [374] Franklin D, Chen Y, Vazquez-Guardado A, Modak S, Boroumand J, Xu D, Wu S-T and Chanda D 2015 Polarization-independent actively tunable colour generation on imprinted plasmonic surfaces *Nat. Commun.* **6** 7337
- [375] Park J, Moon J, Shin H, Wang D and Park M 2006 Direct-write fabrication of colloidal photonic crystal microarrays by ink-jet printing *J. Colloid Interface Sci.* **298** 713–9
- [376] Ding H, Zhu C, Tian L, Liu C, Fu G, Shang L and Gu Z 2017 Structural color patterns by electrohydrodynamic jet printed photonic crystals *ACS Appl. Mater. Interfaces* **9** 11933–41
- [377] Hou J, Zhang H, Su B, Li M, Yang Q, Jiang L and Song Y 2016 Four-dimensional screening anti-counterfeiting pattern by inkjet printed photonic crystals *Chem. Asian J.* **11** 2680–5
- [378] Nam H, Song K, Ha D and Kim T 2016 Inkjet printing based mono-layered photonic crystal patterning for anti-counterfeiting structural colors *Sci. Rep.* **6** 30885
- [379] Sowade E, Blaudeck T and Baumann R R 2016 Self-assembly of spherical colloidal photonic crystals inside inkjet-printed droplets *Cryst. Growth Des.* **16** 1017–26
- [380] Kuang M, Wang J, Bao B, Li F, Wang L, Jiang L and Song Y 2014 Inkjet printing patterned photonic crystal domes for wide viewing-angle displays by controlling the sliding three phase contact line *Adv. Opt. Mater.* **2** 34–8
- [381] Liu G, Zhou L, Zhang G, Li Y, Chai L, Fan Q and Shao J 2017 Fabrication of patterned photonic crystals with brilliant structural colors on fabric substrates using ink-jet printing technology *Mater. Des.* **114** 10–7
- [382] Derby B 2010 Inkjet printing of functional and structural materials: fluid property requirements, feature stability, and resolution *Annu. Rev. Mater. Res.* **40** 395–414
- [383] Ozin G A and Arsenault A C 2008 P-Ink and Elast-Ink from lab to market *Mater. Today* **11** 44–51
- [384] Ge J and Yin Y 2011 Responsive photonic crystals *Angew. Chem. Int. Ed.* **50** 1492–522
- [385] Yue Y and Gong J P 2015 Tunable one-dimensional photonic crystals from soft materials *J. Photochem. Photobiol. C* **23** 45–67
- [386] Kolle M and Lee S 2017 Progress and opportunities in soft photonics and biologically inspired optics *Adv. Mater.* **30** 1702669
- [387] Kolle M, Lethbridge A, Kreysing M, Baumberg J J, Aizenberg J and Vukusic P 2013 Bio-inspired band-gap tunable elastic optical multilayer fibers *Adv. Mater.* **25** 2239–45
- [388] Fudouzi H and Xia Y 2003 Colloidal crystals with tunable colors and their use as photonic papers *Langmuir* **19** 9653–60
- [389] Yue Y, Kurokawa T, Haque M A, Nakajima T, Nonoyama T, Li X, Kajiwarra I and Gong J P 2014 Mechano-actuated ultrafast full-colour switching in layered photonic hydrogels *Nat. Commun.* **5** 4659
- [390] Jia X, Wang J, Wang K and Zhu J 2015 Highly sensitive mechanochromic photonic hydrogels with fast reversibility and mechanical stability *Langmuir* **31** 8732–7
- [391] Yoon J, Lee W and Thomas E L 2008 Thermochromic block copolymer photonic gel *Macromolecules* **41** 4582–4
- [392] Ge J, Hu Y and Yin Y 2007 Highly tunable superparamagnetic colloidal photonic crystals *Angew. Chem. Int. Ed.* **46** 7428–31
- [393] Park T J *et al* 2015 Electrically tunable soft-solid block copolymer structural color *ACS Nano* **9** 12158–67
- [394] Xie Z-Y, Sun L-G, Han G-Z and Gu Z-Z 2008 Optical switching of a birefringent photonic crystal *Adv. Mater.* **20** 3601–4
- [395] Kelly J A, Shukaliak A M, Cheung C C Y, Shopsowitz K E, Hamad W Y and MacLachlan M J 2013 Responsive photonic hydrogels based on nanocrystalline cellulose *Angew. Chem. Int. Ed.* **52** 8912–6
- [396] Haque M A, Kamita G, Kurokawa T, Tsujii K and Gong J P 2010 Unidirectional alignment of lamellar bilayer in hydrogel: one-dimensional swelling, anisotropic modulus, and stress/strain tunable structural color *Adv. Mater.* **22** 5110–4
- [397] Scherer M R J and Steiner U 2015 Gyroid-structured electrodes for electrochromic and supercapacitor applications *Electrochromic Materials and Devices* ed R J Mortimer, D R Rosseinsky and P M Monk (New York: Wiley) 311–36

- [398] Murray S B and Neville A C 1998 The role of pH, temperature and nucleation in the formation of cholesteric liquid crystal spherulites from chitin and chitosan *Int. J. Biol. Macromolecules* **22** 137–44
- [399] National Research Council 1994 *Hierarchical Structures in Biology as a Guide for New Materials Technology* (Washington, DC: National Academies Press) (<https://doi.org/10.17226/2215>)
- [400] Cuthill I C *et al* 2017 The biology of color *Science* **357** eaan0221
- [401] Le T C and Winkler D A 2016 Discovery and optimization of materials using evolutionary approaches *Chem. Rev.* **116** 6107–32
- [402] Noorduyn W L, Grinthal A, Mahadevan L and Aizenberg J 2013 Rationally designed complex, hierarchical microarchitectures *Science* **340** 832–7
- [403] Kaplan C N, Noorduyn W L, Li L, Sadza R, Folkertsma L, Aizenberg J and Mahadevan L 2017 Controlled growth and form of precipitating microsculptures *Science* **355** 1395–9
- [404] Wasik B R, Liew S F, Lilien D A, Dinwiddie A J, Noh H, Cao H and Monteiro A 2014 Artificial selection for structural color on butterfly wings and comparison with natural evolution *Proc. Natl Acad. Sci.* **111** 12109–14
- [405] Huang J, Wang X and Wang Z L 2006 Controlled replication of butterfly wings for achieving tunable photonic properties *Nano Lett.* **6** 2325–31
- [406] Zhang W, Zhang D, Fan T, Ding J, Guo Q and Ogawa H 2006 Fabrication of ZnO microtubes with adjustable nanopores on the walls by the templating of butterfly wing scales *Nanotechnology* **17** 840
- [407] Tan Y *et al* 2012 High-density hotspots engineered by naturally piled-up subwavelength structures in three-dimensional copper butterfly wing scales for surface-enhanced raman scattering detection *Adv. Funct. Mater.* **22** 1578–85
- [408] Lee J H, Fan B, Samdin T D, Monteiro D A, Desai M S, Scheideler O, Jin H-E, Kim S and Lee S-W 2017 Phage-based structural color sensors and their pattern recognition sensing system *ACS Nano* **11** 3632–41